STUDY OF PURE FLUID PHENOMENA

Contract NAS 8-20102

May 28, 1965 - December 15, 1965

Final Report

December 15, 1965

Prepared For: George C. Marshall Space Flight Center
Astrionics Laboratory
National Aeronautics and Space Administration

Prepared By: Sperry Utah Company
Division of Sperry Rand Corporation
Salt Lake City, Utah

FOREWORD AND ACKNOWLEDGEMENTS

This research study was made for the Astrionics Laboratory of the George C. Marshall Space Flight Center, National Aeronautics and Space Administration, by the Sperry Utah Company Division of the Sperry Rand Corporation, under contract NAS 8-20102. The report covers a two-phase program.

Phase I describes the experimental laboratory work conducted to verify the scaling laws developed under contract NAS 8-11236 - June - December 1964. The experimental results have shown it necessary to modify the similarity equations of contract 8-11236. A modified set of similarity laws is presented in this report. A detailed description of a fluid sine wave signal generator developed during the course of the program is also included in this section.

Phase II describes the studies leading to the development of a pure fluid pressure ratio regulator. Several concepts of regulation are considered, and components applicable to pressure regulation systems are discussed.

The following authors have contributed to this report:

Phase I - Dr. E. Groeber

Phase II - C. L. Keller

General - D. F. Folland

ABSTRACT

This report covers two separate investigations. The first is an experiment in dynamic pressure transmission in passive fluid circuits. The second is an investigation of a fluidic circuit for maintaining a constant pressure ratio across a load.

The purpose of the first investigation is to verify the similarity laws for passive circuits. These laws have been developed under an earlier contract NAS 8-11236, and are contained in Volume 1, Chapter 2 of the final report of that contract.

The experiments proved that similar conditions exist when the volume ratio of the passive circuits is constant, and the length to diameter ratio is changed to satisfy the similarity laws. This is better called a dynamic similarity, which means that the same amplitude ratios of output to input oscillations are obtained at corresponding frequencies.

The similarity equations of contract NAS 8-11236 have been found to contain too many assumed conditions. The assumption that the tube length to diameter ratio is constant had to be dropped in order to have sufficient variables. A revised set of similarity laws is presented in this report.

The purpose of the second investigation is the development of a pre fluid pressure ratio regulator. Two concepts of regulation are considered. The first uses a single component operating in a self-regulating mode. It is shown to be feasible for regulating supply pressure variations, but it cannot compensate for changes in load. The second concept makes use of a regulating system, involving sensors, feedback elements and control valves. Components proposed for sensor application are discussed and analyzed. Further component study is found to be necessary.

TABLE OF CONTENTS

CHAPTER 1

THE SIMILARITY LAWS

Chapter 1

1.1 The Similarity Laws

The similarity laws for passive fluidic circuits are a part of the final report of the "Analytical Investigation of Fluid Amplifier Characteristics" of the contract NAS 8-11236, December 30, 1964. The mathematical development of the similarity laws is found in Volume 1, Chapter 2 under the heading "Dynamic Analysis of Passive Circuits and Electrical Analogy" and in Volume 2, Chapter 1 "Dimensional Analysis". Reference is made to the work of A. S. Iberall "Attenuation of Oscillatory Pressures in Instrument Lines", research paper RP 2115 of the National Bureau of Standards, Volume 45, July 1950. The theoretical investigation of Iberall constitutes the basis for the similarity laws developed under the NAS 8-11236 contract.

In general, the performance of devices in fluid mechanics and in fluidics is sensitive to the characteristics of the fluid: viscosity, temperature, and pressure. The problem of the similarity laws for dynamic conditions is to determine the requisite relations under which one system performs similar to another corresponding system.

The similarity laws for oscillatory pressures under contract NAS 8-11236 are developed under the prerequisite that the pipe flow follows Poiseuille's law for laminar flow.

It is the purpose of this work to establish proof for the scaling laws and to make corrections, if necessary. Based on the experiments, such corrections have been made.

1.2 Classification of Fluid Regimes and Similarity Rules

1.2.1 Classification of Dynamic Regimes

It is very important to understand the dynamic classification of fluid regimes and the physical factors entering such classification criterion.

It is well known that the classic Reynolds Number supplies the criterion for the steady-state classification of fluid regimes. Creeping flow, laminar flow, transitional flow and turbulent flow can be denoted by appropriate numerical values of the Reynolds Number.

Similarly, it has been shown that the dimensionless Stokes Number $S = \frac{\omega D^2 \rho}{4 \mu}$ classifies the fluid regimes in regard to dynamic conditions; it is in the nature of a dynamic damping index. Frequency, tube diameter and fluid kinematic viscosity enter into the parameter; it clearly demonstrates that frequency alone is not sufficient to denote dynamic state in a fluid dynamic situation.

Three basic dynamic fluid regimes can be identified, as will be discussed below.

1.2.1.1 High Damping Regime

This area comprises the S-range from 0 to 1.0; at S = 0, of course, there is steady-state flow. Here it is essential to have similarity for both R_e and S_1 since the steady-state flow is the boundary of the area, and quasi-steady-state flow may be assumed for the mathematical solution.

The elementary solution may be used if tube compressibility can be neglected and the chamber processes are isothermal. A criterion for the neglect of tube compressibility is as follows:

$$\frac{32\ \omega\ \mu}{D^2 n p} \leq \frac{1}{100}$$

Generally, the corrected theory should be used. The corrected theory is quite complex and is presented in the final report of contract NAS 8-11236, Volume 1, Chapter 2. Each regime has its own set of corrected equations.

1.2.1.2 Intermediate Damping Area

This area comprises the S-range from 1.0 to 100; most practical applications of proportional fluid control circuitry are expected to fall in this area.

The elementary solution should not be used in this area since the compressibility of the gas in the tube will be important and the chamber processes will be approaching adiabatic. The corrected theory should be used.

1.2.1.3 Low Damping Area

This area comprises the S-range above 100; the upper limit is not defined by a S value, but by another parameter, i.e. $\frac{\omega D}{C} = 3.68$. This area may be also termed the elementary longitudinal acoustic area and its upper limit of applicability is given by the onset of transverse acoustic waves. When such waves occur, the full three-dimensional analysis is required.

1.2.2 Dimensionless Parameters

The theory has shown that the amplitude attenuation ratio and the phase angle is dependent on the following dimensionless parameters:

$$S = \frac{\omega D^2 \rho}{4 \mu}$$

$$\chi_{T_o} = \frac{32\ \omega\ \mu}{n\ p} \left(\frac{L}{D}\right)^2$$

Tube to tank volume ratio = $\frac{V}{AL} \quad \frac{m}{n}$

$$Z = \frac{\omega L}{C}$$

In addition, the classic Reynolds Number $R_e = \frac{UD\varsigma}{\mu}$ should also be considered, to account for steady-state similarity in the tube (pressure-loss and transverse velocity distribution).

The geometric similarity parameters are $\frac{L}{D}$ and $\frac{V}{AL}$.

The heat transfer similarity parameters $\frac{m}{n}$ are explicitly and also implicitly in the velocity of sound.

If in addition to the Reynolds Number R_e and the Stokes Number S (both basic parameters which can be derived directly from the fluid equations of motion) an acoustical Reynolds Number is considered, with the form:

$R_{ea} = \frac{CD\varsigma}{\mu}$

Then it has been shown that χ_{T_o} and Z can be expressed in terms of S and R_{ea}.

Indeed $\chi_{T_o} = \frac{\omega D^2 \varsigma}{4\mu} \quad \frac{\mu^2}{C^2 D^2 \varsigma^2} \quad \left(\frac{L}{D}\right)^2 128$

thus $\chi_{T_o} = 128 \quad \frac{S}{R_{e_a}^2} \quad \left(\frac{L}{D}\right)^2$

also $Z = \frac{\omega D^2 \varsigma}{4\mu} \quad \frac{\mu}{CD\varsigma} \quad \frac{4L}{D}$

thus $Z = \frac{4 \quad S}{R_{e_a}} \quad \frac{L}{D}$

Dynamic similarity in fluidic circuits exists when the amplitude ratio of pressure oscillations is equal. A passive fluidic circuit is shown in Fig. 1-1. The amplitudes in passive circuits are measured at the input to the tube and at the tank. Considering two fluidic circuits, let the index 1 denote the first circuit and the index 2 stand for the

second circuit. Then in case of similarity

$$S = \frac{\omega_1 \rho_1 D_1^2}{\mu_1} = \frac{\omega_2 \rho_2 D_2^2}{\mu_2}$$

or
$$\frac{\omega_1}{\omega_2} \quad \frac{\rho_1}{\rho_2} \quad \frac{\mu_2}{\mu_1} \quad \left(\frac{D_1}{D_2}\right)^2 = 1 \qquad (1\text{-}1)$$

The second requirement is that

$$\chi T_o = \frac{128\ S_1}{Re_{a_1}^2} \left(\frac{L_1}{D_1}\right)^2 = \frac{128\ S_2}{Re_{a_2}^2} \left(\frac{L_2}{D_2}\right)^2$$

since $S_1 = S_2$ and $R_{e_a} = \frac{CD\rho}{\mu}$

$$\frac{\mu_1^2}{C_1^2 D_1^2 \rho_1^2} \left(\frac{L_1}{D_1}\right)^2 = \frac{\mu_2^2}{C_2^2 D_2^2 \rho_2^2} \left(\frac{L_2}{D_2}\right)^2$$

or
$$\frac{\mu_1}{\mu_2} \quad \frac{C_2}{C_1} \quad \left(\frac{D_2}{D_1}\right)^2 \quad \frac{\rho_2}{\rho_1} \quad \frac{L_1}{L_2} = 1 \qquad (1\text{-}2a)$$

$$Z = 4 \frac{S_1}{R_{ea_1}} \frac{L_1}{D_1} = 4 \frac{S_2}{R_{ea_2}} \frac{L_2}{D_2}$$

or again
$$\frac{\mu_1}{\mu_2} \quad \frac{C_2}{C_1} \quad \left(\frac{D_2}{D_1}\right)^2 \quad \frac{\rho_2}{\rho_1} \quad \frac{L_1}{L_2} = 1 \qquad (1\text{-}2b)$$

Equation (1-2a) and (1-2b) are the same.

The third requirement is that

$$\frac{V_1}{A_1 L_1} \quad \frac{m_1}{n_1} = \frac{V_2}{A_2 L_2} \quad \frac{m_2}{n_2}$$

The polytropic expansion ratio $\frac{m}{n}$ is unity in nearly all practical cases. The cross section $A = \frac{\pi D^2}{4}$, so that

$$\frac{V_1}{V_2} \quad \left(\frac{D_2}{D_1}\right)^2 \quad \frac{L_2}{L_1} = 1 \qquad (1\text{-}3)$$

The fourth requirement is that the Reynolds number is equal. (When the mean flow is zero, as it is the case in passive circuits, then the fourth requirement drops out.)

$$R_e = \frac{U_1 D_1 \rho_1}{\mu_1} = \frac{U_2 D_2 \rho_2}{\mu_2}$$

or

$$\frac{U_1}{U_2} \quad \frac{D_1}{D_2} \quad \frac{\rho_1}{\rho_2} \quad \frac{\mu_2}{\mu_1} = 1$$

One should note that these similarity laws are developed with the assumption of laminar flow in the tube. Laminar flow exists when $R_e \leq 2000$. The flow in the tube consists of a constant velocity and a superimposed oscillatory velocity component. The amplitude ratios are clearly defined in the laminar flow region, but when the flow extends into the critical flow region ($R_e \geq 2000$), the amplitude ratios become undefined.

Summarized, the similarity laws for oscillatory pressures in fluid lines consist of a set of four equations which are:

$$\frac{\omega_1}{\omega_2} \quad \frac{\rho_1}{\rho_2} \quad \frac{\mu_2}{\mu_1} \quad \left(\frac{D_1}{S_2}\right)^2 = 1 \qquad (1\text{-}1)$$

$$\frac{C_2}{C_1} \quad \frac{\rho_2}{\rho_1} \quad \frac{\mu_1}{\mu_2} \quad \left(\frac{D_2}{D_1}\right)^2 \quad \frac{L_1}{L_2} = 1 \qquad (1\text{-}2)$$

$$\frac{V_1}{V_2} \quad \left(\frac{D_2}{D_1}\right)^2 \quad \frac{L_2}{L_1} = 1 \qquad (1\text{-}3)$$

$$\frac{U_1}{U_2} \quad \frac{\rho_1}{\rho_2} \quad \frac{\mu_2}{\mu_1} \quad \frac{D_1}{D_2} = 1 \qquad (1\text{-}4)$$

This set of equations constitutes a similarity which renders the same amplitude ratio for a model at corresponding frequencies. The dimensions of the model, however, are not proportional.

There is a difference between the scaling laws of the final report of contract NAS 8-11236 and the similarity laws of this report. The tube length to diameter ratio $\frac{L}{D}$ was a fixed value, but now has become a variable factor. The similarity equations are indetermined when $\frac{L}{D}$ is a constant. Therefore, $\frac{L}{D}$ has to be variable.

Example: A model shall be built for a passive circuit for which the tube diameter is 1/2 the original diameter, and air of 14.6 psia shall be replaced by CO_2 of the same pressure. Index 1 is used for model 1, Index 2 is used for the model 2. The following values are given:

$$D_2 = \frac{1}{2} D_1$$

$$\frac{\mu_{air}}{\mu_{CO_2}} = \frac{3.82 \times 10^{-7}}{3.092 \times 10^{-7}} = 1.235$$

$$\frac{\rho_{air}}{\rho_{CO_2}} = \frac{2.365 \times 10^{-3}}{3.58 \times 10^{-3}} = 0.66$$

$$\frac{C_{air}}{C_{CO_2}} = \frac{1130}{880} = 1.285$$

Equation (1) determines the frequencies for which equal amplitude ratios are obtained

$$\omega_2 = \frac{.66}{1.235} \times 4 \quad \omega_1$$

$$\underline{\omega_2 = 2.135 \quad \omega_1}$$

Equation (2) determines the length of the tube.

$$L_2 = \frac{1.235 \quad \times 1}{1.285 \times .66 \times 4} \quad L_1$$

$$\underline{L_2 = 0.64 \quad L_1}$$

and equation (3) determines the volume of the tank of the model

$$V_2 = 1.4 \times .364 \quad V_1$$

$$\underline{V_2 = .091 \quad V_1}$$

The dynamic response of model (2) is similar to model (1) when it is built to these relationships.

1.3 Test Equipment

The similarity tests required the following instruments and parts:

A sinusoidal fluid signal generator - figure 1-5.
A set of test tubes and volumes - figure 1-6.
Two model KP-15 "PACE" pressure transducers - figure 1-3.
Two model CD25 "PACE" transducer indicators - figure 1-3.
A dual beam oscilloscope - figure 1-2.
A tektronix oscilloscope camera - figure 1-2.
A barometer - figure 1-2.
A mercury monometer - figure 1-2.
Cylinders of compressed carbon dioxide with pressure reducing valves, interconnection lines, tanks, and valves - figure 1-2.
Cylinders of compressed helium with pressure reducing valves - figure 1-2.

These instruments are standard laboratory equipment except for the sinusoidal fluid signal generator (figure 1-5), and a set of tubes and tanks (figure 1-6).

Figures 1-2, 1-3, and 1-7 show the test arrangement which is the same for all tests except for the supply line. The supply line must be adapted to the various gases because it is important that in each case the line delivers constant pressure to the pressure chamber of the signal generator. A pressure regulator is sufficient for air and helium but not for carbon dioxide. Carbon dioxide freezes and forms ice in the process of expansion in the pressure regulator. But ice in the regulator causes random pressure changes. The forming of ice must be prevented by adding heat and by expanding in two stages. In the test arrangement (figure 1-2) a heat gun blows hot air over the pressure regulator and de-ices it effectively. In order to cushion and smooth any remaining pressure variations the carbon dioxide enters a tank which acts as an accumulator. The pressure in the tank is kept 25% to 50% above the chamber pressure of the fluid signal generator and the tank discharge is regulated by a needle valve. Satisfactory pressure conditions are obtained with this arrangement. A mercury monometer indicates the supply pressure before the gas enters the fluid signal generator. In the signal generator the gas flows through a fixed orifice into a pressure chamber and exhausts through a variable outlet orifice. A sinusoidal change of the outlet orifice area causes a pressure sine wave in the pressure chamber. (A more complete description is given below.)

The test tubes are connected to the pressure chamber and the test tanks are connected to the tubes. Since the test tanks are closed, the mean flow in the tube is zero (passive circuit). There is, however, an oscillatory movement of the gas in the tube caused by a pressure difference between input and output. The input and the output pressures are picked up by two "PACE" diaphragm pressure transducers which translate the pressures into electrical signals. The "PACE" pressure transducer indicators amplify the electrical signals for observation of the average value on a meter and the AC value on an oscilloscope.

The diaphragm pressure transducers are low inertia sensors and well capable of following the pressure oscillations up to two or three thousand Hertz. However, the transducer indicator amplifiers are limited to one thousand Hertz. Far more important than the average pressures of the input and output are the instantaneous pressures or pressure oscillations. A dual beam oscilloscope displays pictures of the input and output pressure wave simultaneously. The "PACE" transducer indicators are easily calibrated to correlate the display of the oscilloscope with the gage pressures. Finally, an oscilloscope Polaroid camera is used to photograph the input - output traces from which it is possible to determine accurately the frequency and the pressure amplitudes and to keep a permanent record of the tests. A series of input and output pressure pictures is taken for each passive circuit.

All test tubes have the same inside diameter (0.136) and a cross section of 0.0145 square inch. Table 1 contains the dimensions of the complete set of tubes and test tanks.

Table 1

Test Tubes and Tanks

	L/D for Tube	Tube Length (in)	Tube Volume (in)	Tank Volume	Volume Ratio Tank - Tube
1	200	27.2	.3951	19.756	50 x tube 1
2	150	20.4	.2963	14.817	50 x tube 2
3	100	13.6	.1976	9.878	50 x tube 3
4	75	10.2	.1482	7.408	50 x tube 4
5	50	6.8	.0988	4.939	50 x tube 5
6	37.5	5.1	.0741	3.704	50 x tube 6
7	25	3.4	.0494	2.470	50 x tube 7
8	18.75	2.55	.037	1.852	50 x tube 8
9	12.5	1.7	.0247	1.235	50 x tube 9
				0.926	25 x tube 8
				0.6174	25 x tube 9
				0.463	12.5 x tube 8
				0.3087	12.5 x tube 9
				0.232	6.25 x tube 8
				0.1544	6.25 x tube 9
				0.1157	3.125 x tube 8
				0.0772	3.125 x tube 9

1.4 Description of the Fluid Signal Generator

Clean and undistorted pressure sine waves are a prerequisite for exact measurements. To provide this a new signal generator was designed and built which produces a clean pressure oscillation (figure 1-5). The fluid signal generator is a mechanical device using a rotating wobble plate faced by an open jet. Variation of the distance from the face of the plate and the jet produces pressure variations in the attached chamber. At higher frequencies vibration increases, and signal distortions can be observed. About 200 Hertz can be considered as the frequency limit for measurements using this signal source. Amplitude measurements show large amplitudes for low frequencies and gradually decreasing amplitudes for higher frequencies (figures 1-8 to 1-12). An invention disclosure for the apparatus has been submitted in compliance with the "new technology" clause of the contract.

The fluid signal generator consists of a small pressure chamber (figure 1-13), which is fed by the gas supply line through a small restriction of 1/16-inch diameter. A small 1/8-inch diameter outlet orifice is covered by a wobble plate driven by an air turbine. One small channel leads to the pressure sensor, and finally a 1/8-inch diameter opening serves as connection to the test circuits.

There is a small adjustable distance between the wobble plate and the outlet orifice. The slant of the wobble plate determines the maximum and minimum distance from the outlet orifice. At constant angular speed the outlet area changes sinusoidally. A corresponding pressure change occurs in the pressure chamber. The chamber pressure is a nonlinear function of the outlet area, and a pure sine wave is induced only for small amplitudes. Larger pressure oscillations do not follow a pure sine function. However, a good approximation can be obtained by making a suitable correction in the slant of the wobble plate.

The chamber pressure oscillations change when fluidic circuits are connected. To the volume of the chamber is added the volume of the circuit which causes lower amplitudes, and second order oscillation distortions of the pressure sine wave. This necessitates measurement of the chamber pressure for each experiment.

The output frequency of the generator can be determined either by taking oscilloscope pictures and measuring the time for one cycle, or by using a frequency counter. The signal generator is mechanically driven by an air turbine. The air turbine simply consists of a small spur gear towards which a tangential air jet is directed. Simple and quiet operation characterizes this inexpensive power source. Also the air turbine cannot introduce electrical distortion into the measurements.

1.5 Signal Generator for Signals Above 200 Hertz

Pressure oscillations of higher frequencies are desirable for testing very short lines and very thin lines. The natural frequencies of such lines are generally higher than 200 Hertz. Lines with higher natural frequencies may be very practical in fluidic lines to obtain fast response without change in signal amplitude. The mechanical fluid signal generator described above can be used for higher frequencies, also, if the rotating wobble plate is replaced by a vibrating membrane. An Altec 806A driver loudspeaker has been used as a replacement for the wobble plate (figure 1-14). The loudspeaker has a frequency range from 500 to 22,000 cps. It is driven by an electronic signal generator and amplifier. A piezo type "Sensonic" transducer is used instead of the "PACE" sensors to be compatible with the frequency range of the loudspeaker. The limit for the "PACE" indicator is 1000 Hertz, the "Sensonic" transducer indicates up to 10^5 Hz.

There are two serious complications in using this generator. First, the vibration of the membrane is well in the acoustical region and the sound waves are transmitted through the environment and the hardware, as well as through the gas in the tube. The "Sensonic" transducers pick up the sound waves from the environment and from the tube. It is, therefore, impossible to measure the pure fluid transmission of the oscillation because the pressure waves in the fluid cannot be isolated from the sound waves. Secondly, the membrane of the loudspeaker driver is very soft and the stagnation pressure of the air jet stops the vibration where the jet hits the membrane. Only a very minute change in the area of the orifice occurs. The generated pressure oscillations are not satisfactory.

Another loudspeaker approach was tried. This time, the gas flow and the compression chamber are eliminated (figures 1-15 and 1-16). The membrane is enclosed and the passive circuit is mounted directly above the vibrating membrane. Also the "PACE" pressure sensors are used again to avoid acoustic interference.

The result of this arrangement is satisfactory. The most interesting oscillatory pressure transfer conditions occur between 200 and 500 Hz, which is below the specified operating range of the available driver loudspeaker. The speaker membrane ruptured during a test run.

1.6 Test Plan

The purpose of the experiments is to prove the practical validity of the similarity laws. We recall that similarity between circuits exists when the similarity factors S, χ_{T_0}, $\frac{V}{AL}$, and R_e are equal. R_e is zero for passive circuits because the mean flow is zero. The similarity factors mentioned above contain characteristic values of the fluid as well

as geometrical relationships. Three different gases have been chosen: air, carbon dioxide, and helium, with greatly different gas characteristics.

	AIR	CO_2	HE	
Absolute viscosity μ	3.82×10^{-7}	3.092×10^{-7}	4.05×10^{-7}	$\frac{lb\ sec}{ft^2}$
Mass Density ϱ	2.365×10^{-3}	3.58×10^{-3}	3.033×10^{-4}	$\frac{lb\ sec^2}{ft^4}$
Velocity of sound C	1130	880	3325	ft/sec
Acoustic Reynolds number R_{ea}	7.92×10^4	11.55×10^4	2.82×10^4	

These values apply for an input pressure of 14.6 psia for air and carbon dioxide and 13.6 psia for helium. The tests were made at an altitude of 4200 ft above sea level and an atmospheric pressure of 12.6 psia. All test tube diameters are equal but the lengths of the tubes are different. The lengths have been chosen in such a way that the test tubes and tanks can be combined conveniently into passive circuits of constant volume ratios. Experiments were made with two volume ratios, namely: $\frac{V}{AL} = 6.25$ and 25. The passive circuits are connected to the pressure chamber of the fluid signal generator.

The tests themselves consist of the observation and the taking of pictures of the oscilloscope display. The pressure sine wave frequencies are changed step by step and pictures are taken from the input and output wave at each step. This has been done for each passive circuit and for each gas. Series of pictures were obtained and evaluated for various frequencies and amplitudes.

But, since these frequencies and amplitudes are not the final result of the tests, we must go one step further. The final result is obtained when the amplitude ratios are plotted over the attenuation factor χ_{T_0} for constant damping factor S. It is easy to find χ_{T_0} when we chose the factor S and remember that the χ_{T_0} is a linear function of the angular velocity ω or the frequency f. χ_{T_0} can be calculated for each length to volume ratio from the equation

$$\chi_{T_0} = 128 \frac{S}{R_{ea}^2} \left(\frac{L}{D}\right)^2. \qquad (1\text{-}5)$$

Now the amplitude ratios can be plotted versus χ_{T_0} for constant S and various gases. Similarity is obtained when those curves coincide.

1.7 Test Results

The test set-up is shown in figure 1-2. After calibration of the "PACE" transducer indicator the testing is routine. Chamber pressures of 2 psi for air and carbon dioxide and 1.0 psi for helium were used. The average chamber pressure is indicated on the "PACE" transducer indicator. The frequency is chosen between 3 and 200 Hertz and set by regulating the air supply to the turbine. The input pressure oscillation is displayed at the lower part of the oscilloscope picture tube and the output at the upper part. The following data was entered on each picture: type of gas, ratio $\frac{L}{D}$, volume ratio, chamber pressure, amplification in the horizontal and vertical direction for the upper and lower beam, and the relation between pressure and voltage of the "PACE" transducer. Samples are shown on pages through . These pictures represent three sets of actual tests, one for air, one for carbon dioxide, and one for helium. Each set delivers one curve of amplitude ratio versus frequency. But, to draw the amplitude ratio versus frequency the amplitudes are measured and the amplitude ratio computed. Also the period of pressure oscillation is measured and the frequency calculated. All the curves obtained in this manner for various circuit combinations are shown in figures 1-17 through 1-21. All curves for the same gas and the same volume ratio are plotted on one sheet. Since all tube diameters D are equal and the damping factor $S = \frac{\omega D^2 \varrho}{4 \mu}$ is proportional to the frequency, one can calculate the frequency for any S. Arbitrarily, three factors of S are chosen, namely: 15, 25 and 100. The corresponding frequencies are:

S	AIR	CO_2	He	
15	12	6.4	100	Hz
25	20	10.7	166.5	Hz
100	80	42.8	--	Hz

The attenuation factor $\chi_{T_0} = 128 \frac{S}{R_{ea}^2} \left(\frac{L}{D}\right)^2$ can now be calculated for each passive circuit and gas and damping factor S (table 2).

Table 2

T_o for S =

L/D	AIR 15	AIR 25	AIR 100	CO_2 15	CO_2 25	CO_2 100	He 15	He 25
400	4.88×10^{-2}	8.15×10^{-2}	3.26×10^{-1}	2.3×10^{-2}	3.84×10^{-2}	1.526×10^{-1}	--	--
300	2.76×10^{-2}	4.59×10^{-2}	1.836×10^{-1}	1.3×10^{-2}	2.16×10^{-2}	8.64×10^{-2}	--	--
200	1.22×10^{-2}	2.04×10^{-2}	8.15×10^{-2}	5.75×10^{-3}	9.6×10^{-3}	3.84×10^{-2}	9.65×10^{-2}	1.61×10^{-1}
150	---	---	---	---	---	---	5.43×10^{-2}	9.05×10^{-2}
100	3.06×10^{-3}	5.1×10^{-3}	2.04×10^{-2}	1.44×10^{-3}	2.4×10^{-3}	9.6×10^{-2}	2.42×10^{-2}	4.02×10^{-2}
50	7.65×10^{-4}	1.275×10^{-3}	5.1×10^{-3}	3.6×10^{-4}	6×10^{-4}	2.4×10^{-3}	6.02×10^{-3}	1.0×10^{-2}
25	1.92×10^{-4}	3.19×10^{-4}	1.275×10^{-3}	9×10^{-5}	1.5×10^{-4}	6×10^{-4}	1.5×10^{-3}	2.51×10^{-3}
12.5	4.77×10^{-5}	7.95×10^{-5}	3.19×10^{-4}	2.24×10^{-5}	3.74×10^{-5}	1.5×10^{-4}	---	6.25×10^{-4}

With the attenuation factor χ_{T_0} known, every corresponding amplitude ratio known, the final curves can be plotted. Figures 1-22 through 1-25 show these amplitude ratio vs. attenuation factor curves for constant S and $\frac{V}{AL}$. The fact that corresponding curves coincide for various gases and at any arbitrary damping factor S and volume ratio proves that the similarity law is correct.

1.8 Additional Observations

The program to measure experimentally the dynamic behavior of each passive circuit, or in other words to produce the amplitude ratio vs. frequency curves, has been rewarding. It eliminated mistakes because the characteristic path of the curve is so obvious that wrong measurements are detected immediately. It provided the amplitude ratios for each circuit at any arbitrarily chosen frequency or Stokes number, and in addition it gave the possibility of comparing the various sets of curves. One cannot help but notice, for example, that the amplitude ratios of the passive circuit for air with $\frac{L}{D}$ of 100 and $\frac{V}{AL}$ of 6.25 (figure 1-17) is almost identical with the amplitude ratios of the circuit with $\frac{L}{D}$ of 50 and $\frac{V}{AL}$ of 25 (figure 1-20). The same is true for other curves. These new facts suggest that there may also be dynamic similarity between circuits of different volume ratios. Therefore, the assumption of constant volume ratios may not be necessary. A new, broader law for dynamic similarity might explain this observation. Such an extended law could mean that the dynamic behavior of fluid transmission lines could be altered and controlled by geometric combinations of varying $\frac{L}{D}$ and $\frac{V}{AL}$. A study in this direction would be of value for fluidic transmission lines.

1.9 Limitation of the Similarity Laws

It was indicated earlier that the similarity laws depend on Poiseuille's law for laminar flow. The limit for this flow region is reached at a Reynolds number R_e of 2000. The critical flow region is entered when R_e exceeds 2000 and the flow resistance in a pipe becomes random.

When the experiments were performed with helium, random amplitude ratios were obtained. Since the mean flow in the tubes of passive circuits is zero, and only oscillating flow exists, the conclusion was drawn that the instantaneous velocity exceeded the laminar flow region. In order to drop back into the laminar region the chamber pressure was lowered from 2.0 psi to 1.0 psi which produced acceptable results. It shows clearly that the similarity laws are only valid for the relatively small laminar region, and that the limit is the maximum instantaneous velocity in the tube.

Lines for inter-connecting fluidic devices might be affected by this limitation. Proper control over the dynamic behavior in the turbulent region and more knowledge in the critical flow region are desirable. It is recommended that a study extend the similarity laws into these regions.

1.10 Conclusion

This report contains the experimental verification of similarity laws for lines with volumes and in particular for closed passive circuits. It was necessary to modify slightly the similarity laws of a previous contract (NAS 8-11236). The similarity laws are:

$$\frac{\omega_1}{\omega_2}\ \frac{\rho_1}{\rho_2}\ \frac{\mu_2}{\mu_1}\ \left(\frac{D_1}{D_2}\right)^2 = 1 \qquad (1\text{-}1)$$

$$\frac{C_2}{C_1}\ \frac{\rho_2}{\rho_1}\ \frac{\mu_1}{\mu_2}\ \left(\frac{D_2}{D_1}\right)^2\ \frac{L_1}{L_2} = 1 \qquad (1\text{-}2)$$

$$\frac{V_1}{V_2}\ \left(\frac{D_2}{D_1}\right)^2\ \frac{L_2}{L_1} = 1 \qquad (1\text{-}3)$$

$$\frac{U_1}{U_2}\ \frac{\rho_1}{\rho_2}\ \frac{\mu_2}{\mu_1}\ \frac{D_1}{D_2} = 1 \qquad (1\text{-}4)$$

These laws determine how the geometric parameters and frequencies have to change for various gases to obtain equal amplitude ratios. The laws are valid in the laminar flow region.

As by-product, a satisfactory sine wave fluid signal generator has been developed with a frequency range of 3 to 200 Hz. Attempts to produce a high frequency generator have not been completely successful.

The results of the experiments point the way for further, valuable studies and tests which would broaden the knowledge in the field of fluidics particularily for fluid transmission lines.

1.11 List of Symbols used in Chapter 1

A	Pipe cross section	(ft^2)
C	Speed of sound	(ft/sec)
D	Pipe diameter	(ft)
f	Frequency	(Hertz)
L	Length of pipe	(ft)
m,n	Exponents for polytropic expansion	(o)
P_0	Chamber pressure	(lb/ft^2)
R_e	Reynolds number	(o)
R_{ea}	Acoustic Reynolds number	(o)
S	Stokes Number	(o)
u	Velocity of flow	(ft/sec)
V	Tank volume	(ft^3)
χ_{T_o}	Attenuation factor	(1/sec)
Z	Attenuation factor	(1/sec)
μ	Absolute fluid viscosity	$(\frac{lb\ sec}{ft^2})$
ϱ	Mass Density	($lb\ sec^{\ 2}/ft^4$)
ω	Angular velocity	(1/sec)

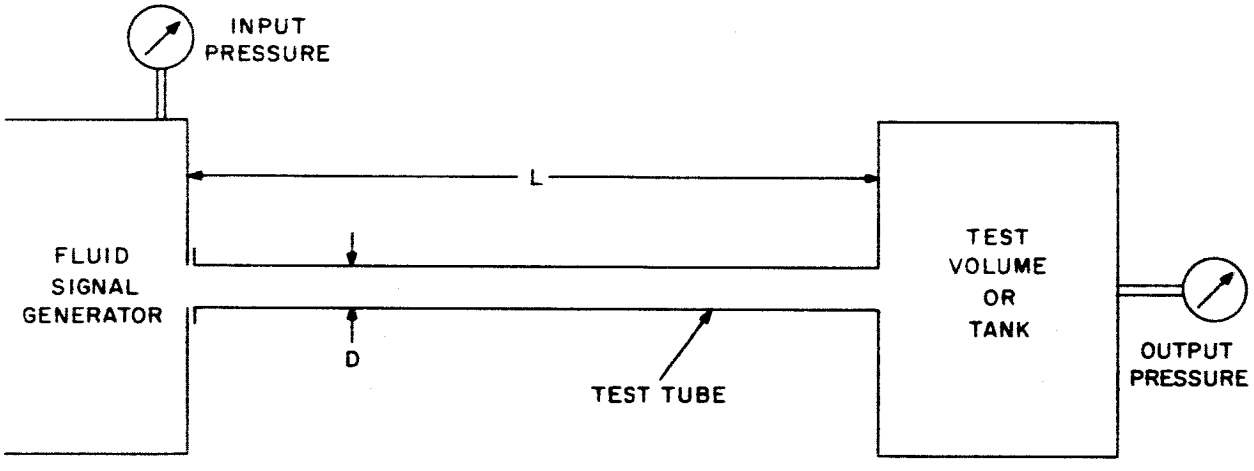

FIGURE 1.— PASSIVE FLUIDIC CIRCUIT

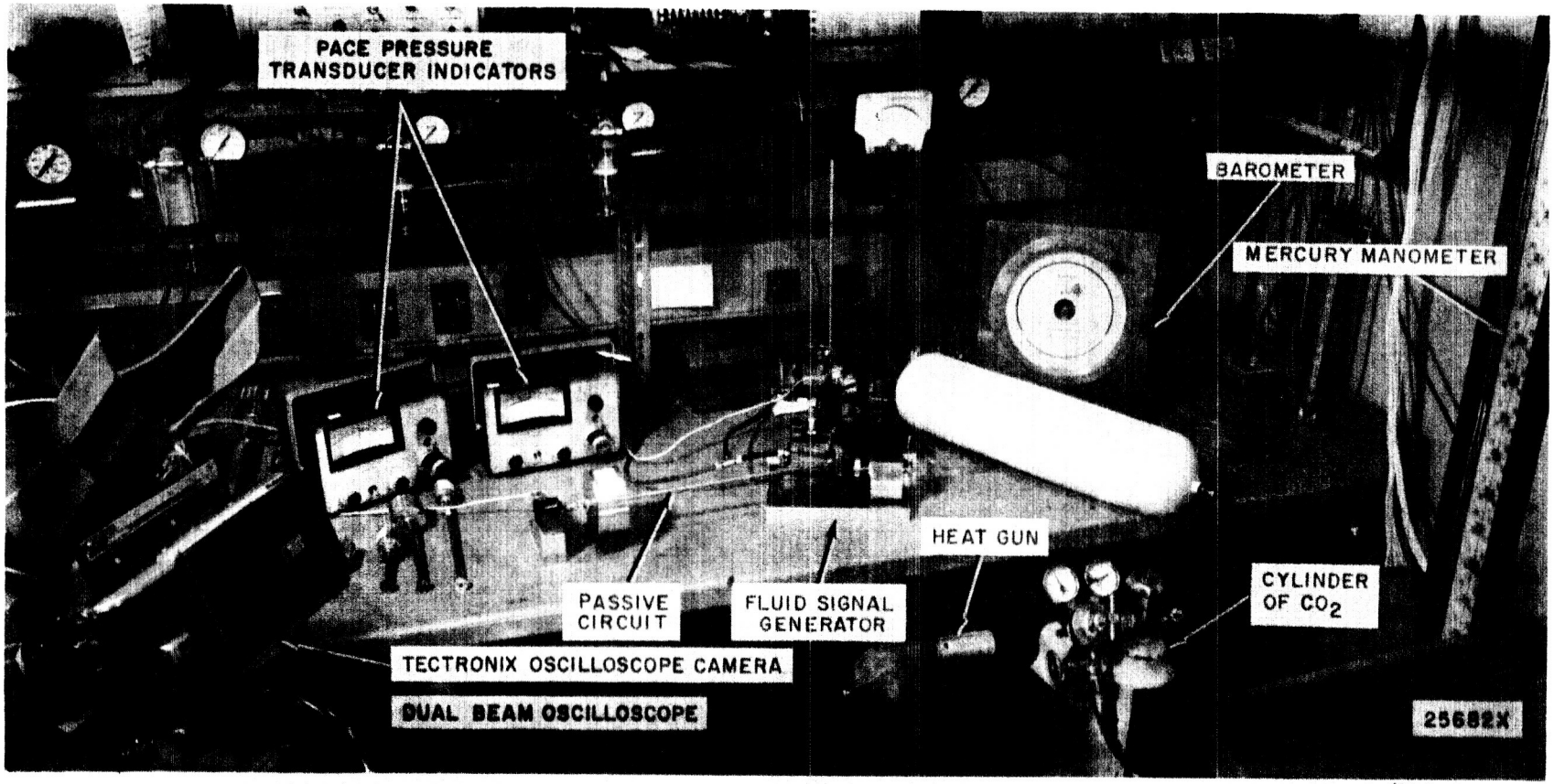

FIGURE 2. SIMILARITY TEST ARRANGEMENT FOR CO_2

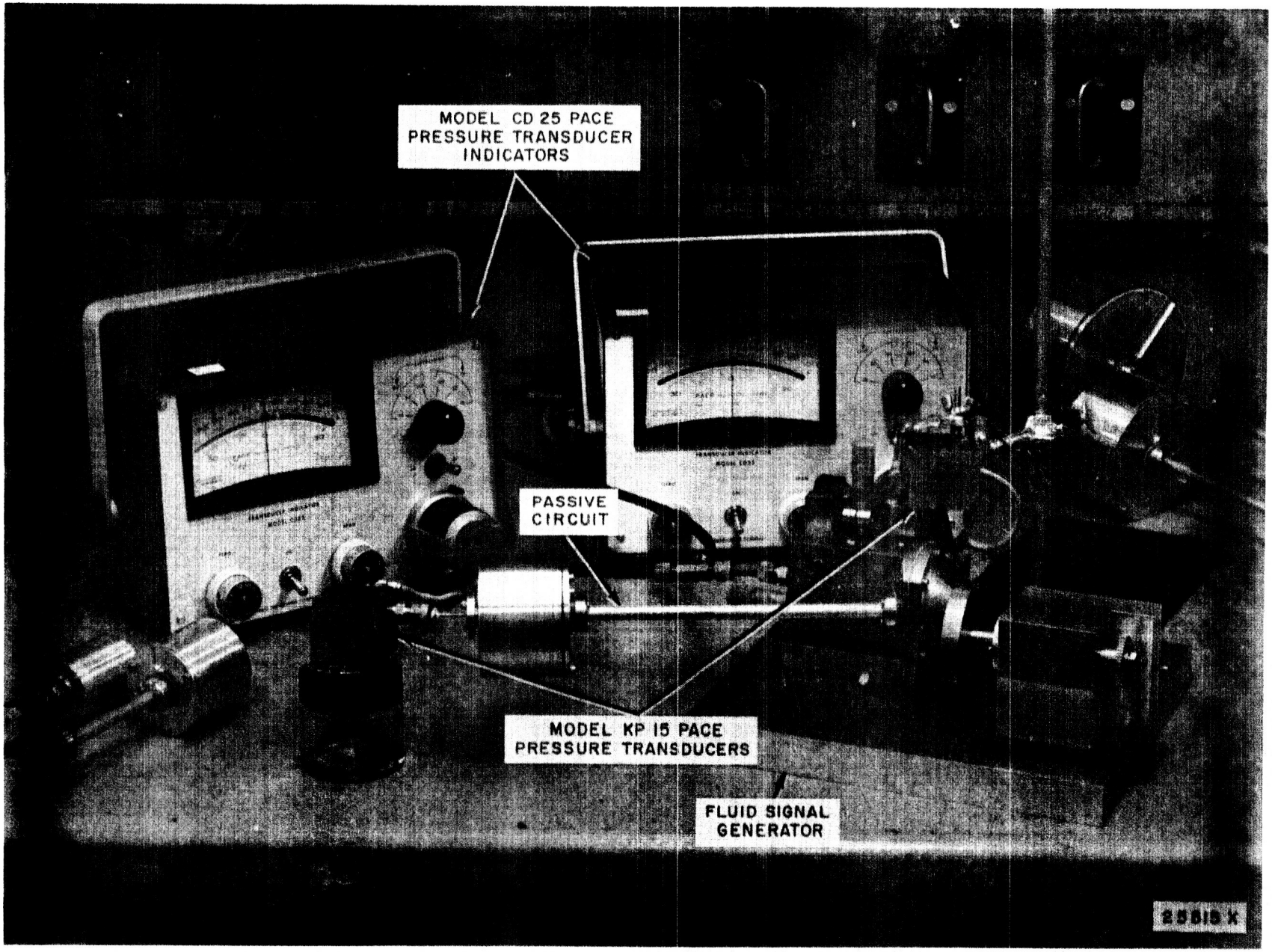

FIGURE 3. SIMILARITY TEST SET UP

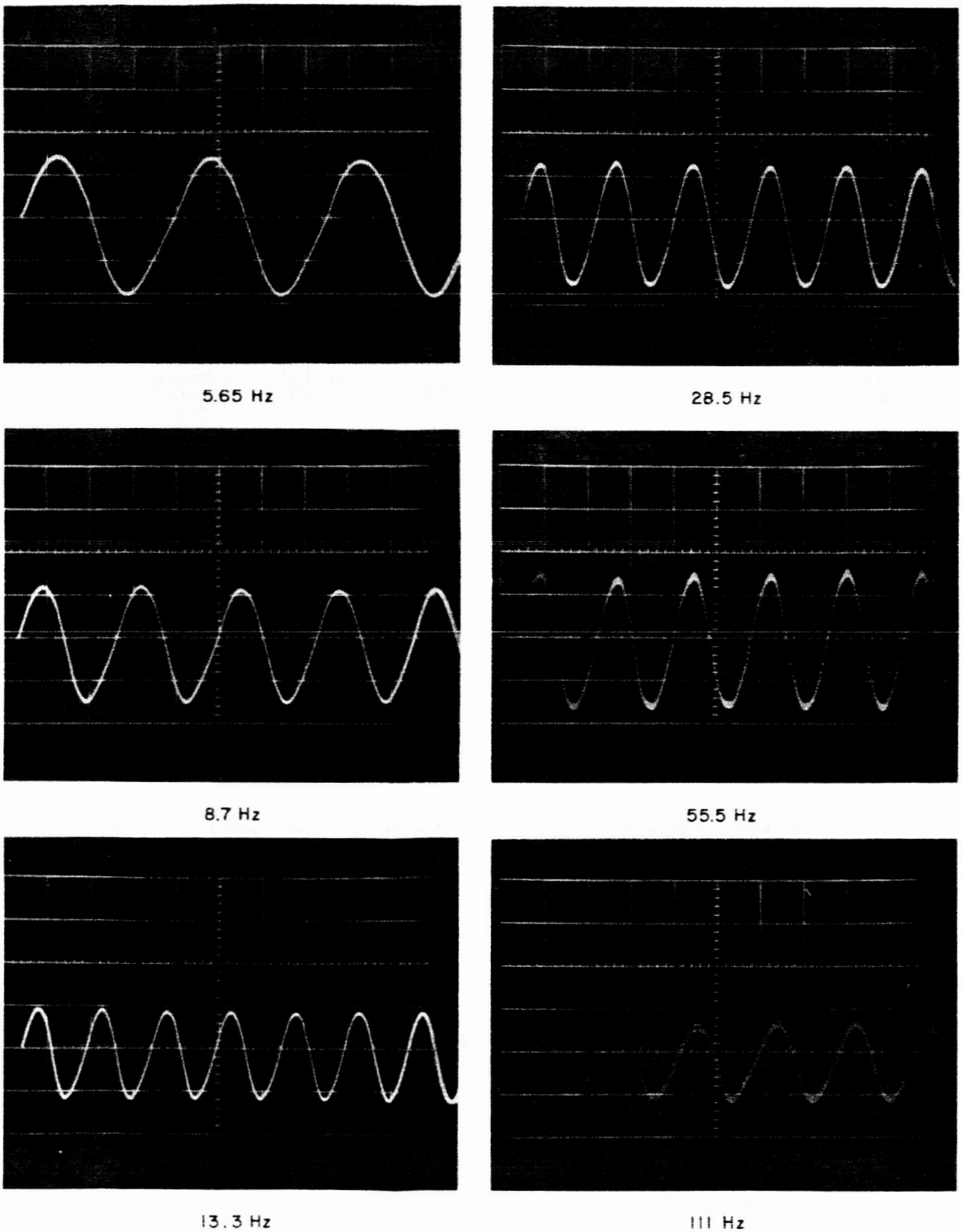

FIGURE 4. PRESSURE OSCILLATION OF FREQUENCY GENERATOR AT VARIOUS FREQUENCIES AND INFINITE LOAD.

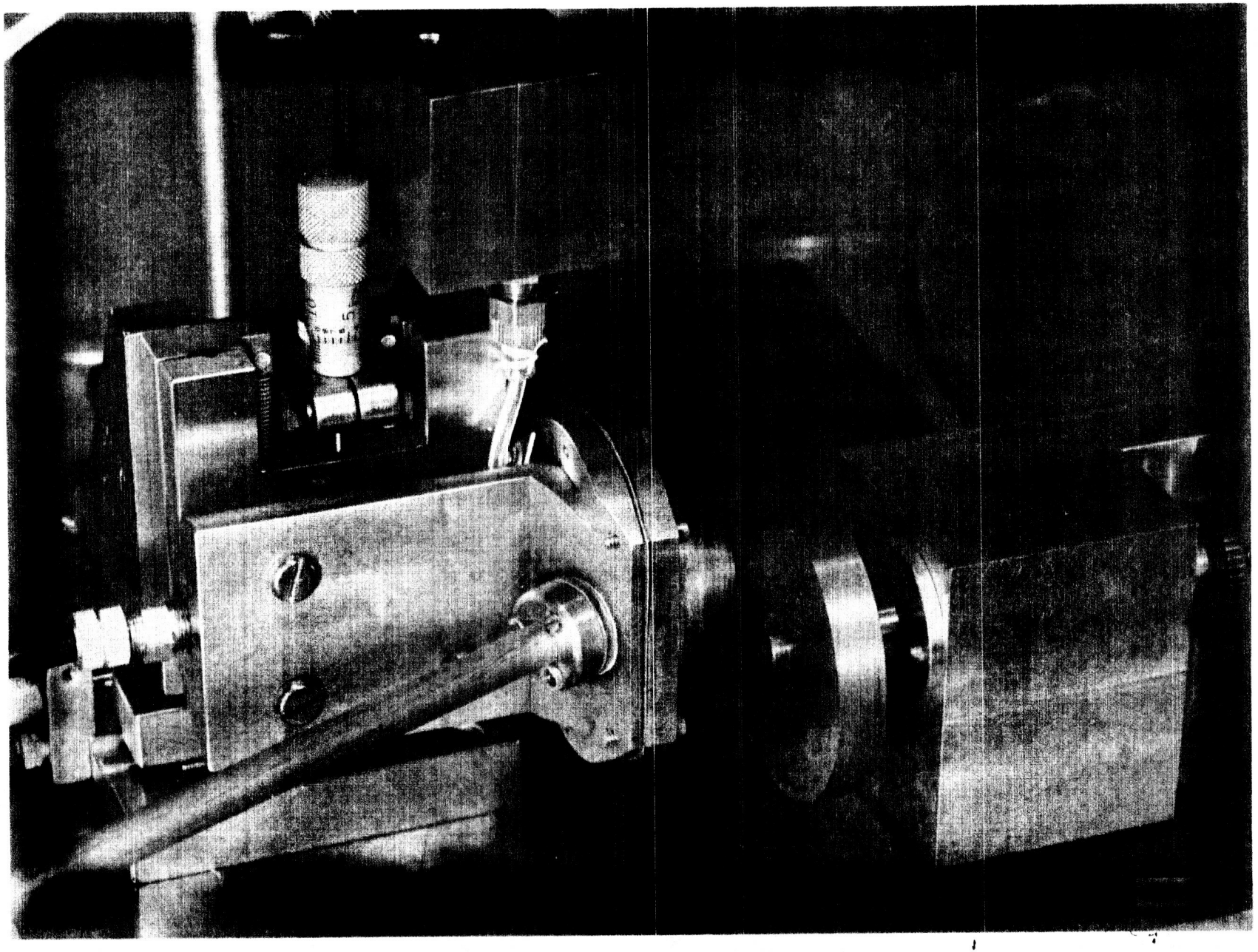

FIGURE 5. FLUID SIGNAL GENERATOR

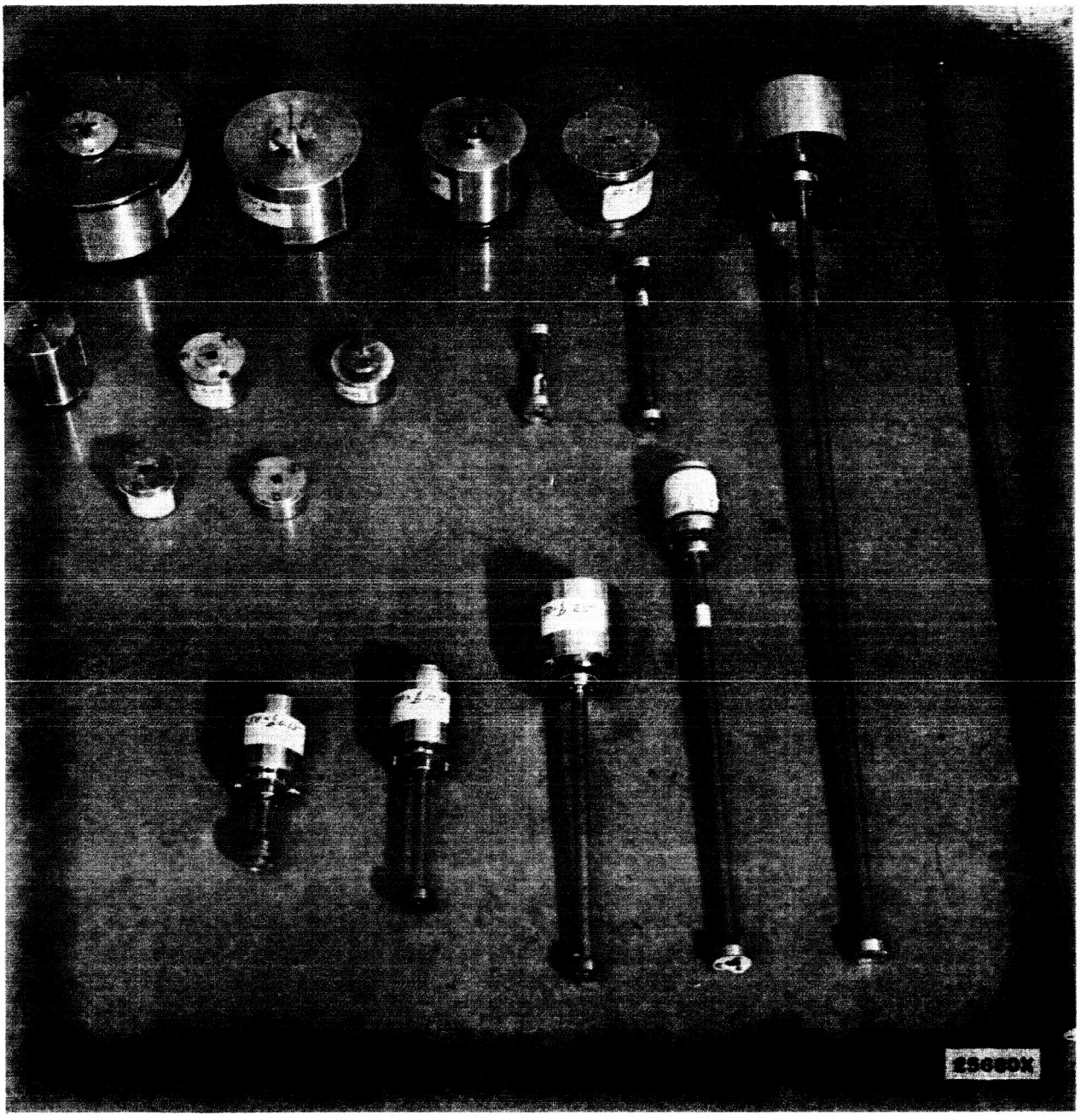

FIGURE 6. SET OF TEST TUBES AND VOLUMES

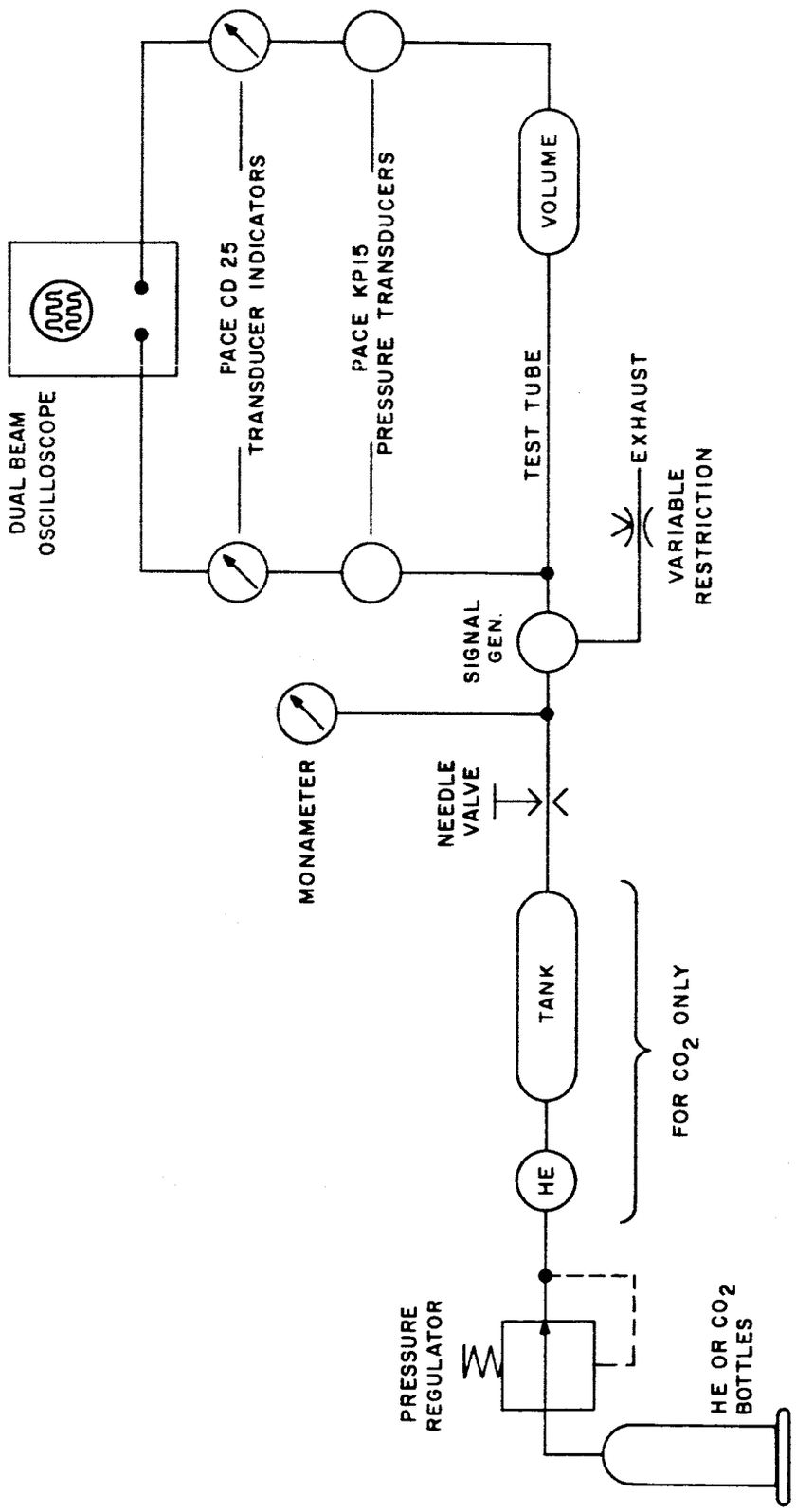

FIGURE 7.— GENERAL TEST ARRANGEMENT SCHEMATIC

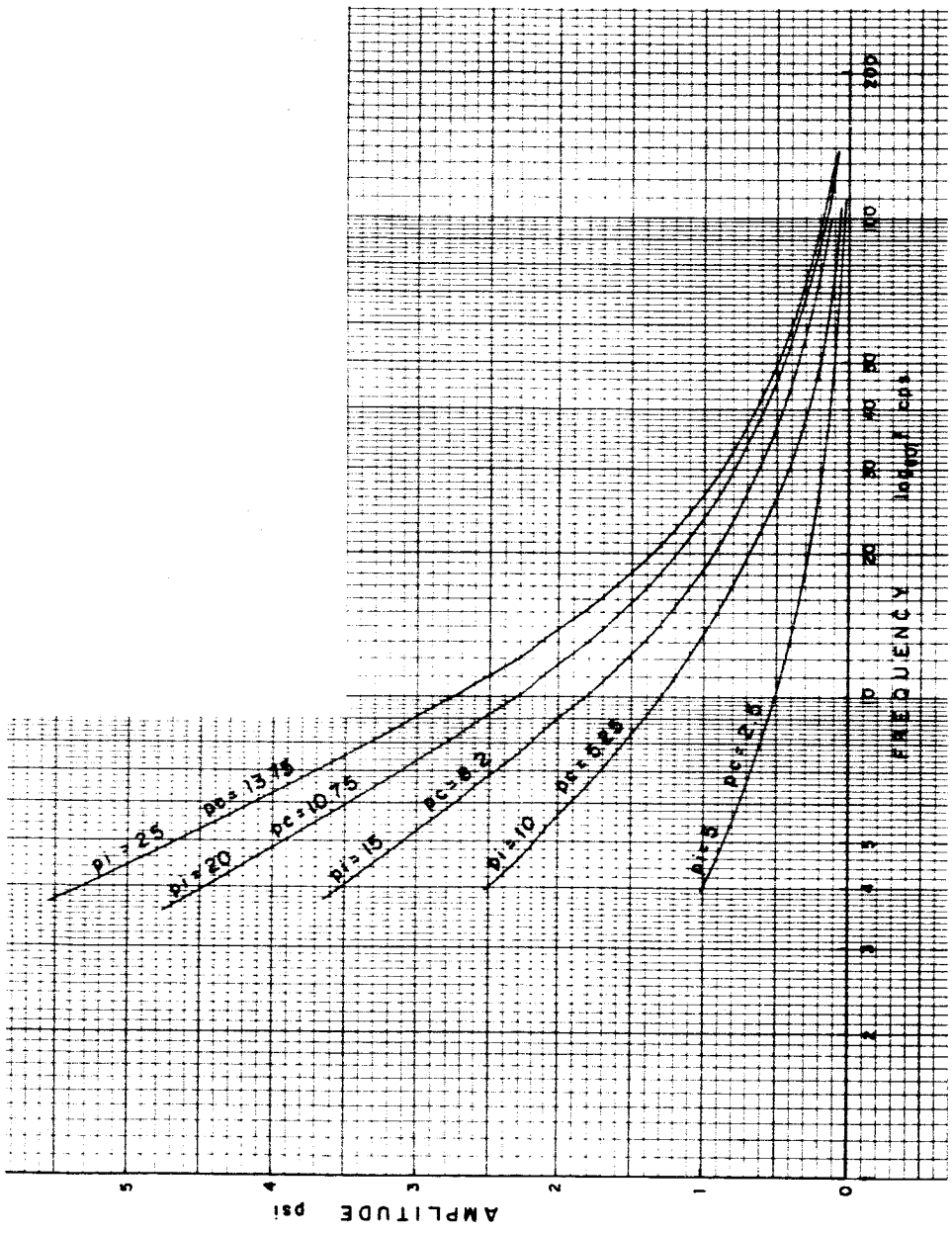

FIGURE 8. PERFORMANCE OF L.F. FLUID SIGNAL GENERATOR
(FOR NOZZLE GAP WIDTH .002 (MIN.)).

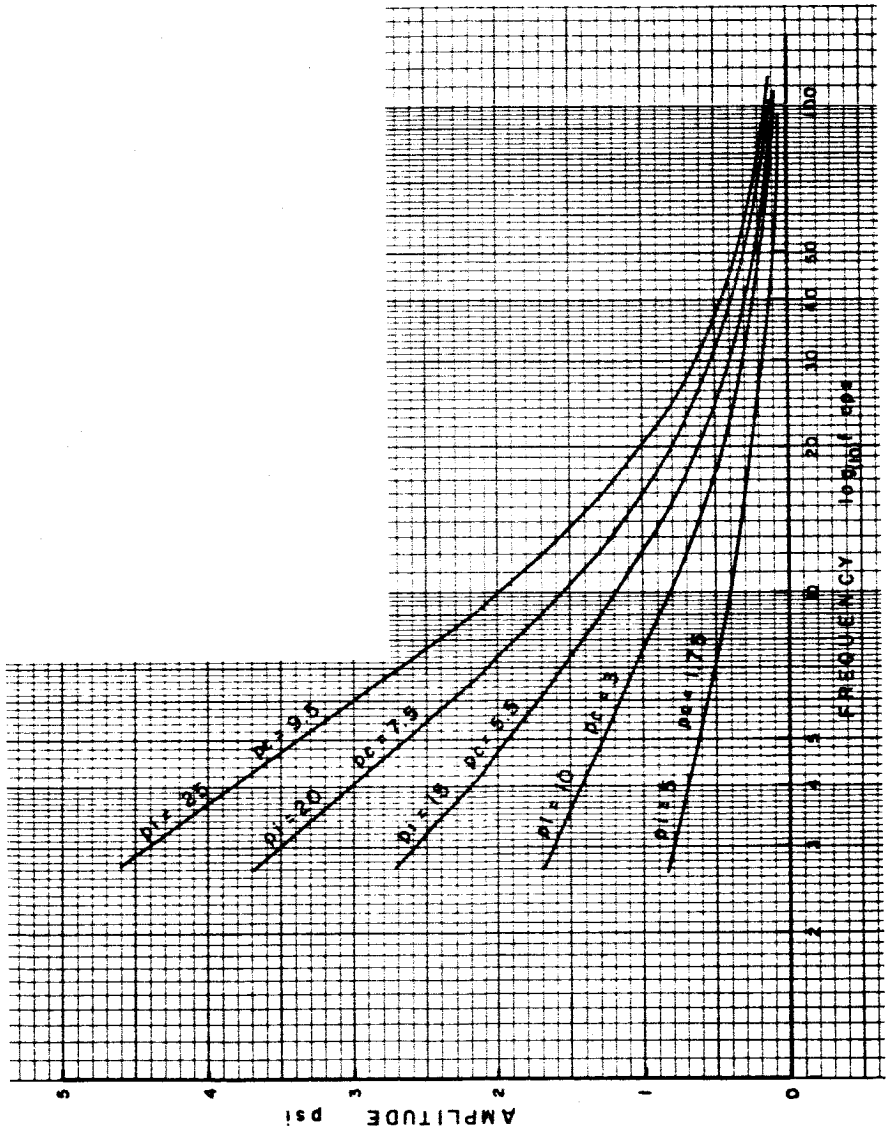

FIGURE 9. PERFORMANCE OF L.F. FLUID SIGNAL GENERATOR (FOR NOZZLE GAP WIDTH .005(MIN.)).

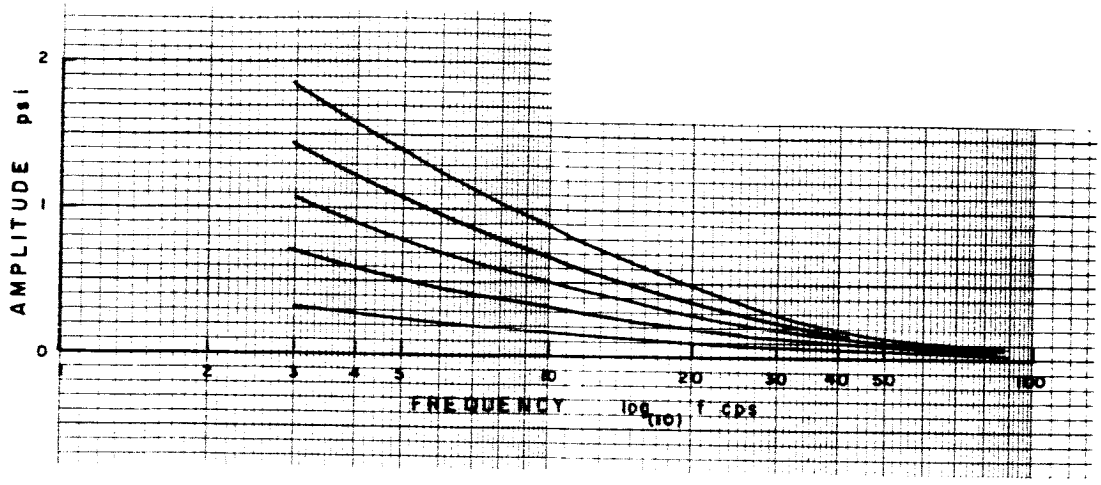

FIGURE 10. PERFORMANCE OF L.F. FLUID SIGNAL GENERATOR
(FOR NOZZLE GAP WIDTH .010 (MIN.)).

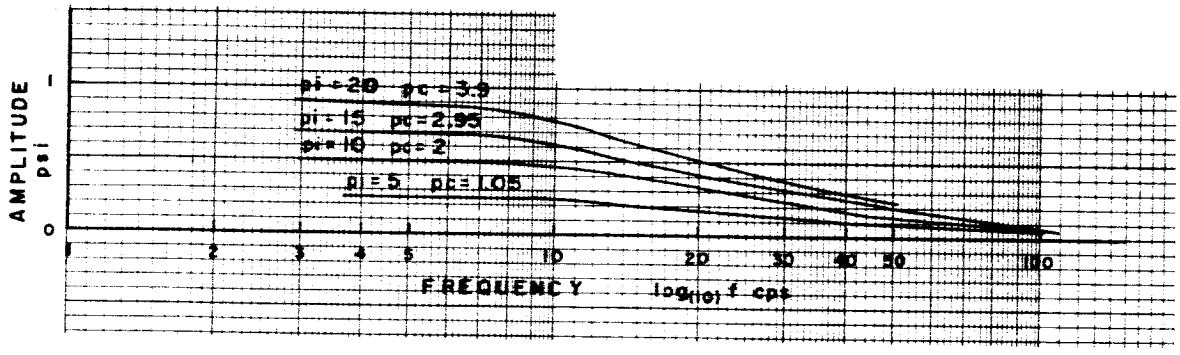

FIGURE 11. PERFORMANCE OF L. F. FLUID SIGINAL GENERATOR
(FOR NOZZLE GAP WIDTH .015 (MIN.)).

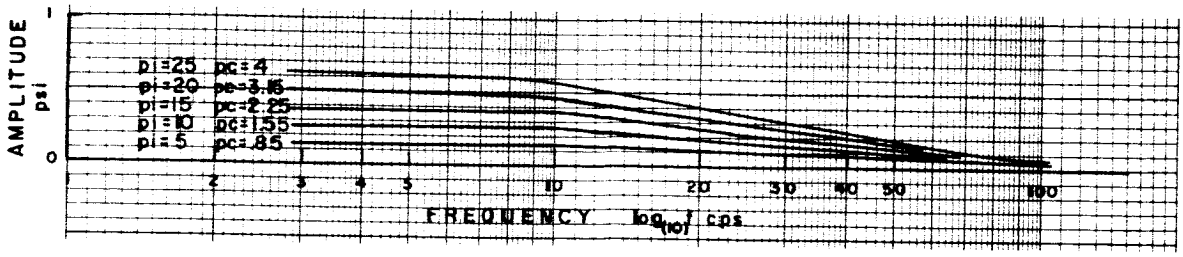

FIGURE 12. PERFORMANCE OF L.F FLUID SIGNAL GENERATOR
(FOR NOZZLE GAP WIDTH .020 (MIN.)).

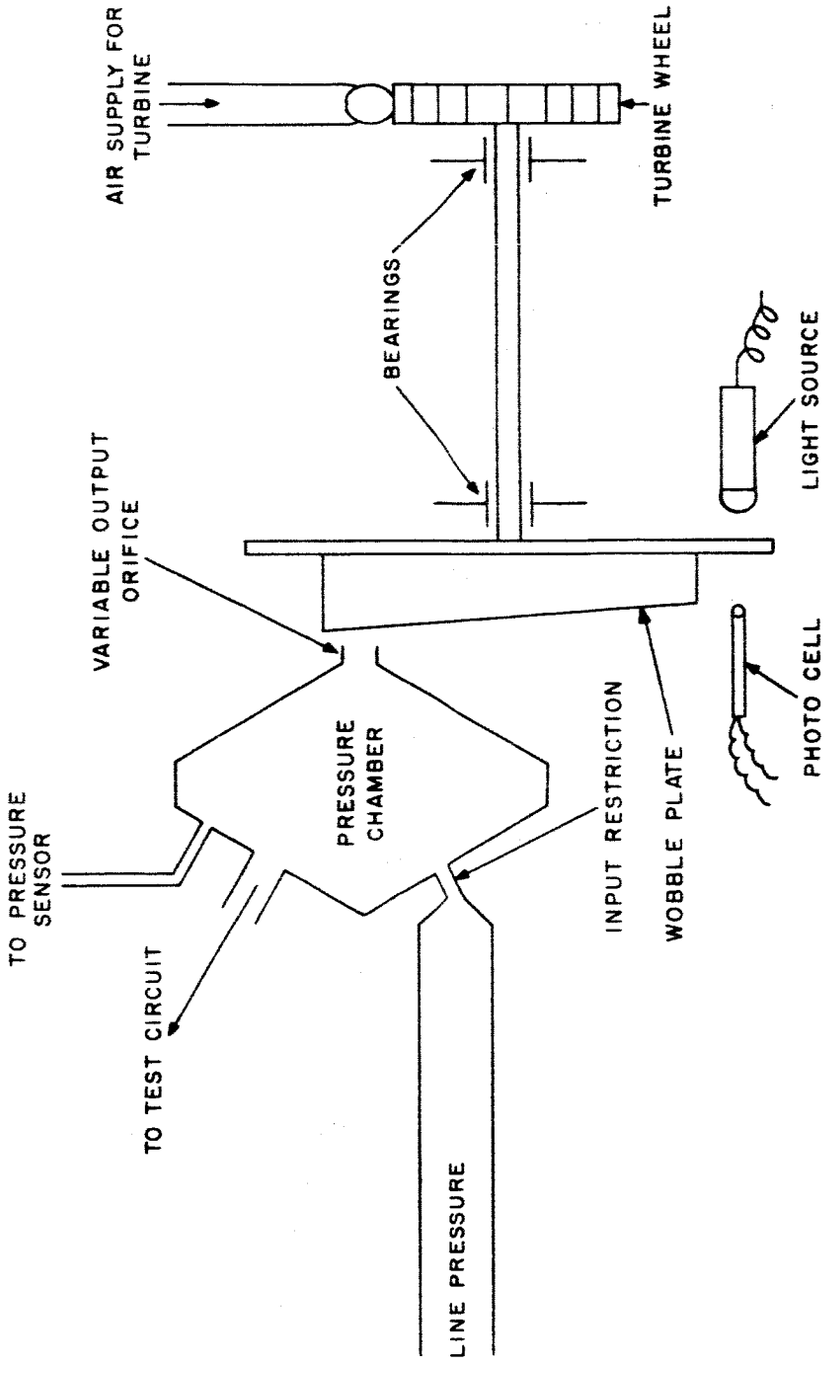

FIGURE 13.— SCHEMATIC OF FLUID SIGNAL GENERATOR

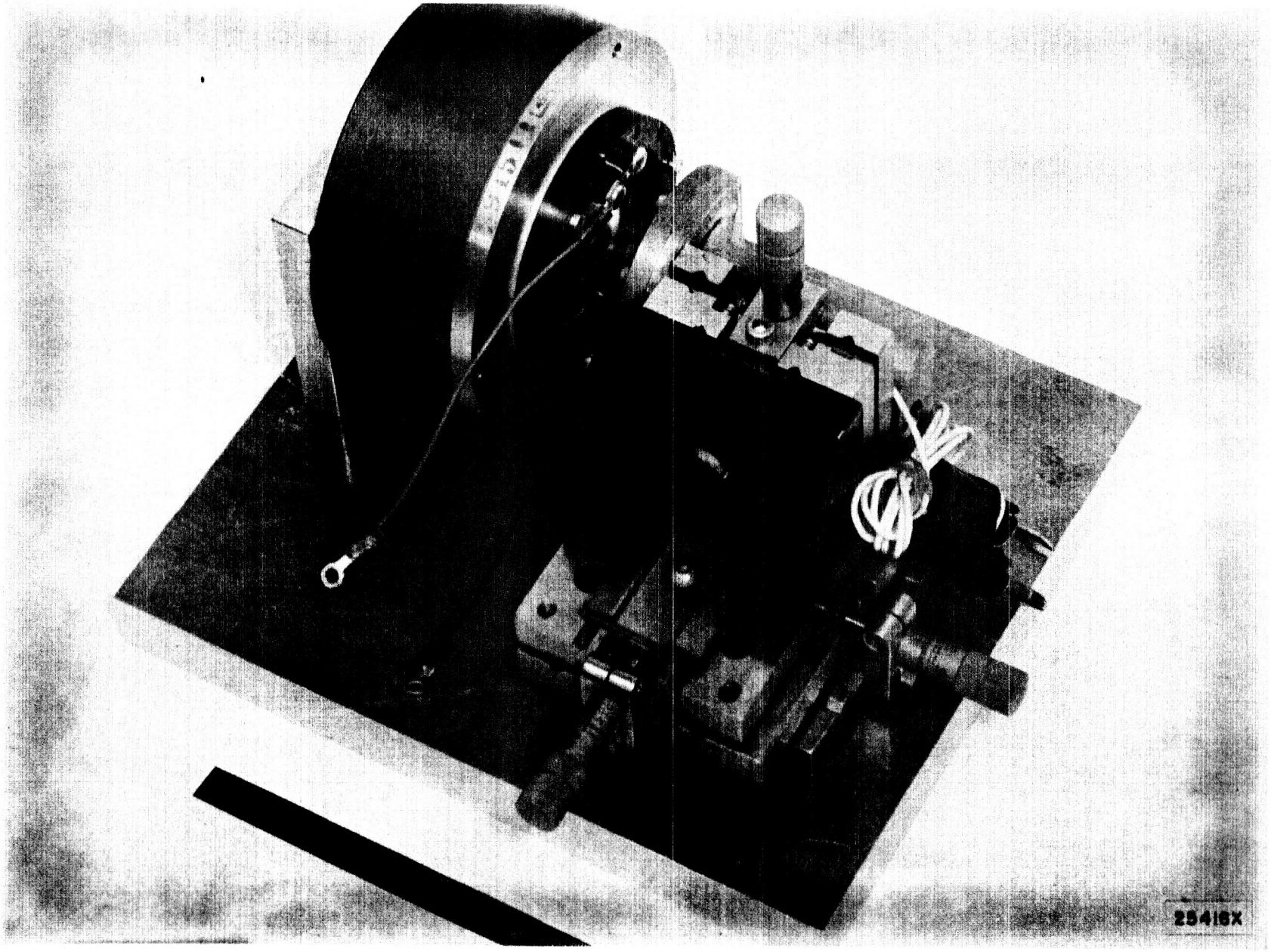

FIGURE 14. HIGH FREQUENCY SIGNAL GENERATOR MODEL. I

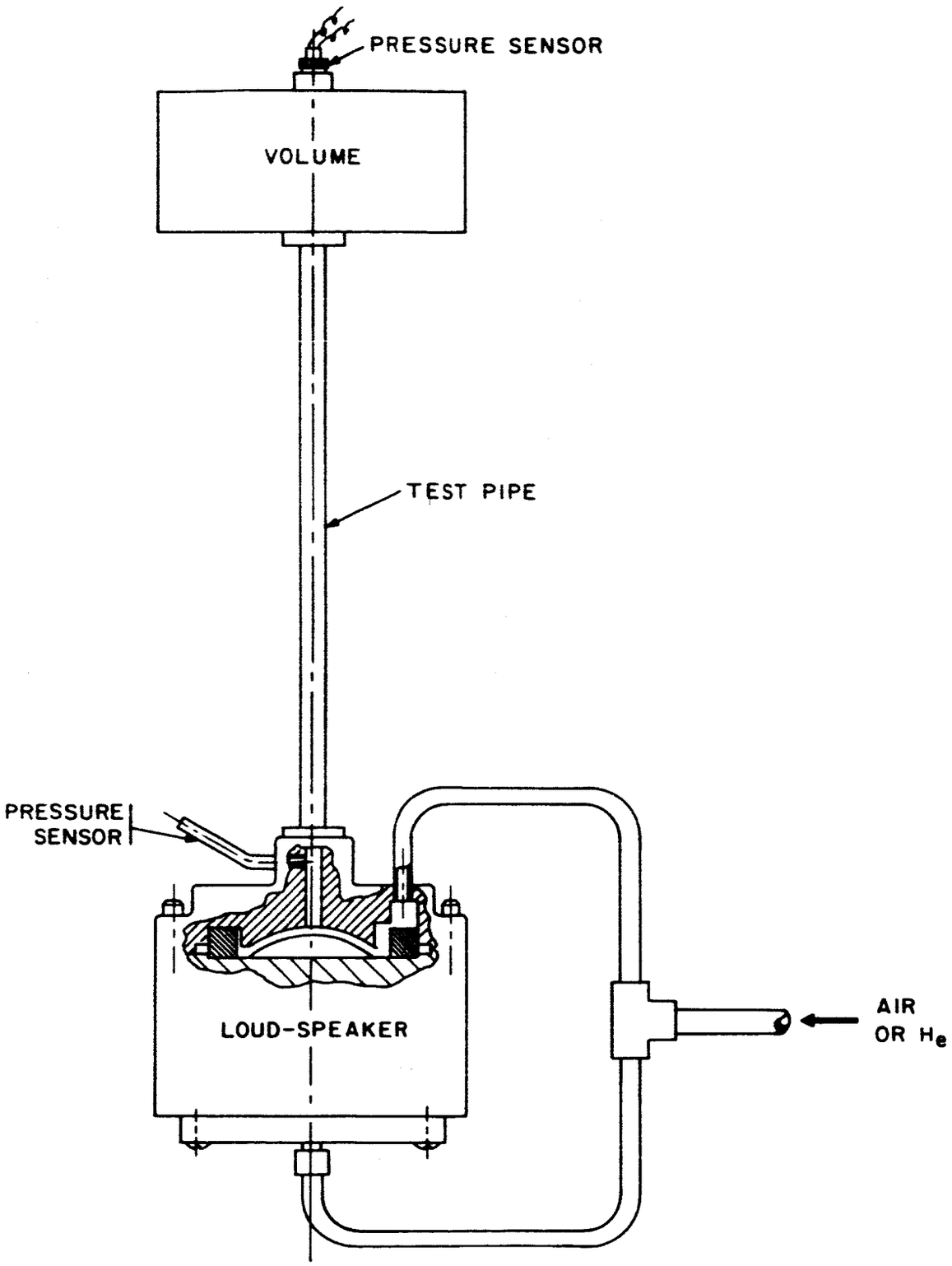

FIGURE 15. H. F. TEST ARRANGEMENT

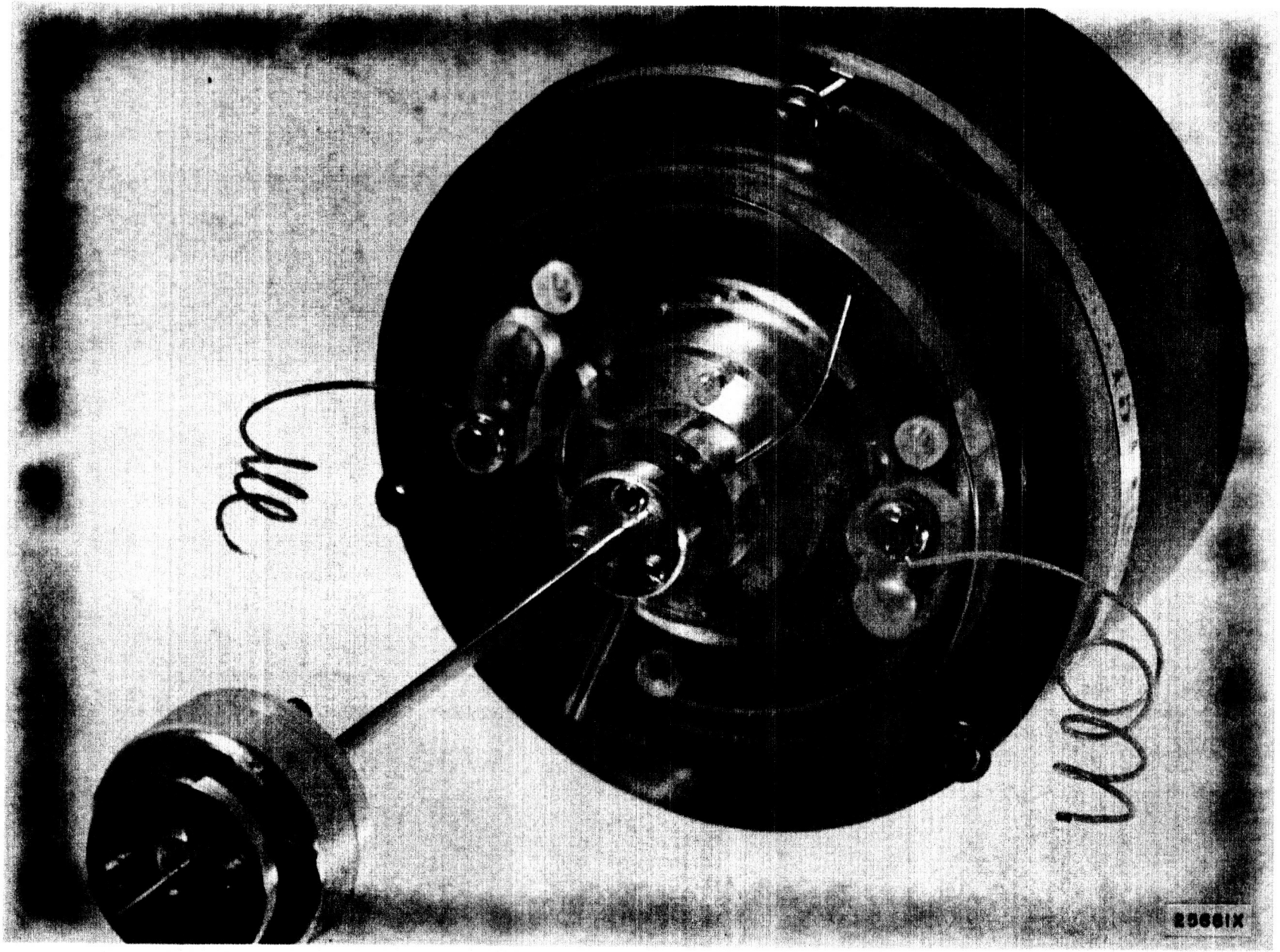

FIGURE 16. HIGH FREQUENCY SIGNAL GENERATOR MODEL 2

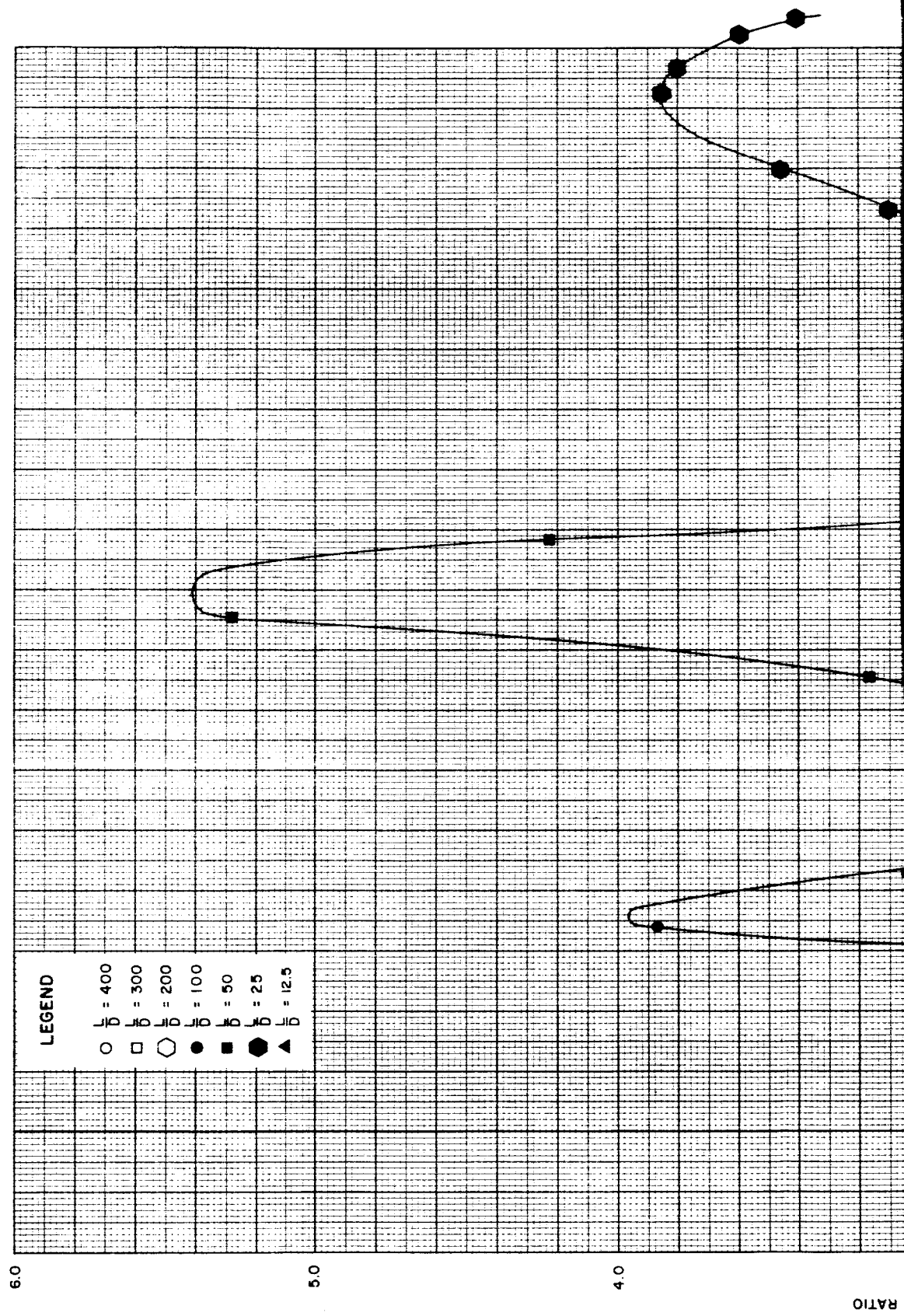

FIGURE 17. AMPLITUDE RATIO VS. FREQUENCY CURVES FOR AIR AND $\frac{V}{AL} = 6.25$

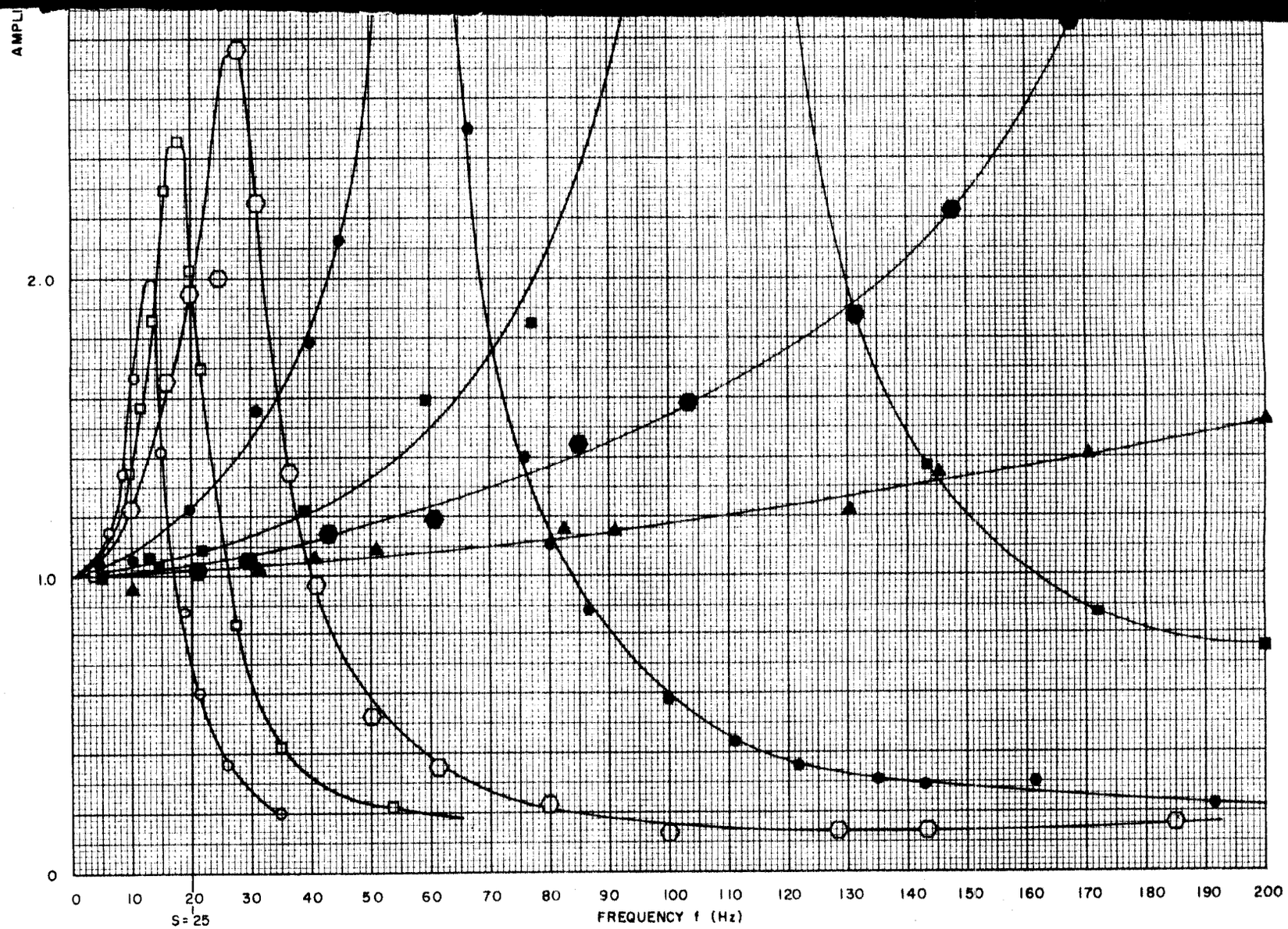
AMPLI
2.0
1.0
0
0
10
20
30
40
50
60
70
80
90
100
110
120
130
140
150
160
170
180
190
200
S=25
FREQUENCY f (Hz)

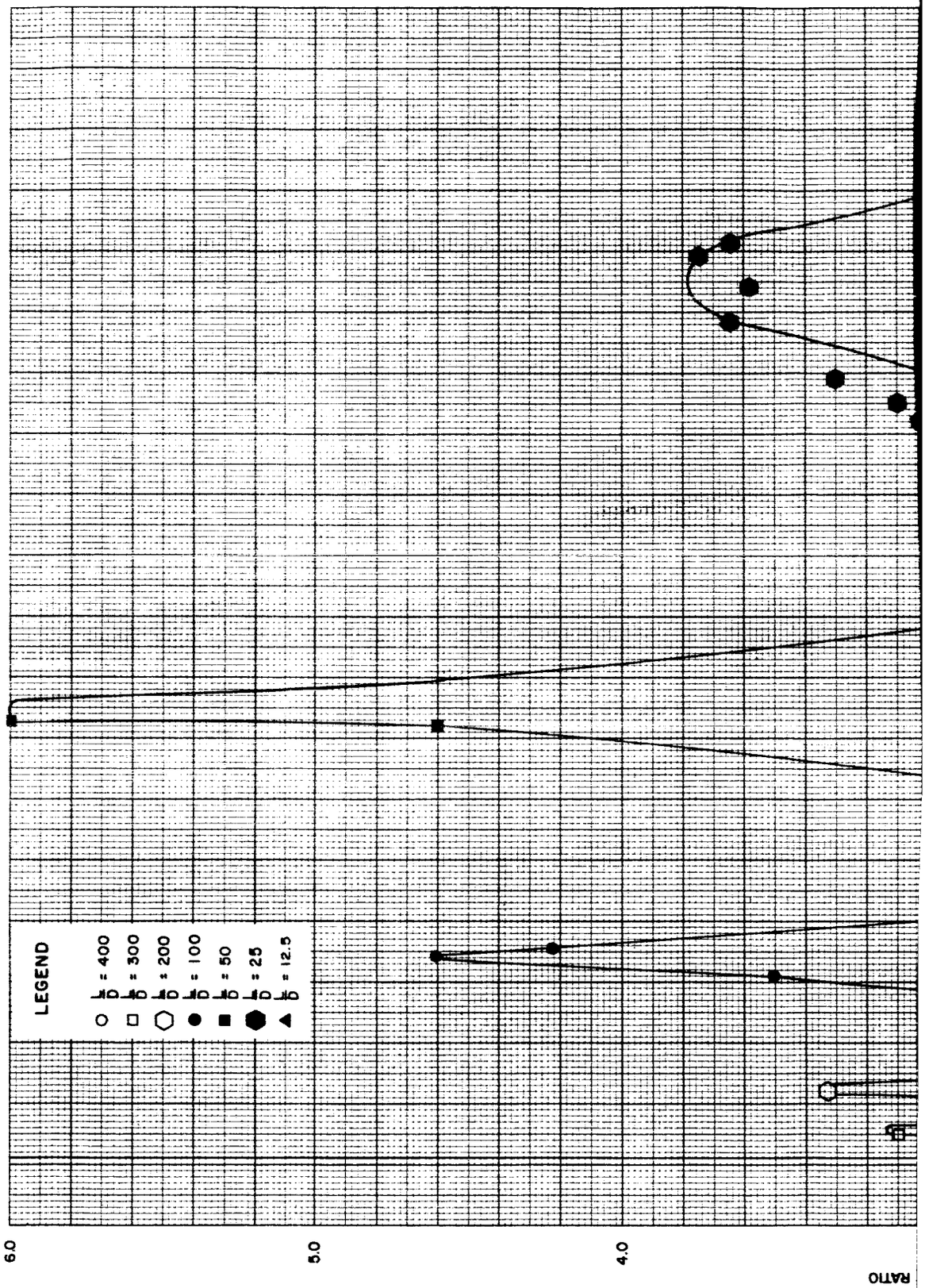

FIGURE 18. AMPLITUDE RATIO VS. FREQUENCY CURVES FOR CO_2 AND $\frac{V}{AL} = 6.25$

2

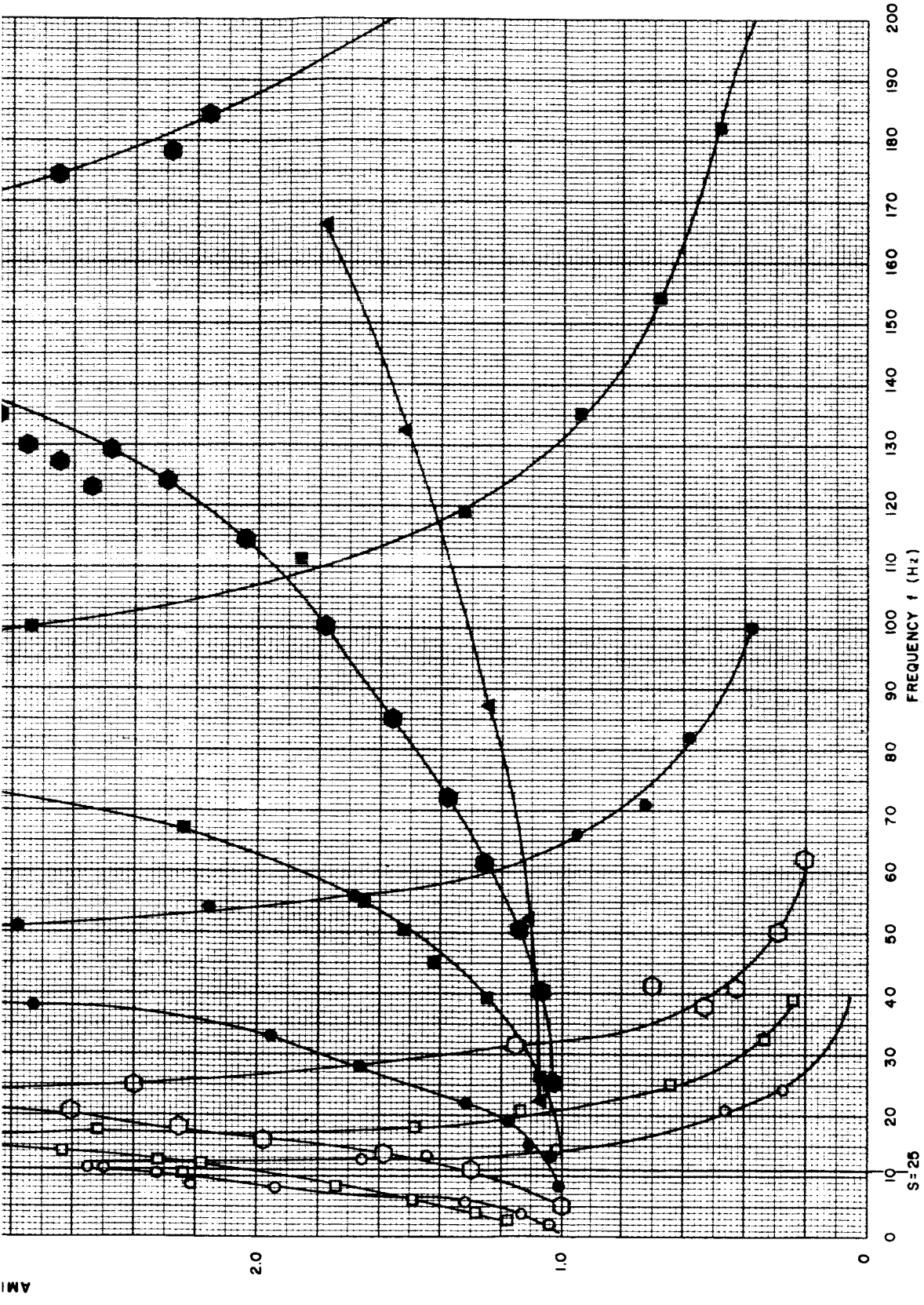
FREQUENCY f (Hz)
0
10
20
30
40
50
60
70
80
90
100
110
120
130
140
150
160
170
180
190
200
S=25
0
1.0
2.0
AMI

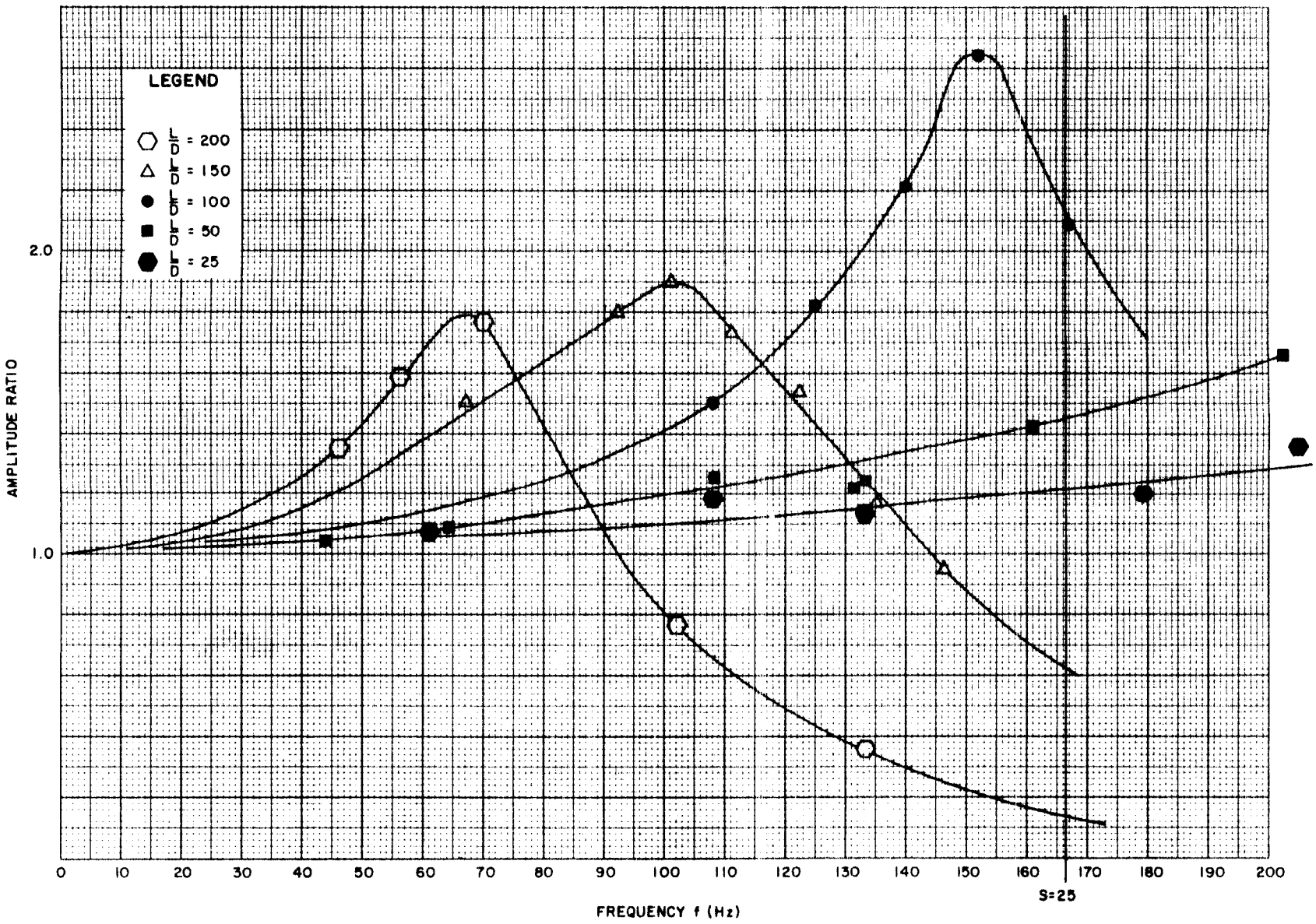

FIGURE 19. AMPLITUDE RATIO VS. FREQUENCY CURVES FOR HELIUM AND $\frac{V}{AL} = 6.25$

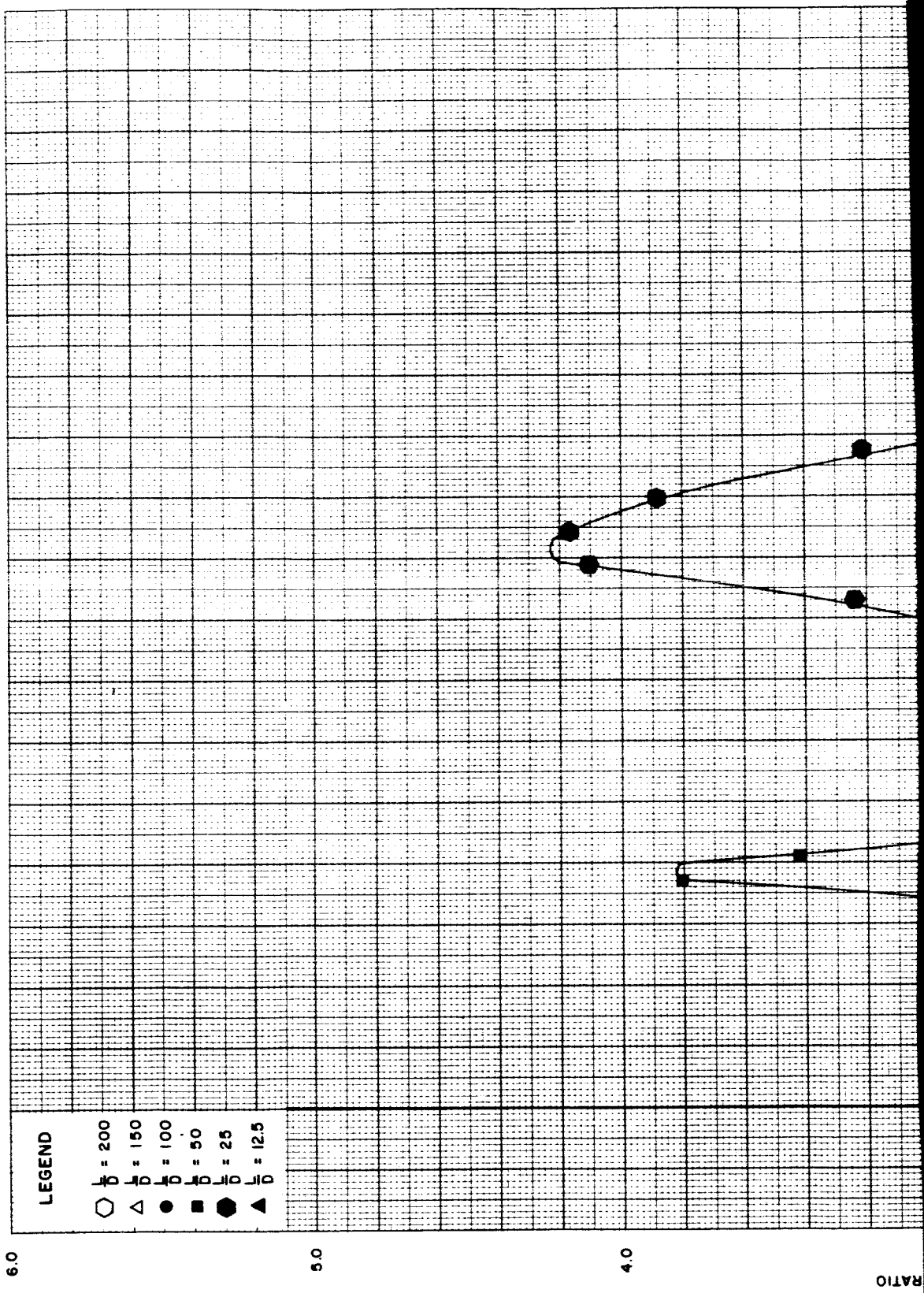

FIGURE 20. AMPLITUDE RATIO VS. FREQUENCY CURVES FOR AIR AND $\frac{V}{AL} = 25$

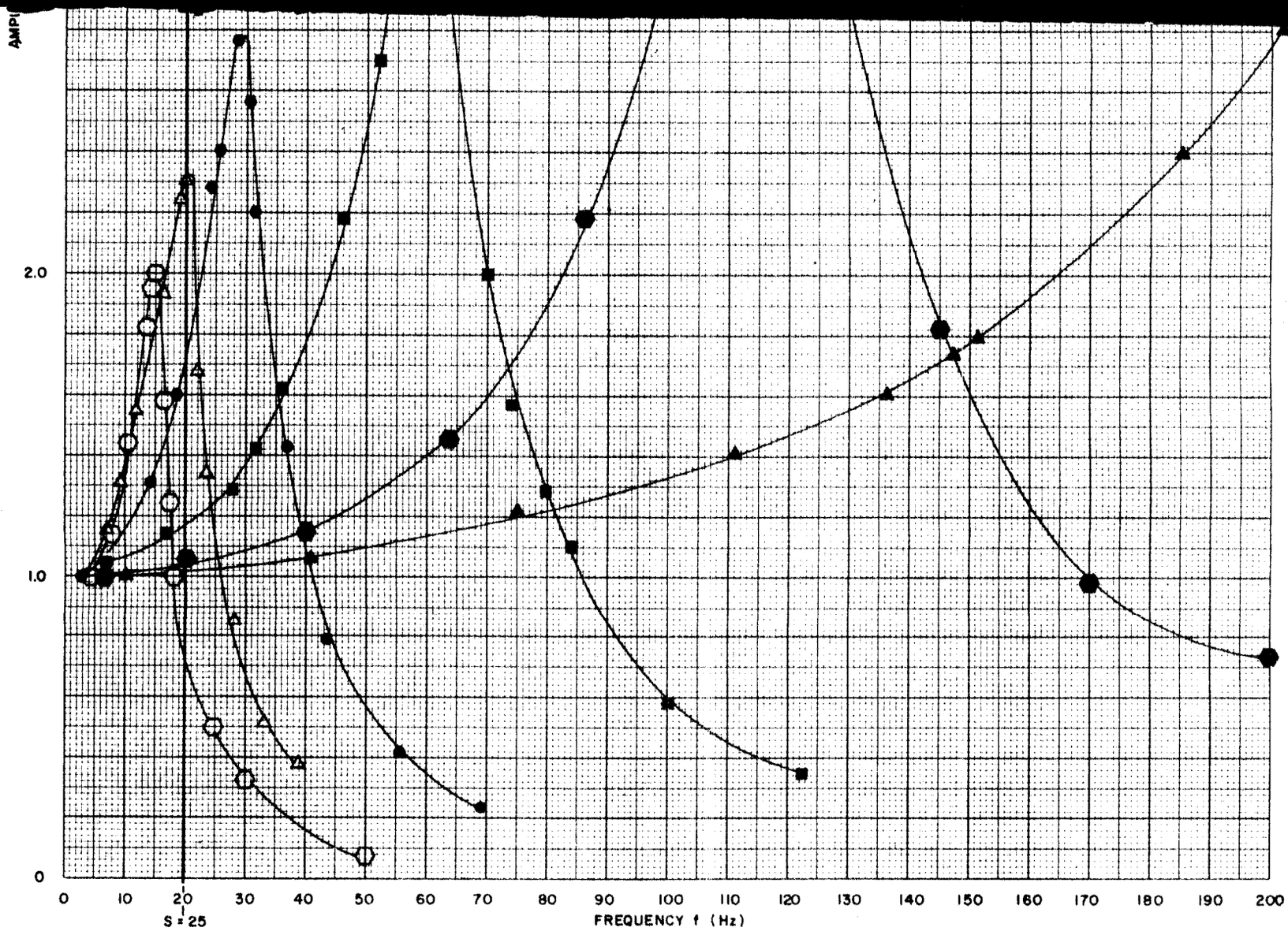
AMPL
2.0
1.0
0
0
10
20
30
40
50
60
70
80
90
100
110
120
130
140
150
160
170
180
190
200
S = 25
FREQUENCY f (Hz)

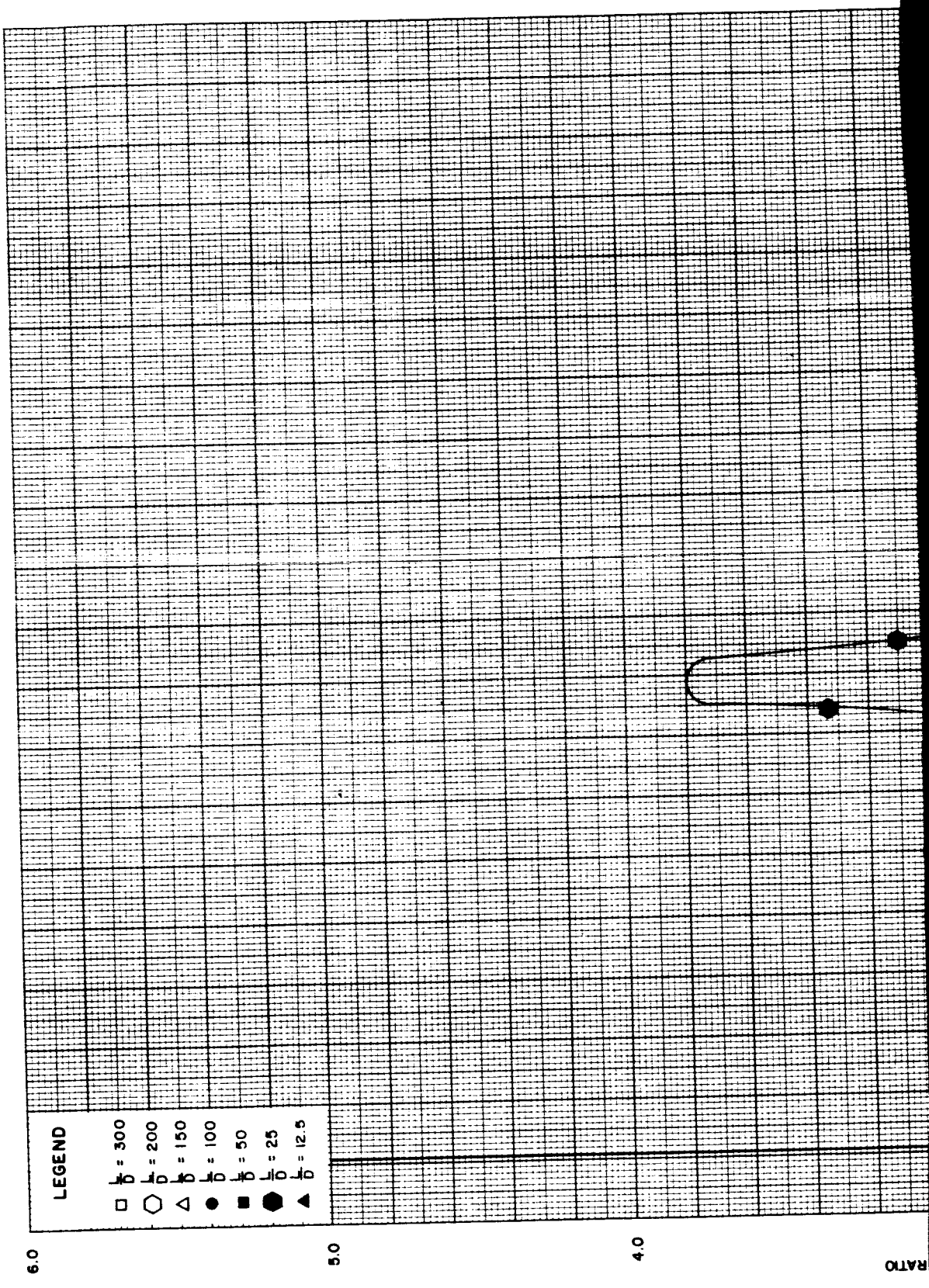

FIGURE 21. AMPLITUDE RATIO VS. FREQUENCY CURVES FOR CO_2 AND $\frac{V}{AL} = 25$

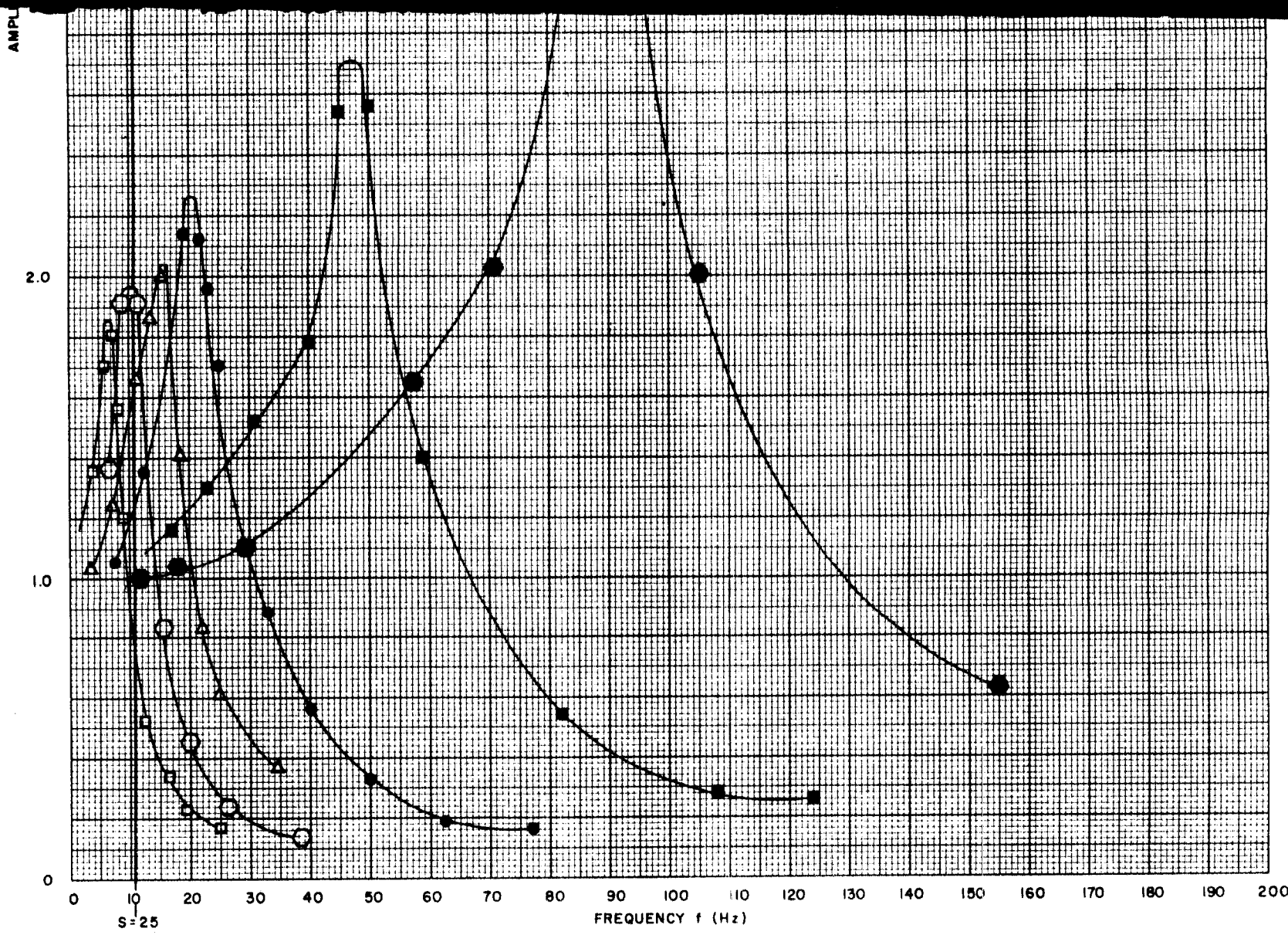
AMPL
2.0
1.0
0
0
10
20
30
40
50
60
70
80
90
100
110
120
130
140
150
160
170
180
190
200
S=25
FREQUENCY f (Hz)

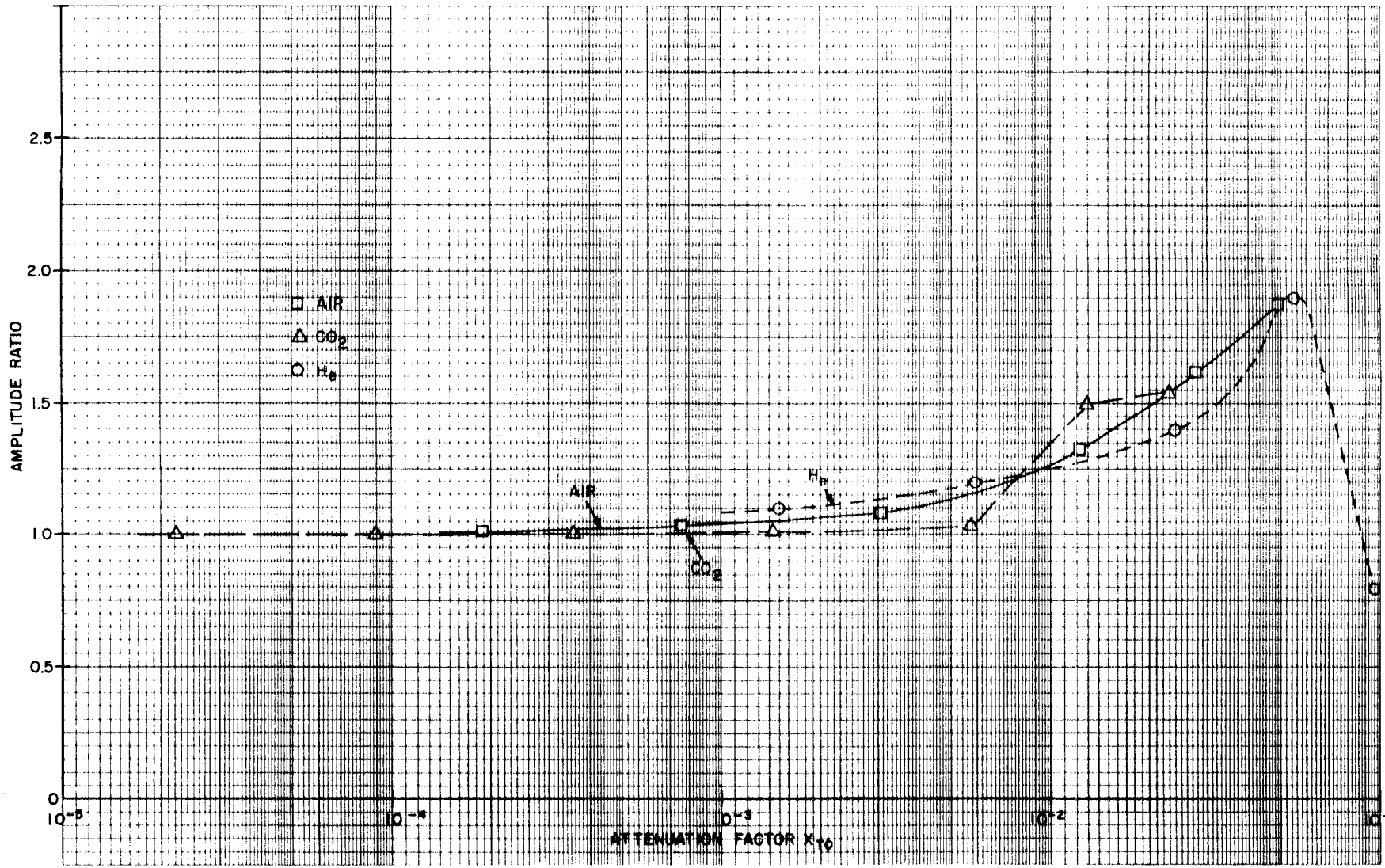

FIGURE 22. AMPLITUDE RATIO VS. ATTENUATION FACTOR FOR S=15 AND $\frac{V}{AL}$ = 6.25

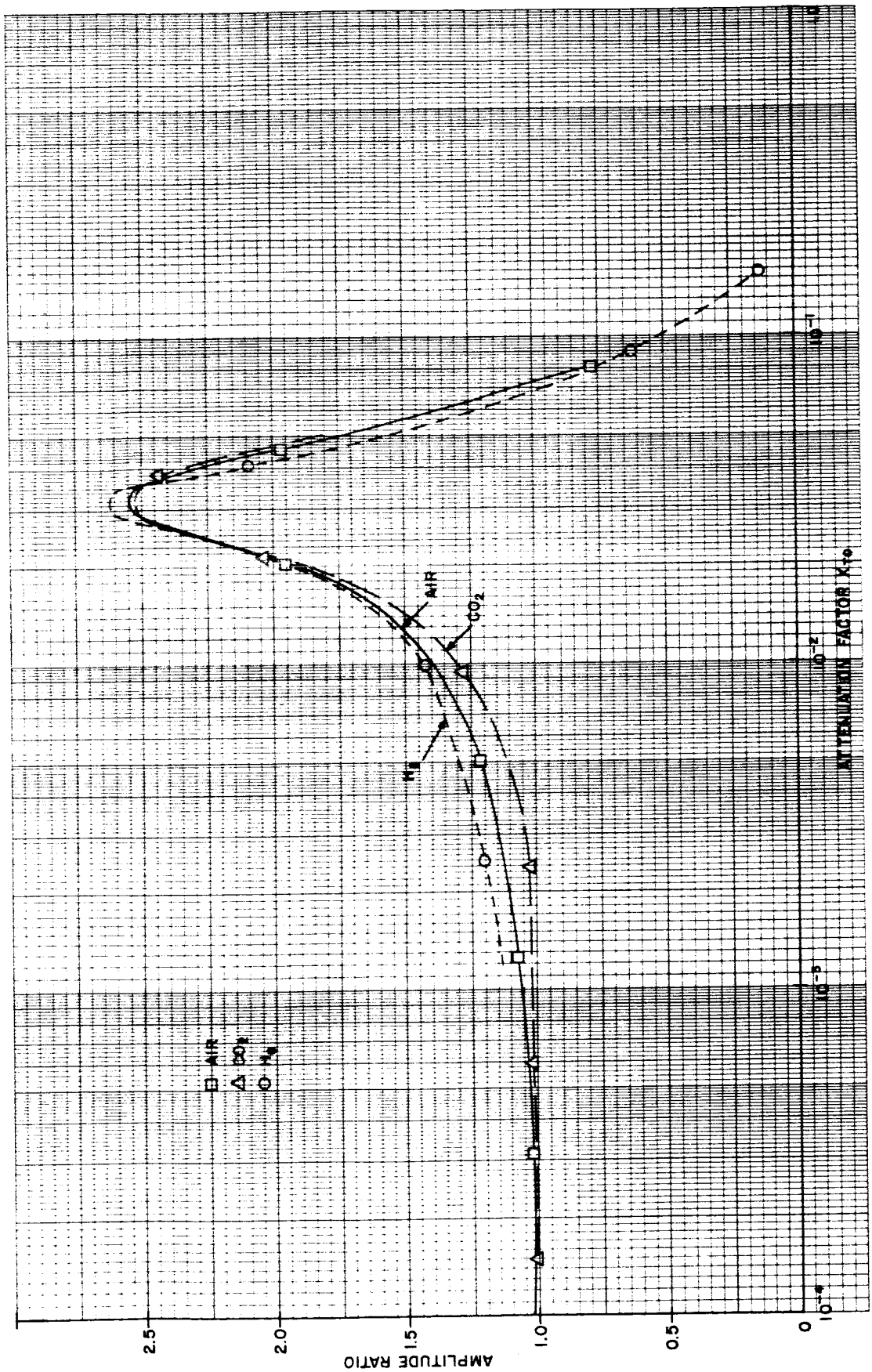

FIGURE 23. AMPLITUDE RATIO VS. ATTENUATION FACTOR FOR S=25 AND $\frac{V}{AL}$ = 6.25.

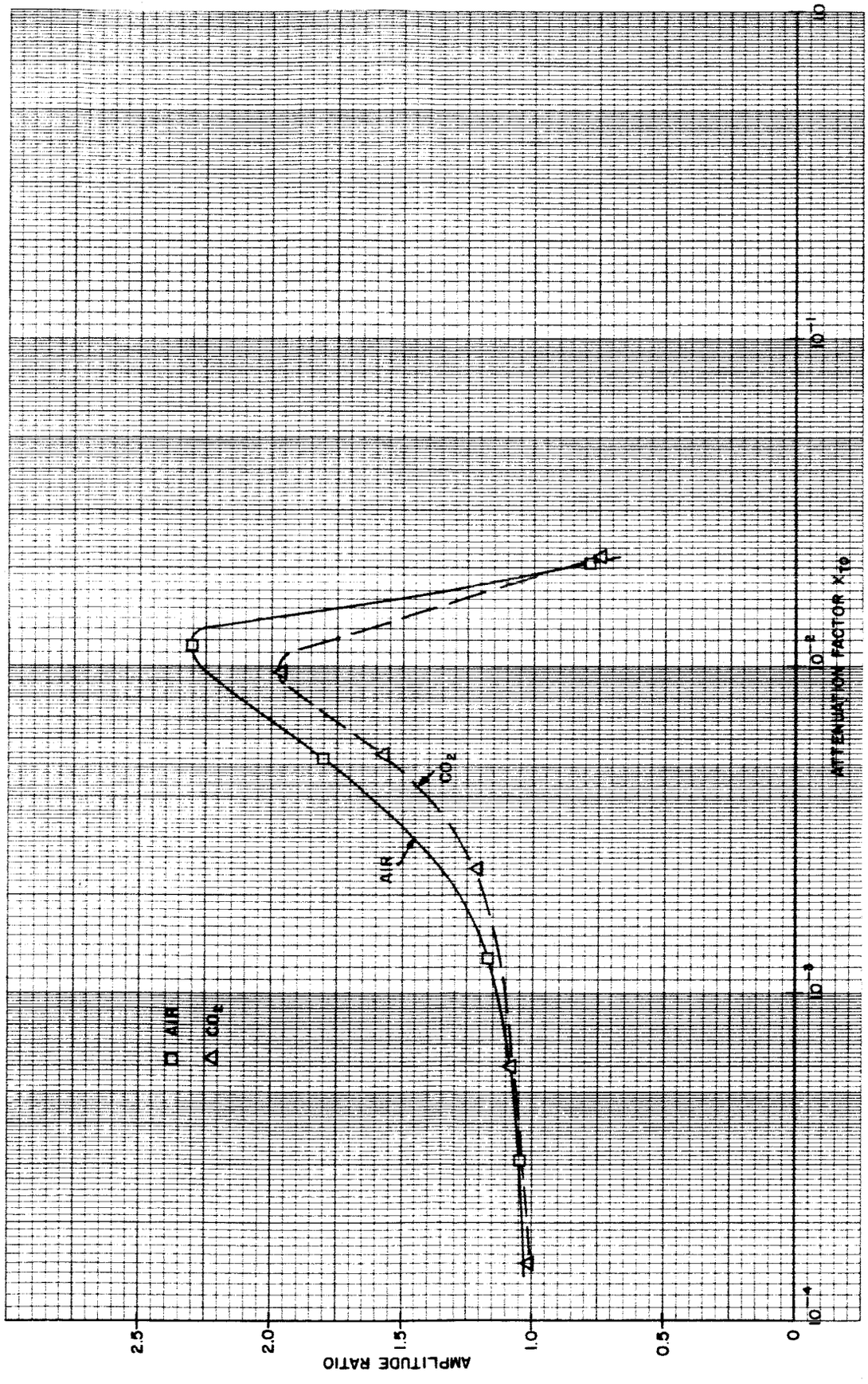

FIGURE 24. AMPLITUDE RATIO VS. ATTENUATION FACTOR FOR S=25 AND $\frac{V}{AL}$ =25.

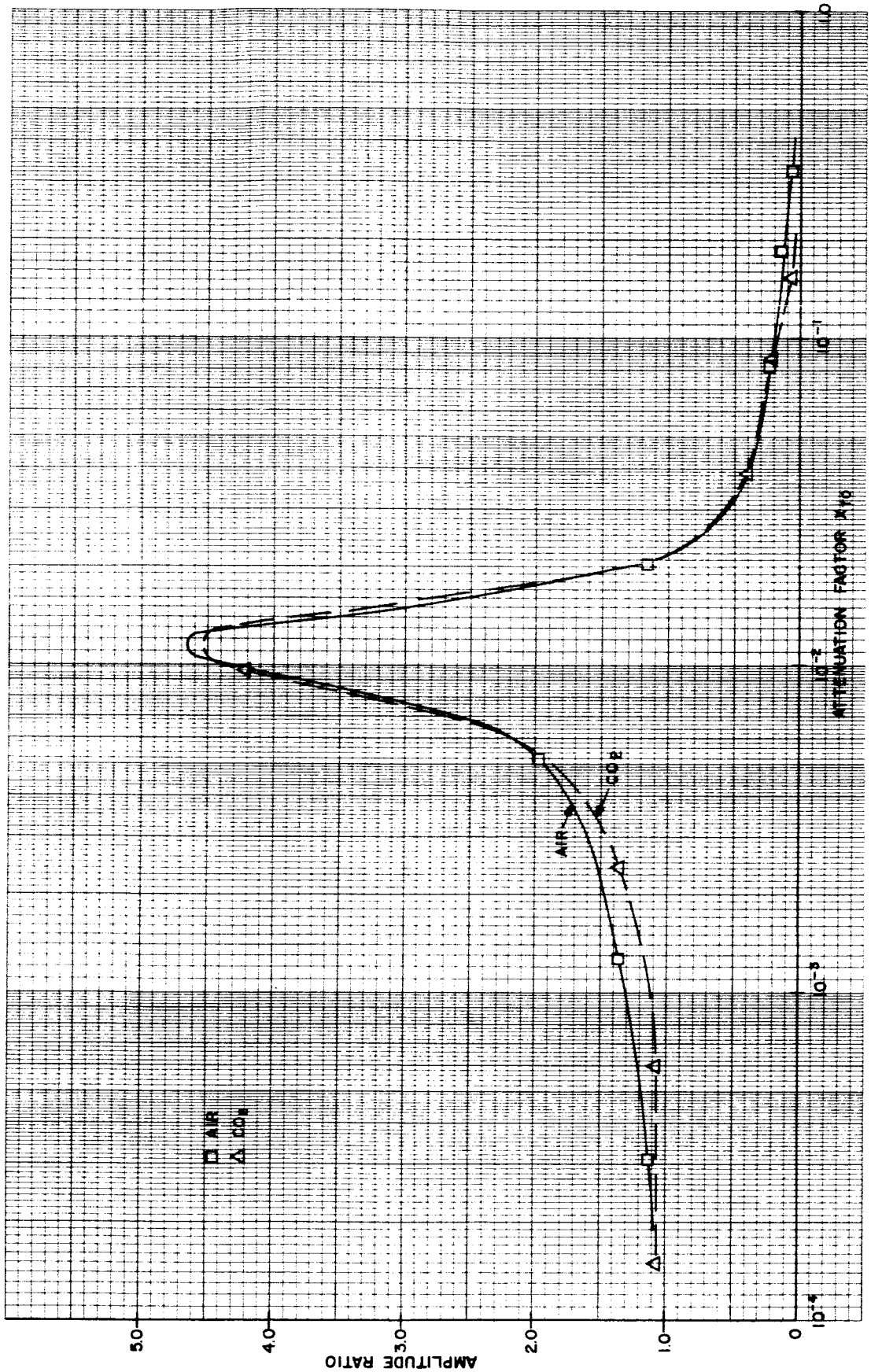

FIGURE 25. AMPLITUDE RATIO VS. ATTENUATION FACTOR FOR S=100 AND $\frac{V}{AL}$ = 6.25.

OSCILLOSCOPE PICTURES OF INPUT AND OUTPUT PRESSURE OF PASSIVE CIRCUITS

TUBE TO TANK VOLUME RATIO 6.25

TUBE LENGTH TO DIAMETER L/D = 100

TESTED WITH AIR

CHAMBER PRESSURE 2.0 psi OR 14.6 psia AT 4200 FT. ALTITUDE

THE PRESSURE TRANSDUCERS ARE ADJUSTED TO 0.5 psi PER VOLT

THE LOWER CURVE IS THE INPUT, THE UPPER CURVE IS THE OUTPUT

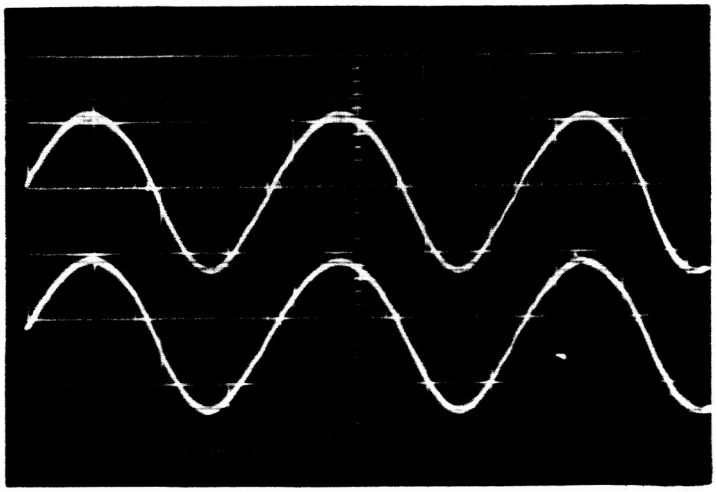

HORIZONTAL SCALE	50	ms/cm
FREQUENCY	5.26	Hz
UPPER VERT SCALE	.5	V/cm
LOWER VERT. SCALE	.5	V/cm
UPPER AMPLITUDE	.575	psi
LOWER AMPLITUDE	.55	psi
AMPLITUDE RATIO	1.04	

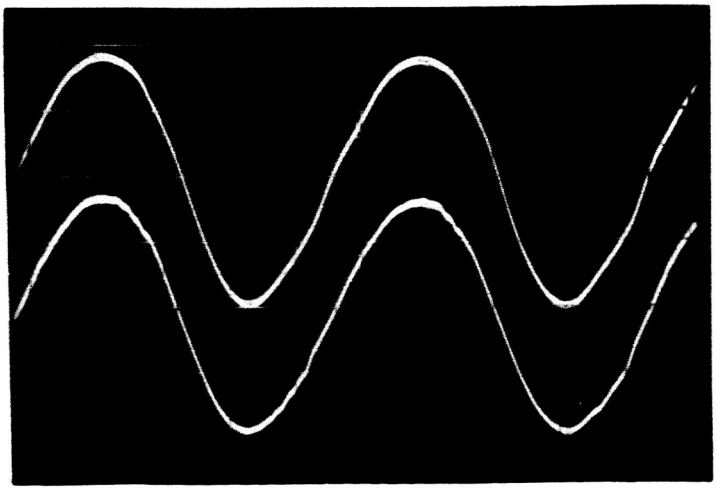

HORIZONTAL SCALE	20	ms/cm
FREQUENCY	10.4	Hz
UPPER VERT. SCALE	.2	V/cm
LOWER VERT. SCALE	.2	V/cm
UPPER AMPLITUDE	.375	psi
LOWER AMPLITUDE	.35	psi
AMPLITUDE RATIO	1.07	

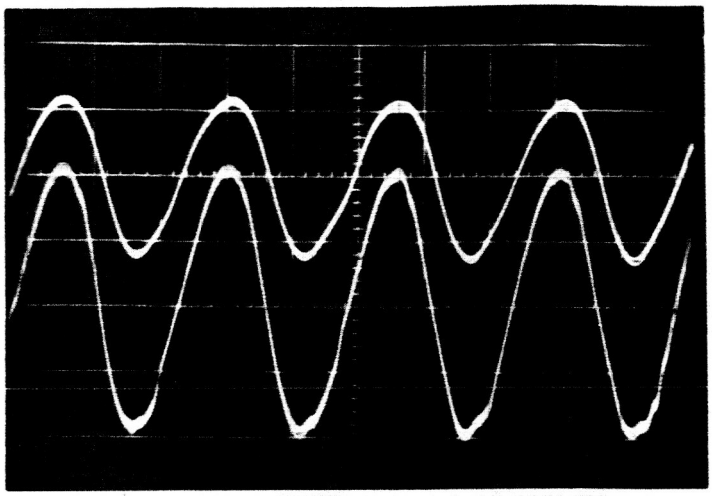

HORIZONTAL SCALE	20	ms/cm
FREQUENCY	19.6	Hz
UPPER VERT. SCALE	.2	V/cm
LOWER VERT. SCALE	.1	V/cm
UPPER AMPLITUDE	.235	psi
LOWER AMPLITUDE	.195	psi
AMPLITUDE RATIO	1.2	

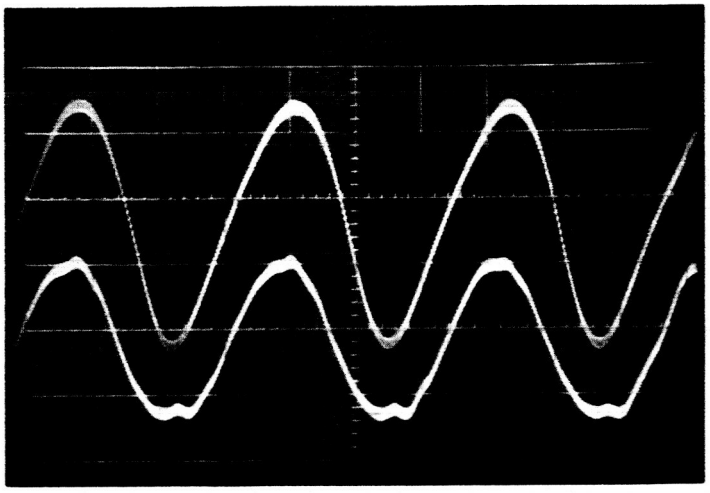

HORIZONTAL SCALE	10	ms/cm
FREQUENCY	30.7	Hz
UPPER VERT. SCALE	.1	V/cm
LOWER VERT. SCALE	.1	V/cm
UPPER AMPLITUDE	.18	psi
LOWER AMPLITUDE	.115	psi
AMPLITUDE RATIO	1.56	

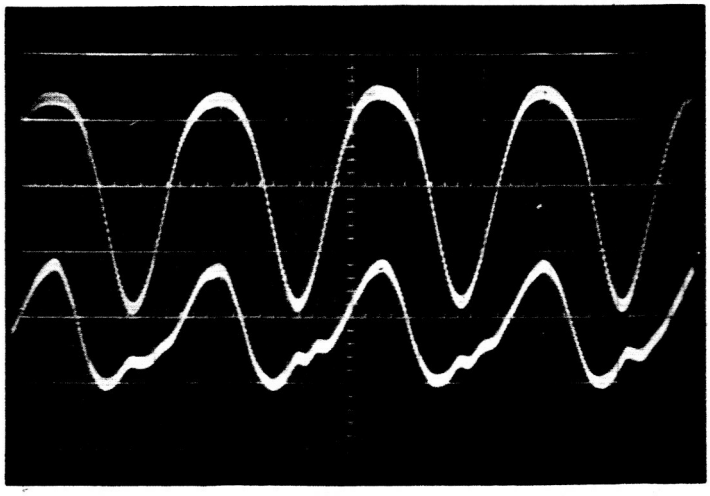

HORIZONTAL SCALE	10	ms/cm
FREQUENCY	40.8	Hz
UPPER VERT. SCALE	.1	V/cm
LOWER VERT. SCALE	.1	V/cm
UPPER AMPLITUDE	.16	psi
LOWER AMPLITUDE	.0875	psi
AMPLITUDE RATIO	1.93	

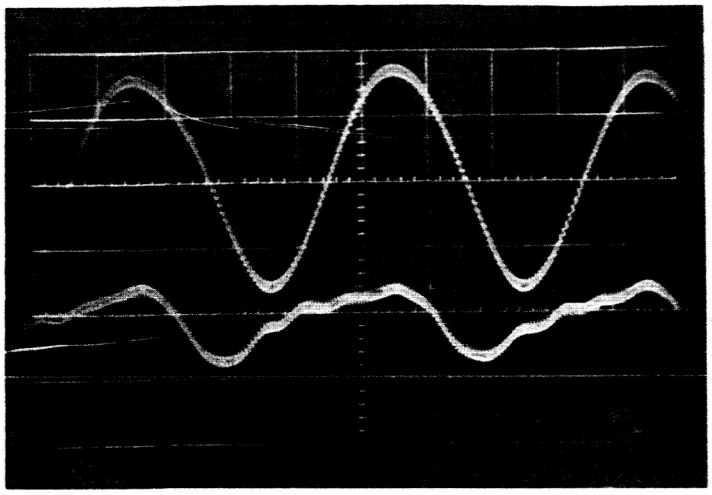

HORIZONTAL SCALE	5	ms/cm
FREQUENCY	51.2	Hz
UPPER VERT. SCALE	.1	V/cm
LOWER VERT. SCALE	.1	V/cm
UPPER AMPLITUDE	.16	psi
LOWER AMPLITUDE	.05	psi
AMPLITUDE RATIO	3.2	

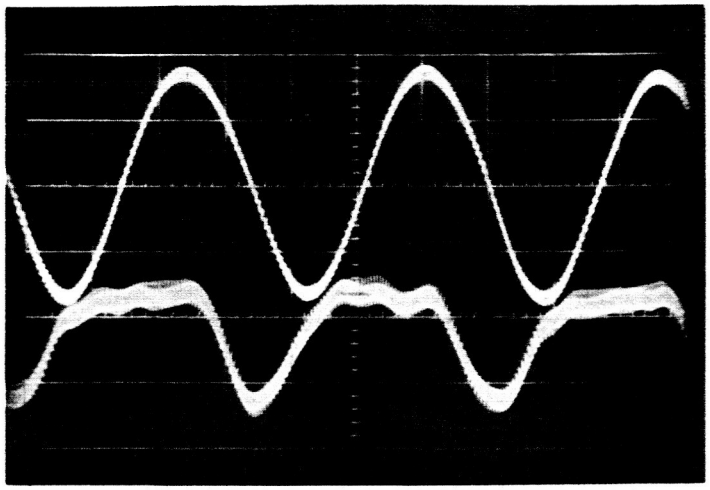

HORIZONTAL SCALE	5	ms/cm
FREQUENCY	55	Hz
UPPER VERT. SCALE	.1	V/cm
LOWER VERT. SCALE	.05	V/cm
UPPER AMPLITUDE	.167	psi
LOWER AMPLITUDE	.041	psi
AMPLITUDE RATIO	4.06	

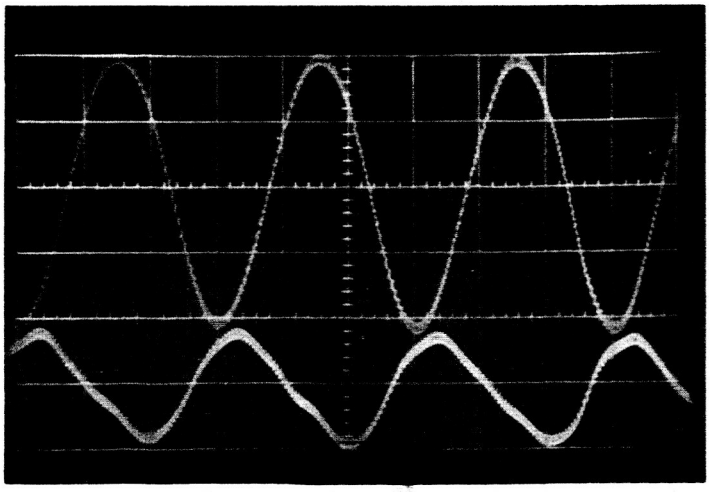

HORIZONTAL SCALE	5	ms/cm
FREQUENCY	66.5	Hz
UPPER VERT. SCALE	.1	V/cm
LOWER VERT. SCALE	.1	V/cm
UPPER AMPLITUDE	.20	psi
LOWER AMPLITUDE	.08	psi
AMPLITUDE RATIO	2.5	

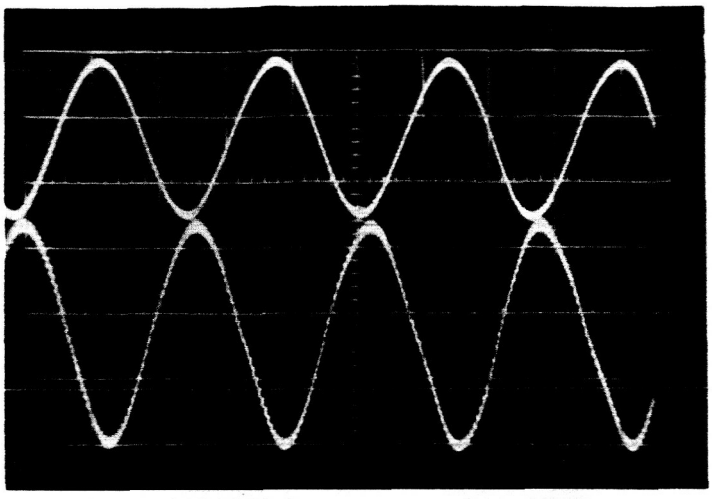

HORIZONTAL SCALE	5	ms/cm
FREQUENCY	77	Hz
UPPER VERT. SCALE	.2	V/cm
LOWER VERT. SCALE	.1	V/cm
UPPER AMPLITUDE	.22	psi
LOWER AMPLITUDE	.167	psi
AMPLITUDE RATIO	1.31	

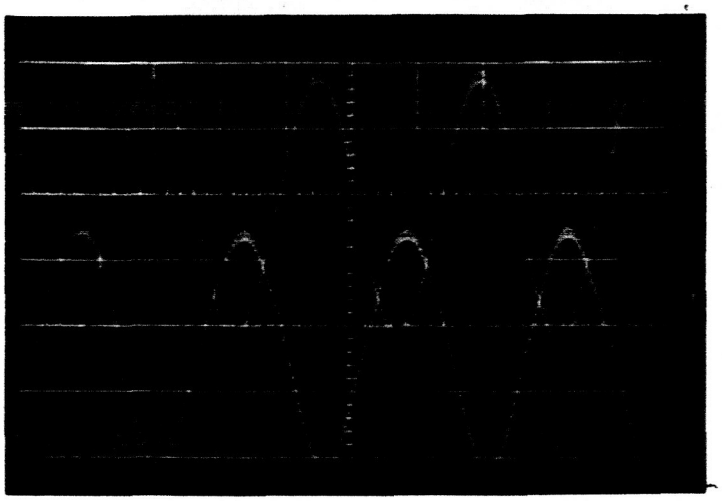

HORIZONTAL SCALE	5	ms/cm
FREQUENCY	81.5	Hz
UPPER VERT. SCALE	.1	V/cm
LOWER VERT. SCALE	.1	V/cm
UPPER AMPLITUDE	.198	psi
LOWER AMPLITUDE	.178	psi
AMPLITUDE RATIO	1.11	

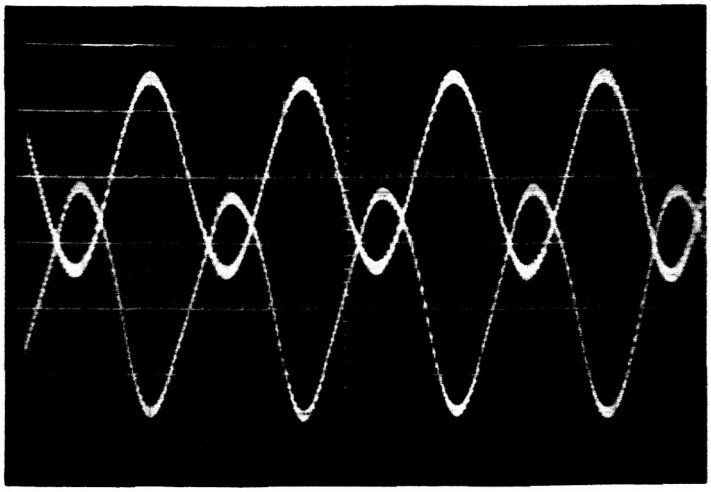

HORIZONTAL SCALE	5	ms/cm
FREQUENCY	87	Hz
UPPER VERT. SCALE	.1	V/cm
LOWER VERT. SCALE	.1	V/cm
UPPER AMPLITUDE	.145	psi
LOWER AMPLITUDE	.17	psi
AMPLITUDE RATIO	.85	

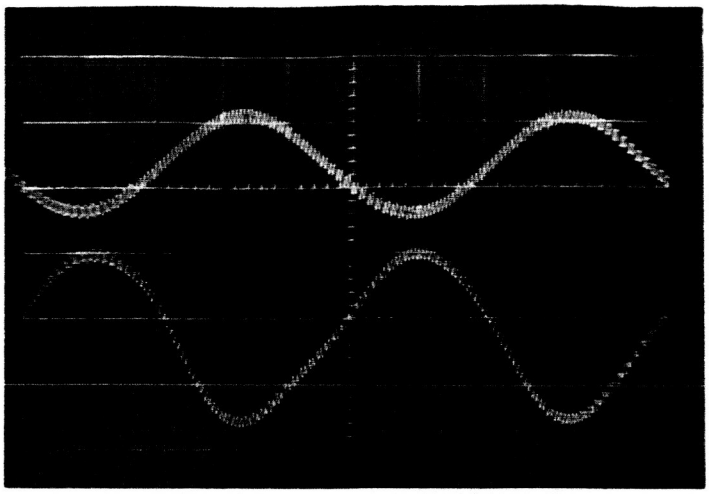

HORIZONTAL SCALE	2	ms/cm
FREQUENCY	100	Hz
UPPER VERT. SCALE	.1	V/cm
LOWER VERT. SCALE	.1	V/cm
UPPER AMPLITUDE	.075	psi
LOWER AMPLITUDE	.125	psi
AMPLITUDE RATIO	.6	

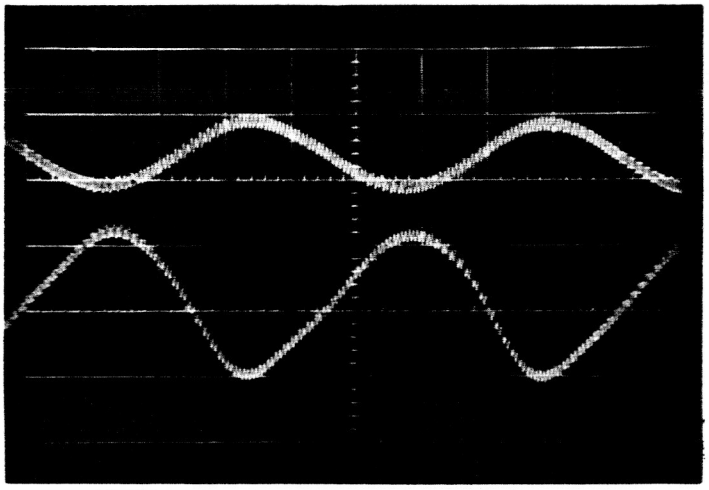

HORIZONTAL SCALE	2	ms/cm
FREQUENCY	111	Hz
UPPER VERT. SCALE	.1	V/cm
LOWER VERT. SCALE	.1	V/cm
UPPER AMPLITUDE	.05	psi
LOWER AMPLITUDE	.108	psi
AMPLITUDE RATIO	.46	

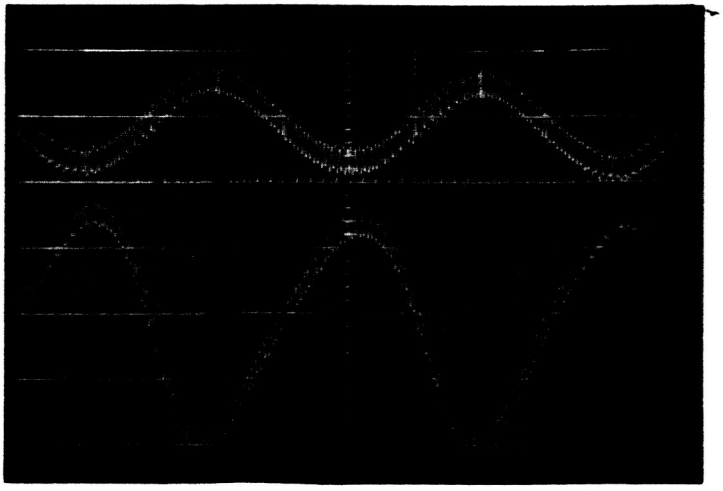

HORIZONTAL SCALE	2	ms/cm
FREQUENCY	125	Hz
UPPER VERT. SCALE	.05	V/cm
LOWER VERT. SCALE	.05	V/cm
UPPER AMPLITUDE	.03	psi
LOWER AMPLITUDE	.077	psi
AMPLITUDE RATIO	.39	

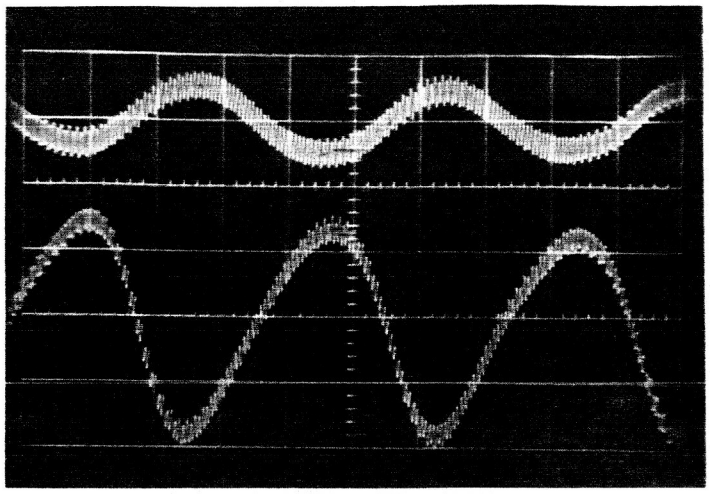

HORIZONTAL SCALE	2	ms/cm
FREQUENCY	133	Hz
UPPER VERT. SCALE	.05	V/cm
LOWER VERT. SCALE	.05	V/cm
UPPER AMPLITUDE	.0225	psi
LOWER AMPLITUDE	.051	psi
AMPLITUDE RATIO	.44	

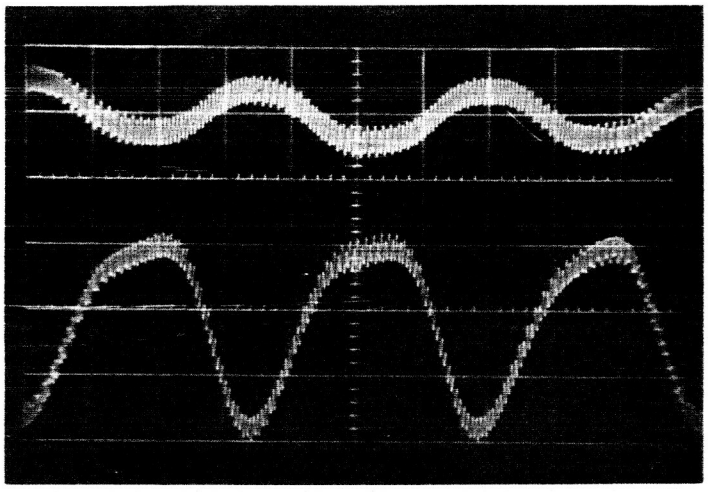

HORIZONTAL SCALE	2	ms/cm
FREQUENCY	143	Hz
UPPER VERT. SCALE	.05	V/cm
LOWER VERT. SCALE	.05	V/cm
UPPER AMPLITUDE	.02	psi
LOWER AMPLITUDE	.0675	psi
AMPLITUDE RATIO	.296	

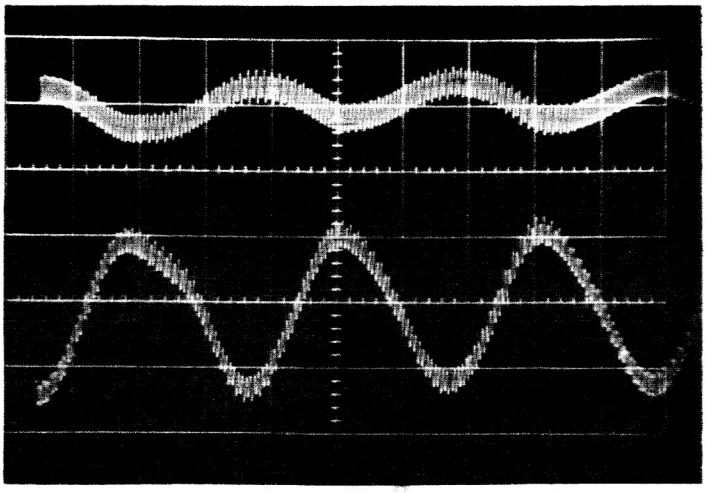

HORIZONTAL SCALE	2	ms/cm
FREQUENCY	161	Hz
UPPER VERT. SCALE	.05	V/cm
LOWER VERT. SCALE	.05	V/cm
UPPER AMPLITUDE	.015	psi
LOWER AMPLITUDE	.0575	psi
AMPLITUDE RATIO	.26	

OSCILLOSCOPE PICTURES OF INPUT AND OUTPUT PRESSURE OF PASSIVE CIRCUITS

TUBE TO TANK VOLUME RATIO 6.25

TUBE LENGTH TO DIAMETER L/D = 100

TESTED WITH CARBON DIOXIDE

CHAMBER PRESSURE 2.0 psi OR 14.6 psia AT 4200 FT. ALTITUDE

THE PRESSURE TRANSDUCERS ARE ADJUSTED TO 0.5 psi PER VOLT

THE LOWER CURVE IS THE INPUT, THE UPPER CURVE IS THE OUTPUT

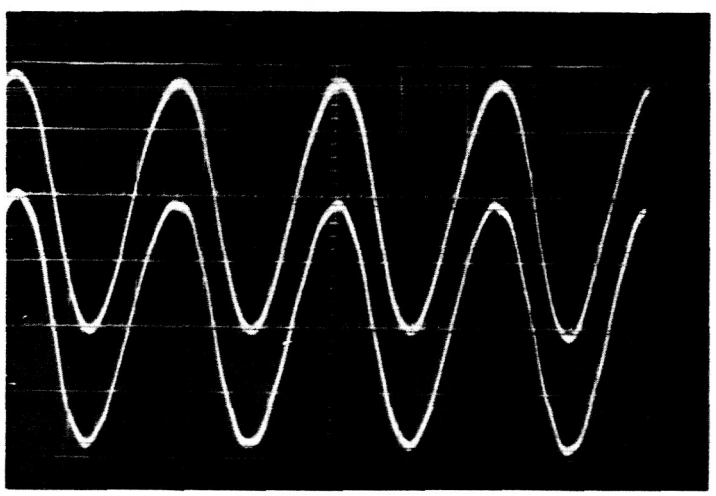

HORIZONTAL SCALE	50	ms/cm
FREQUENCY	8.2	Hz
UPPER VERT SCALE	.2	V/cm
LOWER VERT. SCALE	.2	V/cm
UPPER AMPLITUDE	.75	psi
LOWER AMPLITUDE	.74	psi
AMPLITUDE RATIO	1.01	

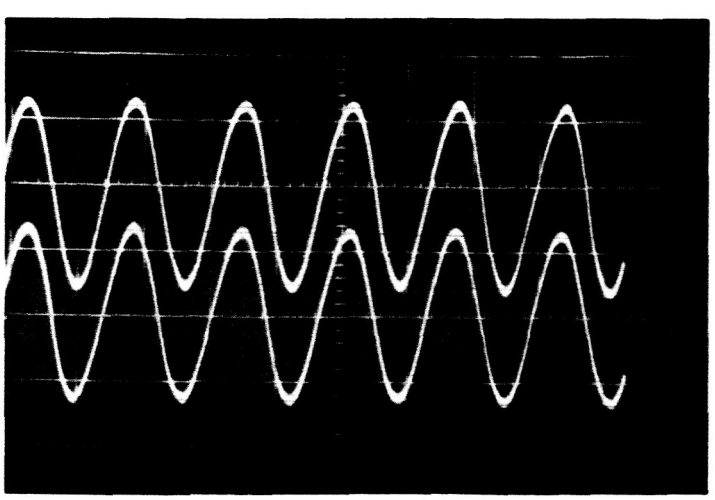

HORIZONTAL SCALE	50	ms/cm
FREQUENCY	13	Hz
UPPER VERT. SCALE	.2	V/cm
LOWER VERT. SCALE	.2	V/cm
UPPER AMPLITUDE	.54	psi
LOWER AMPLITUDE	.52	psi
AMPLITUDE RATIO	1.04	

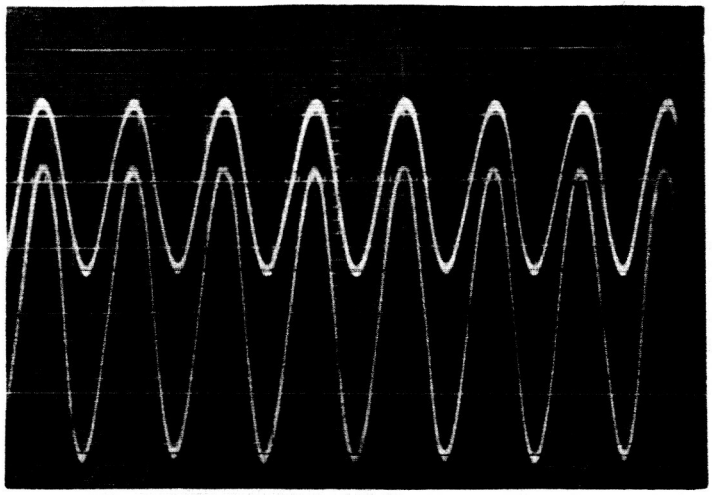

HORIZONTAL SCALE	50	ms/cm
FREQUENCY	15	Hz
UPPER VERT. SCALE	.2	V/cm
LOWER VERT. SCALE	.1	V/cm
UPPER AMPLITUDE	.51	psi
LOWER AMPLITUDE	.435	psi
AMPLITUDE RATIO	1.15	

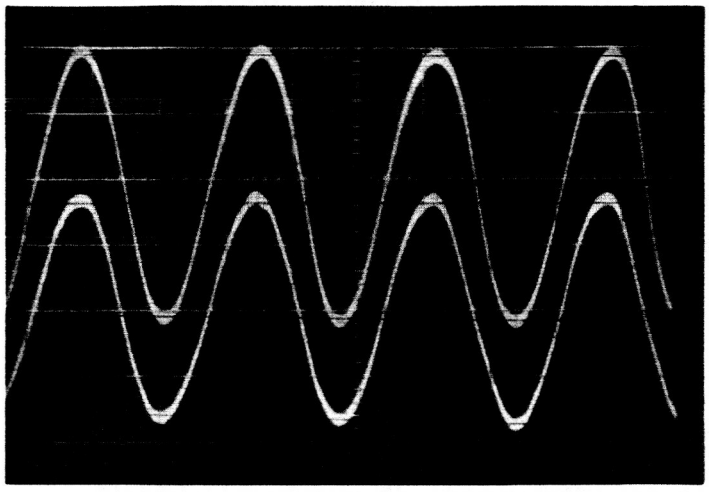

HORIZONTAL SCALE	20	ms/cm
FREQUENCY	19.2	Hz
UPPER VERT. SCALE	.1	V/cm
LOWER VERT. SCALE	.1	V/cm
UPPER AMPLITUDE	.40	psi
LOWER AMPLITUDE	.34	psi
AMPLITUDE RATIO	1.18	

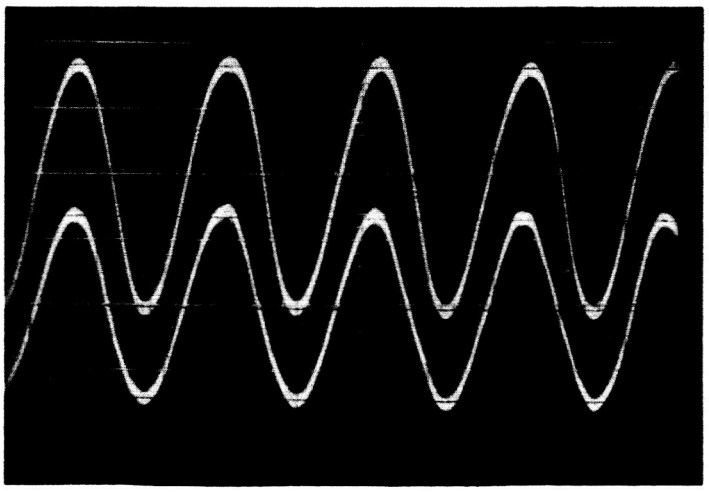

HORIZONTAL SCALE	20	ms/cm
FREQUENCY	22	Hz
UPPER VERT. SCALE	.1	V/cm
LOWER VERT. SCALE	.1	V/cm
UPPER AMPLITUDE	.37	psi
LOWER AMPLITUDE	.28	psi
AMPLITUDE RATIO	1.32	

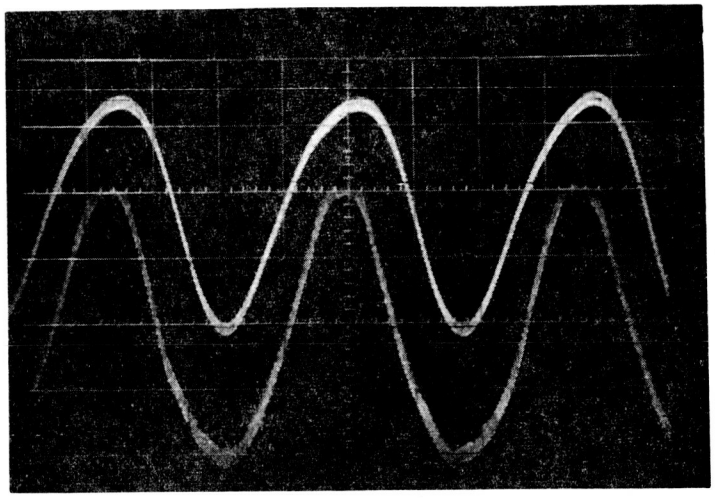

HORIZONTAL SCALE	10	ms/cm
FREQUENCY	28	Hz
UPPER VERT. SCALE	.1	V/cm
LOWER VERT. SCALE	.05	V/cm
UPPER AMPLITUDE	.345	psi
LOWER AMPLITUDE	.207	psi
AMPLITUDE RATIO	1.67	

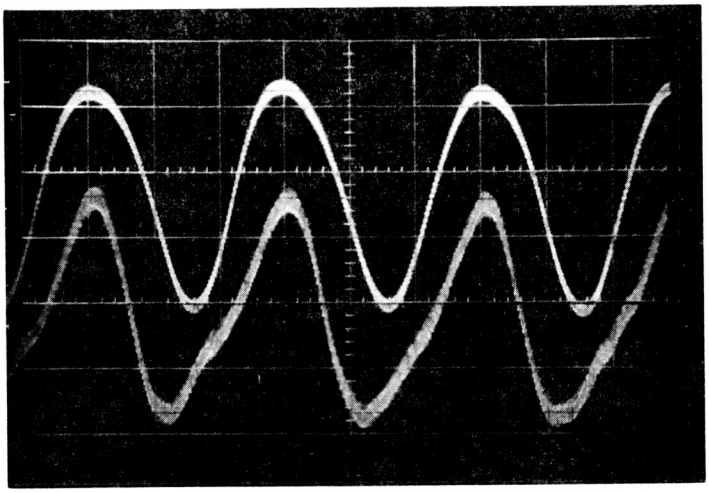

HORIZONTAL SCALE	10	ms/cm
FREQUENCY	33	Hz
UPPER VERT. SCALE	.1	V/cm
LOWER VERT. SCALE	.05	V/cm
UPPER AMPLITUDE	.322	psi
LOWER AMPLITUDE	.165	psi
AMPLITUDE RATIO	1.95	

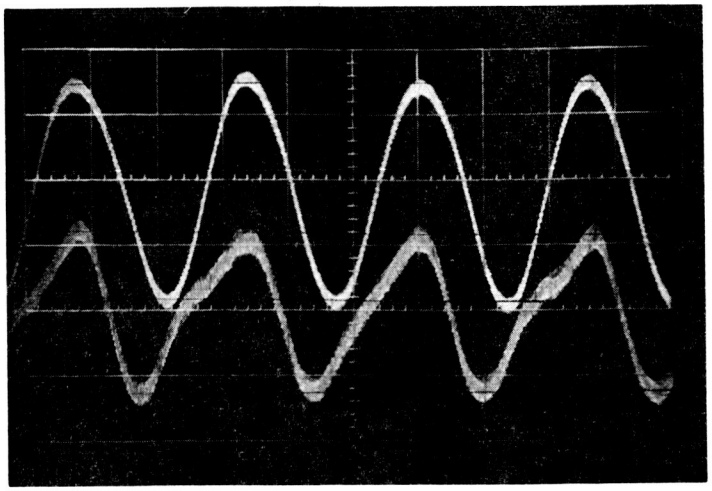

HORIZONTAL SCALE	10	ms/cm
FREQUENCY	38	Hz
UPPER VERT. SCALE	.1	V/cm
LOWER VERT. SCALE	.05	V/cm
UPPER AMPLITUDE	.332	psi
LOWER AMPLITUDE	.1235	psi
AMPLITUDE RATIO	2.73	

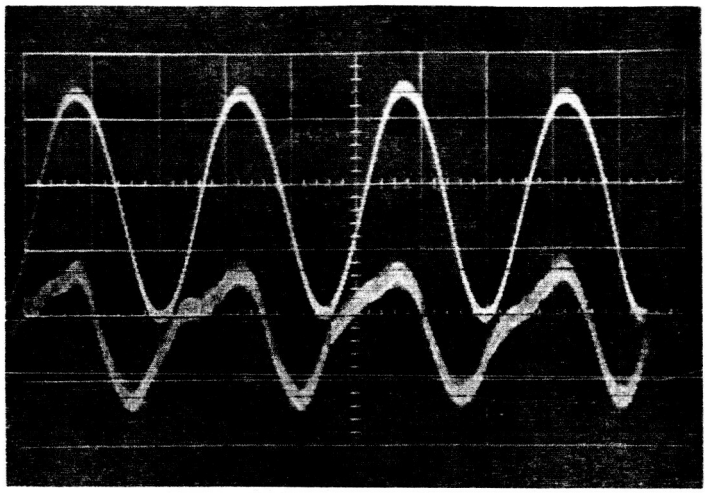

HORIZONTAL SCALE	10	ms/cm
FREQUENCY	41	Hz
UPPER VERT. SCALE	.1	V/cm
LOWER VERT. SCALE	.05	V/cm
UPPER AMPLITUDE	.34	psi
LOWER AMPLITUDE	.095	psi
AMPLITUDE RATIO	3.5	

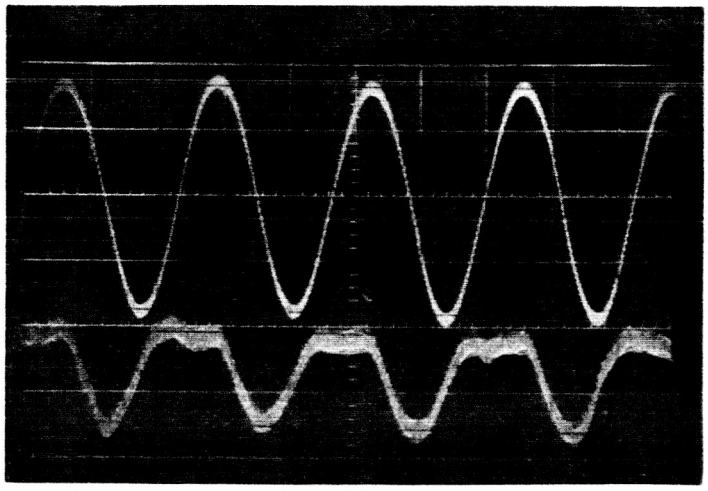

HORIZONTAL SCALE	10	ms/cm
FREQUENCY	44	Hz
UPPER VERT. SCALE	.1	V/cm
LOWER VERT. SCALE	.05	V/cm
UPPER AMPLITUDE	.345	psi
LOWER AMPLITUDE	.075	psi
AMPLITUDE RATIO	4.6	

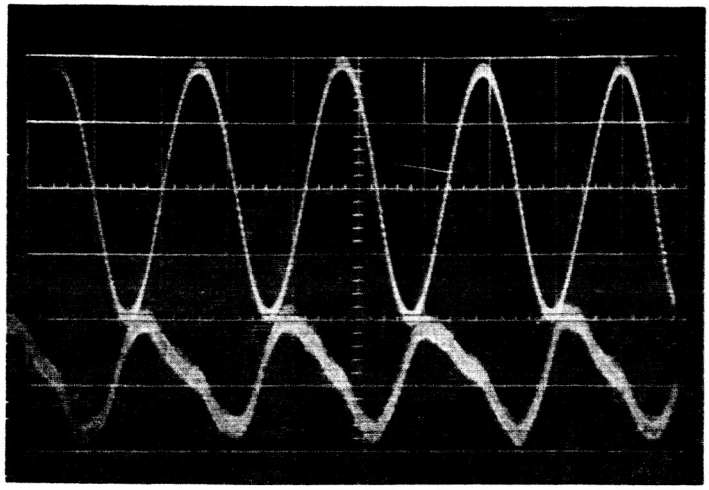

HORIZONTAL SCALE	10	ms/cm
FREQUENCY	45.5	Hz
UPPER VERT. SCALE	.1	V/cm
LOWER VERT. SCALE	.05	V/cm
UPPER AMPLITUDE	.38	psi
LOWER AMPLITUDE	.09	psi
AMPLITUDE RATIO	4.22	

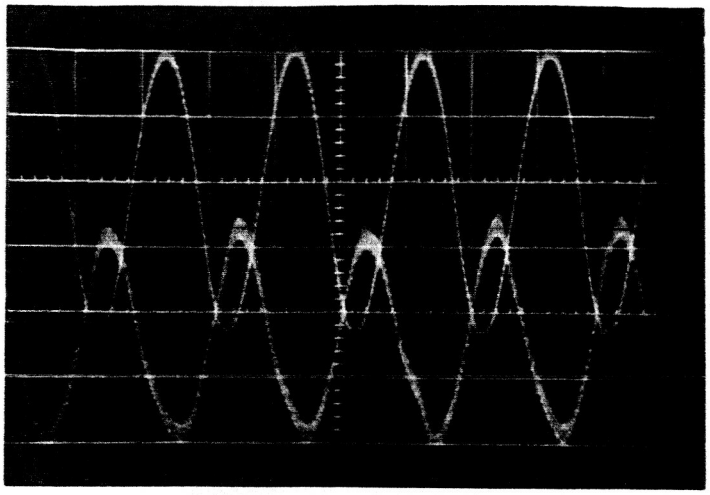

HORIZONTAL SCALE	10	ms/cm
FREQUENCY	51	Hz
UPPER VERT. SCALE	.1	V/cm
LOWER VERT. SCALE	.05	V/cm
UPPER AMPLITUDE	.43	psi
LOWER AMPLITUDE	.155	psi
AMPLITUDE RATIO	2.78	

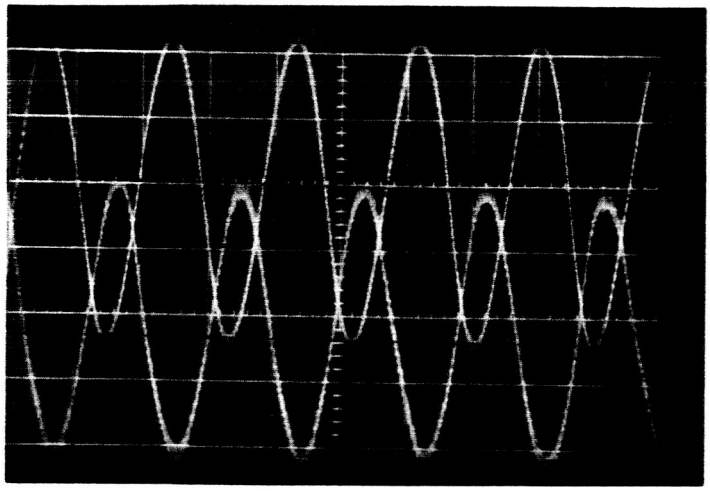

HORIZONTAL SCALE	10	ms/cm
FREQUENCY	54	Hz
UPPER VERT. SCALE	.1	V/cm
LOWER VERT. SCALE	.05	V/cm
UPPER AMPLITUDE	.455	psi
LOWER AMPLITUDE	.21	psi
AMPLITUDE RATIO	2.16	

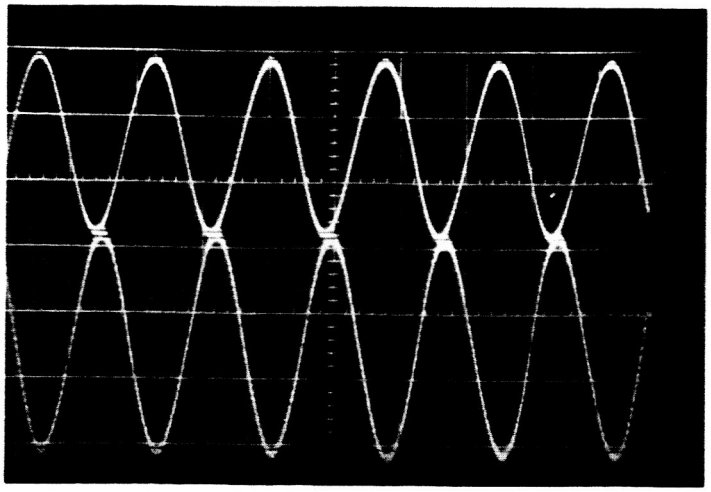

HORIZONTAL SCALE	10	ms/cm
FREQUENCY	56	Hz
UPPER VERT. SCALE	.2	V/cm
LOWER VERT. SCALE	.1	V/cm
UPPER AMPLITUDE	.54	psi
LOWER AMPLITUDE	.32	psi
AMPLITUDE RATIO	1.69	

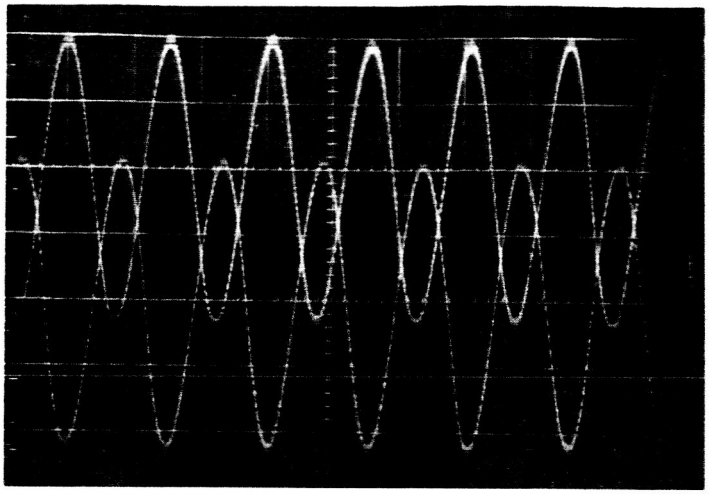

HORIZONTAL SCALE	10	ms/cm
FREQUENCY	66	Hz
UPPER VERT. SCALE	.1	V/cm
LOWER VERT. SCALE	.1	V/cm
UPPER AMPLITUDE	.41	psi
LOWER AMPLITUDE	.43	psi
AMPLITUDE RATIO	.955	

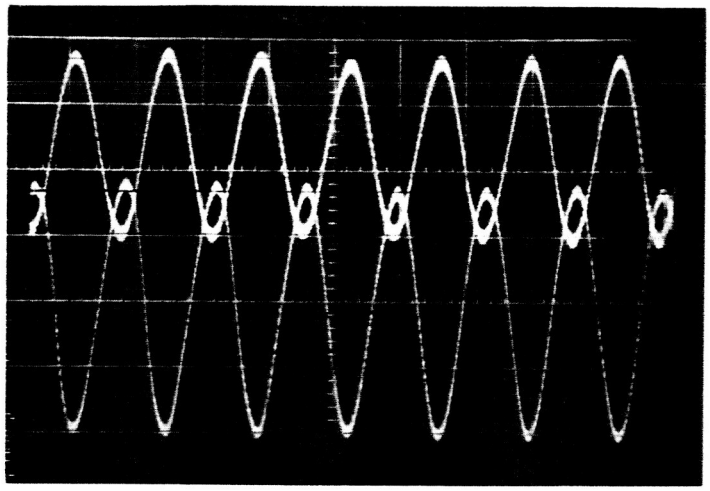

HORIZONTAL SCALE	10	ms/cm
FREQUENCY	71	Hz
UPPER VERT. SCALE	.1	V/cm
LOWER VERT. SCALE	.1	V/cm
UPPER AMPLITUDE	.27	psi
LOWER AMPLITUDE	.37	psi
AMPLITUDE RATIO	.73	

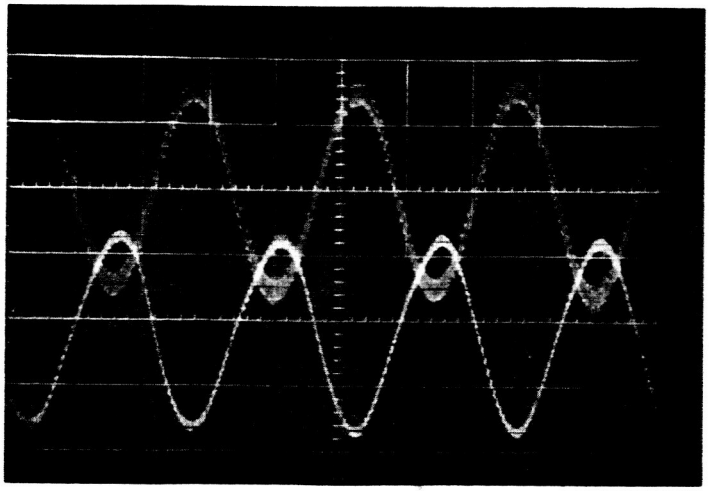

HORIZONTAL SCALE	5	ms/cm
FREQUENCY	.82	Hz
UPPER VERT. SCALE	.05	V/cm
LOWER VERT. SCALE	.1	V/cm
UPPER AMPLITUDE	.172	psi
LOWER AMPLITUDE	.29	psi
AMPLITUDE RATIO	.59	

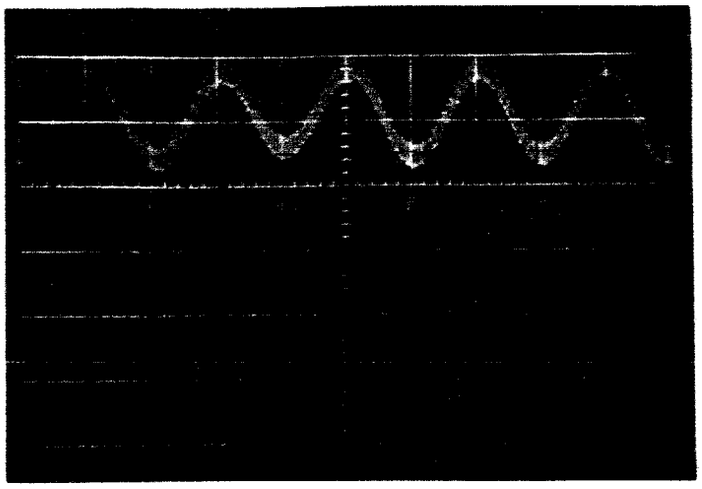

HORIZONTAL SCALE	5	ms/cm
FREQUENCY	100	Hz
UPPER VERT. SCALE	.05	V/cm
LOWER VERT. SCALE	.05	V/cm
UPPER AMPLITUDE	.065	psi
LOWER AMPLITUDE	.2	psi
AMPLITUDE RATIO	.325	

OSCILLOSCOPE PICTURES OF INPUT AND OUTPUT PRESSURE OF PASSIVE CIRCUITS

TUBE TO TANK VOLUME RATIO 6.25

TUBE LENGTH TO DIAMETER L/D = 100

TESTED WITH HELIUM

CHAMBER PRESSURE 1.0 psi OR 13.6 psia AT 4200 FT. ALTITUDE

THE PRESSURE TRANSDUCERS ARE ADJUSTED TO 0.1 psi PER VOLT

THE LOWER CURVE IS THE INPUT, THE UPPER CURVE IS THE OUTPUT

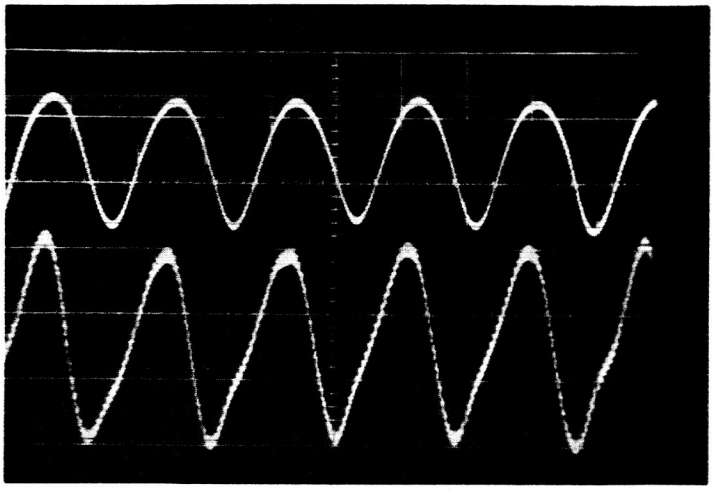

HORIZONTAL SCALE	5	ms/cm
FREQUENCY	108	Hz
UPPER VERT SCALE	.5	V/cm
LOWER VERT. SCALE	.2	V/cm
UPPER AMPLITUDE	.09	psi
LOWER AMPLITUDE	.06	psi
AMPLITUDE RATIO	1.5	

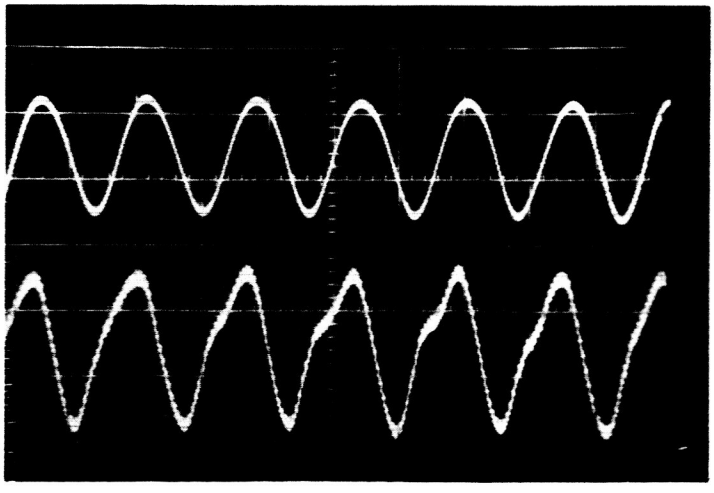

HORIZONTAL SCALE	5	ms/cm
FREQUENCY	125	Hz
UPPER VERT. SCALE	.5	V/cm
LOWER VERT. SCALE	.2	V/cm
UPPER AMPLITUDE	.085	psi
LOWER AMPLITUDE	.047	psi
AMPLITUDE RATIO	1.81	

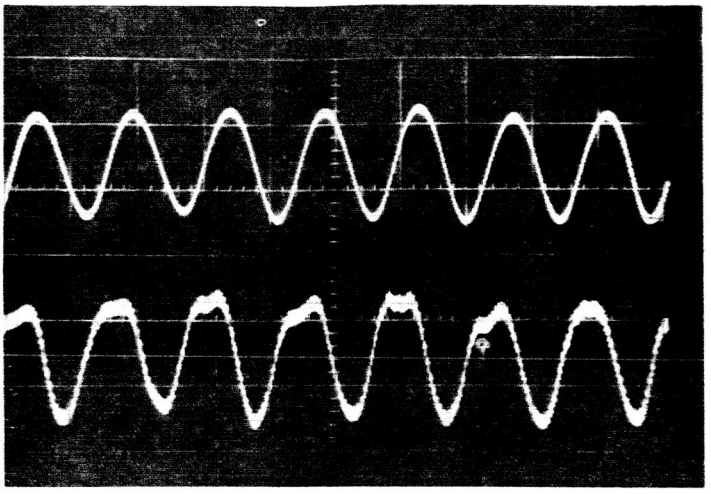

HORIZONTAL SCALE	5	ms/cm
FREQUENCY	140	Hz
UPPER VERT. SCALE	.5	V/cm
LOWER VERT. SCALE	.2	V/cm
UPPER AMPLITUDE	.080	psi
LOWER AMPLITUDE	.0362	psi
AMPLITUDE RATIO	2.21	

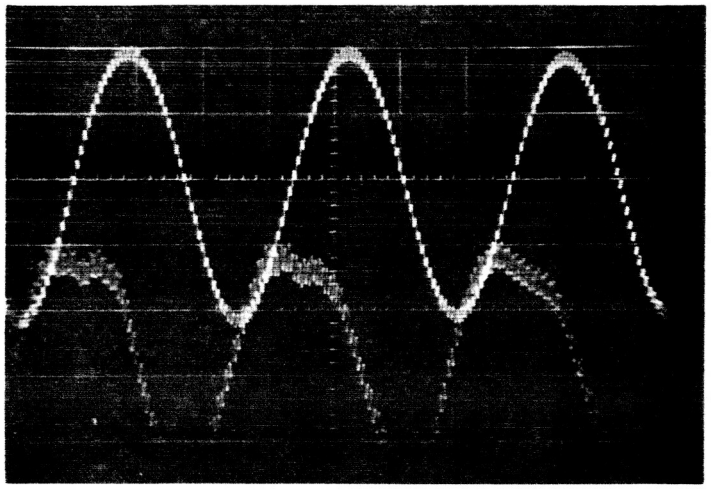

HORIZONTAL SCALE	2	ms/cm
FREQUENCY	152	Hz
UPPER VERT. SCALE	.2	V/cm
LOWER VERT. SCALE	.1	V/cm
UPPER AMPLITUDE	.08	psi
LOWER AMPLITUDE	.030	psi
AMPLITUDE RATIO	2.65	

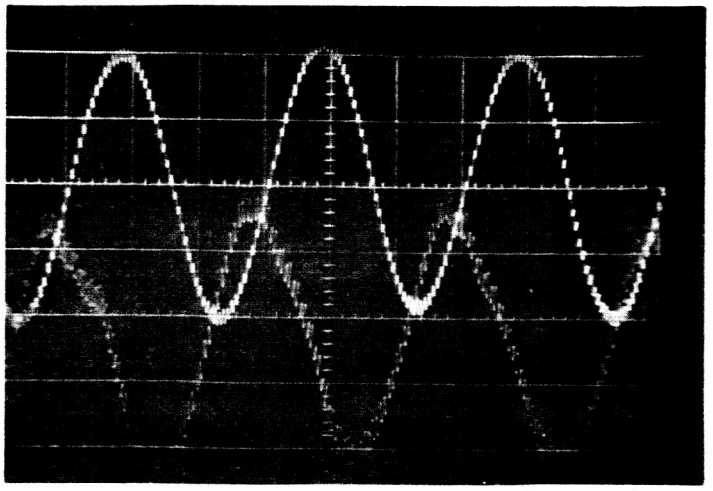

HORIZONTAL SCALE	2	ms/cm
FREQUENCY	167	Hz
UPPER VERT. SCALE	.2	V/cm
LOWER VERT. SCALE	.1	V/cm
UPPER AMPLITUDE	.08	psi
LOWER AMPLITUDE	.0385	psi
AMPLITUDE RATIO	2.08	

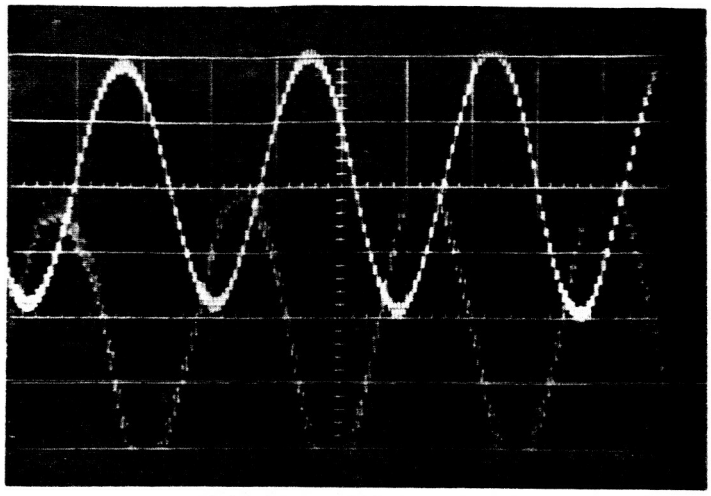

HORIZONTAL SCALE	2	ms/cm
FREQUENCY	175	Hz
UPPER VERT. SCALE	.2	V/cm
LOWER VERT. SCALE	.2	V/cm
UPPER AMPLITUDE	.076	psi
LOWER AMPLITUDE	.092	psi
AMPLITUDE RATIO	.825	

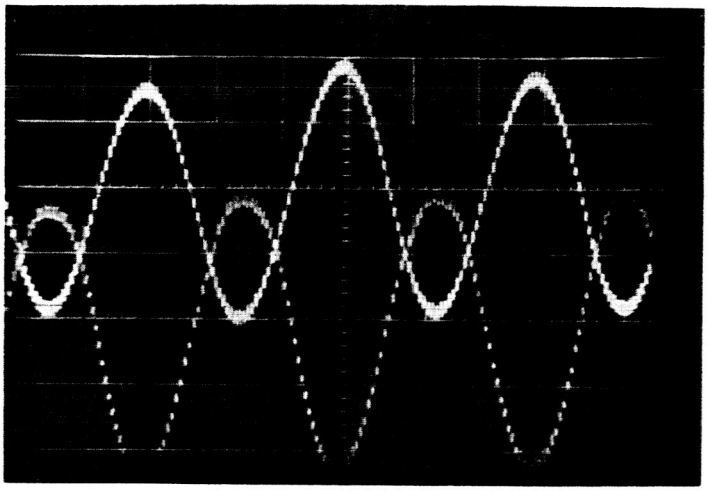

HORIZONTAL SCALE	2	ms/cm
FREQUENCY	167	Hz
UPPER VERT. SCALE	.2	V/cm
LOWER VERT. SCALE	.2	V/cm
UPPER AMPLITUDE	.071	psi
LOWER AMPLITUDE	.084	psi
AMPLITUDE RATIO	.845	

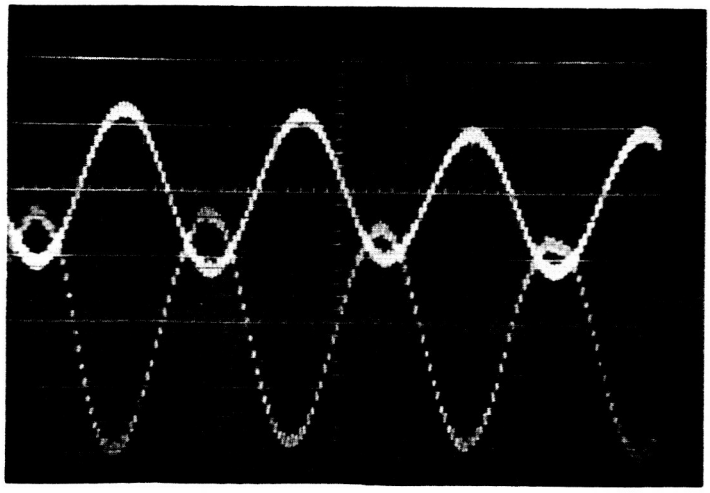

HORIZONTAL SCALE	.2	ms/cm
FREQUENCY	185	Hz
UPPER VERT. SCALE	.2	V/cm
LOWER VERT. SCALE	.2	V/cm
UPPER AMPLITUDE	.044	psi
LOWER AMPLITUDE	.072	psi
AMPLITUDE RATIO	.59	

CHAPTER 2

STUDIES LEADING TO PRESSURE REGULATOR DEVELOPMENT

Chapter 2 Studies Leading to Pressure Regulator Development

2.1 Introduction

The pressure regulator of a fluidic system might be compared to the power supply of an electronic system. The components used to make up the system are designed to operate at a specified pressure level and do not always perform well at other pressures. This is particularly true of proportional devices, where an extreme sensitivity to pressure variations is exhibited.

There are three parameters to be considered in pressure regulation:

1. Primary supply pressure variations
2. Variations in load
3. Variations in the ambient pressure.

The primary supply of fluid may originate at a pump or within a fixed volume, high pressure source. In either case, the pressure at which the fluid is supplied cannot be expected to be constant; if it were, there would be no need for pressure regulation, only pressure reduction.

The load consists of the units being supplied with fluid from the regulator at the regulated pressure. This includes components incidental to the regulation as well as those in the fluidic system. Variations in load must be expected whenever variable flow devices are used and must be accommodated by the regulation unit or system.

The importance of ambient pressures may not be immediately apparent until it is remembered that the pressure drop across a component vented to atmosphere is a drop between supply and ambient pressures. For airborne fluidic systems the ambient pressures may vary widely. A unit operating at a subcritical pressure ratio at sea level soon finds itself operating in critical pressure ratios as the vehicle ascends. In many cases, the performance of a unit under such circumstances changes radically. Fluidic operational amplifiers have been found to be sensitive to ambient changes encountered due to change in location within the United States, suggesting that supply pressure for the unit should be specified as a supply pressure ratio rather than a simple gage pressure, and emphasizing the importance of pressure ratio regulation.

The need for pressure regulation devices -- or more specifically, pressure ratio regulation devices, is apparent. For the purposes of the study reported herein, the regulation was specified to be accomplished with pure fluid devices -- that is, devices with no moving parts. The desired regulated pressure ratios were taken to be 2:1 to 3:1, and regulation was to be accurate to within plus or minus two per cent ($\pm$ 2%). Flow rates through the regulator were set at 0.5 lb/min, with air as the working fluid. Although these figures were somewhat arbitrarily

chosen, they are representative of supply requirements of components in operation today.

Two concepts of pure fluid pressure ratio regulation were taken under study. The first was based upon a single unit, presumably a proportional valve, operating in a self regulating mode, while the second made use of numerous components operating in concert to form a pressure regulation system. As will be seen in subsequent paragraphs, the first approach, while showing some promise of success, ultimately requires the support of additional components, thereby degenerating into the category of the second concept.

2.2 Self Regulation -- Variable Supply Pressure

Self regulation is accomplished by a unit performing all pressure regulation functions within itself. Unregulated supply pressure goes into the unit, and regulated pressure comes out. This implies control based upon the pressures or flows on each side of the unit.

Consider, first, a self regulating component required to regulate only variations in supply pressure. Without specifying the type of unit to be used, assume its operation can be described in terms of pressures alone. Then, based upon the diagram shown, the output pressure may be described as

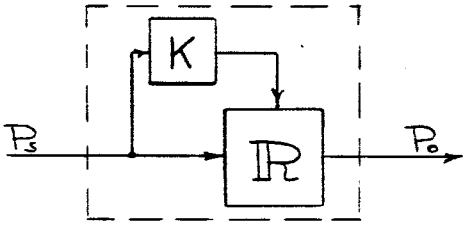

Figure 2-1

$$P_o = \frac{\partial P_o}{\partial P_s} P_s + K \frac{\partial P_o}{\partial P_c} P_s$$

$$= \left[\frac{\partial P_o}{\partial P_s} + K \frac{\partial P_o}{\partial P_c} \right] P_s \qquad (2\text{-}1)$$

If the output is to be insensitive to supply pressure variations,

$$\frac{\partial P_o}{\partial P_s} = 0 = \frac{\partial P_o}{\partial P_s} + K \frac{\partial P_o}{\partial P_c} \qquad (2\text{-}2)$$

in which case

$$K = - \frac{\partial P_o / \partial P_s}{\partial P_o / \partial P_c} \qquad (2\text{-}3)$$

If the output pressure sensitivity to control is greater than its sensitivity to supply, $\frac{\partial P_o}{\partial P_c} > \frac{\partial P_o}{\partial P_s}$, then the constant K is a simple restrictor, or resistance, whose value may be specified from the known characteristics of the chosen unit. This simple derivation, then, suggests that through the self regulation procedure of feeding unregulated supply pressure forward to be used as control pressure, perfect compensation for supply pressure variations can be realized — provided, of course, the unit being used has the assumed linearity.

2.2.1 Impact Modulator

The above theory was examined in practice with the use of an impact modulator. This proportional valve was developed by the Johnson Service Company. Its operation is based upon controlling the impact of stagnation point between two opposing streams. The streams are generated by a primary and secondary supply pressure, each applied to its own convergent nozzle. The secondary nozzle is enclosed by a collector chamber which, in turn, feeds the output tubes. The secondary supply pressure is adjusted to bring the impact, or stagnation point between the two streams into, or near the boundary of, the collector chamber. A control jet is located adjacent to the primary supply nozzle, but with its axis normal to that of the nozzle. Any flow through the control jet tends to weaken the primary stream, thereby moving the impact point toward the primary nozzle and away from the collector chamber. The end result, of course, is a decrease in output pressure.

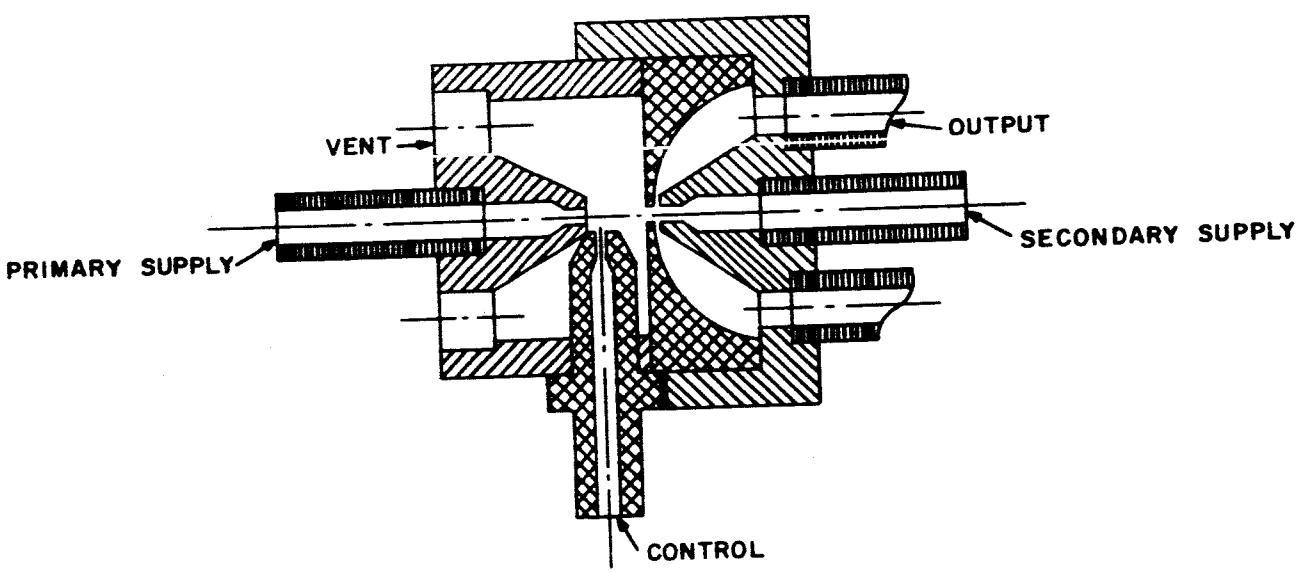

Impact Modulator

Figure 2-2

Typical performance characteristics of the impact modulator are shown in figures 2-3a and 2-3b. The first figure presents data for a 1/2 inch diameter unit having 0.025 inch diameter jets. The secondary supply pressure was adjusted for maximum output pressure without input flow. The data in the second figure shows the characteristics of the unit when the secondary pressure is adjusted for maximum gain. In both cases the output was blocked; since there was no output flow, the output pressures shown are peak values to be expected from a unit of this size.

The impact modulator is extremely sensitive to the secondary supply pressure adjustment, as shown in figure 2-4. The dashed line represents a locus of points for which no secondary pressure is supplied. If the secondary port were plugged and the pressure within it were measured, the pressures would fall on this dashed line. It suggests that the blocked secondary port would have pressures in excess of the output pressures; this, of course, is due to the additional stagnation pressure increment that the output ports cannot sense. The figure implies that the impact modulator could be operated without secondary supply pressures without compromising its performance. This is true, but the secondary supply does improve the linearity of the unit.

The experimental results of the impact modulator operating in a self regulating mode are shown in figure 2-5. The supply pressure was fed forward, through a needle valve, to the control port. The needle valve was adjusted such that the control pressure was a fraction (K) of the supply pressure. Since the needle valves are not linear restrictors, the resistance settings were all measured at a supply pressure of 8 psig. The constant K is defined in figure 2-1 as

$$K = \frac{P_C}{P_S} \qquad (2\text{-}4)$$

and is used in that manner in figure 2-5. As the amount of control is increased, the curves of output versus supply pressures become flatter. When the constant K is increased to 0.250, the point of optimum performance appears to have been passed. The fact that the curves do not become completely flat was attributed to the nonlinearity of the unit itself (see figure 2-3) and the needle valve. When calibrated, however, the latter showed itself to have surprisingly good characteristics, as seen in figure 2-6. A capillary tube was selected to provide a resistance in the most desirable range, and the impact modulator was tested with it in place of the needle valve. That data is shown in figure 2-5, and the characteristics of the capillary alone are shown in figure 2-6.

Consider the curve for the unit with the capillary tube in figure 2-5. If the nominal output pressure were chosen as 3.25 psig, then a two per cent variation would allow the output pressure to vary from 3.185 to 3.3125 psig. The curve shows the output pressure to remain within this range while supply pressure drops as low as 6.75 psig, or rises as high as 10.25 psig. If the midpoint of this supply pressure range is

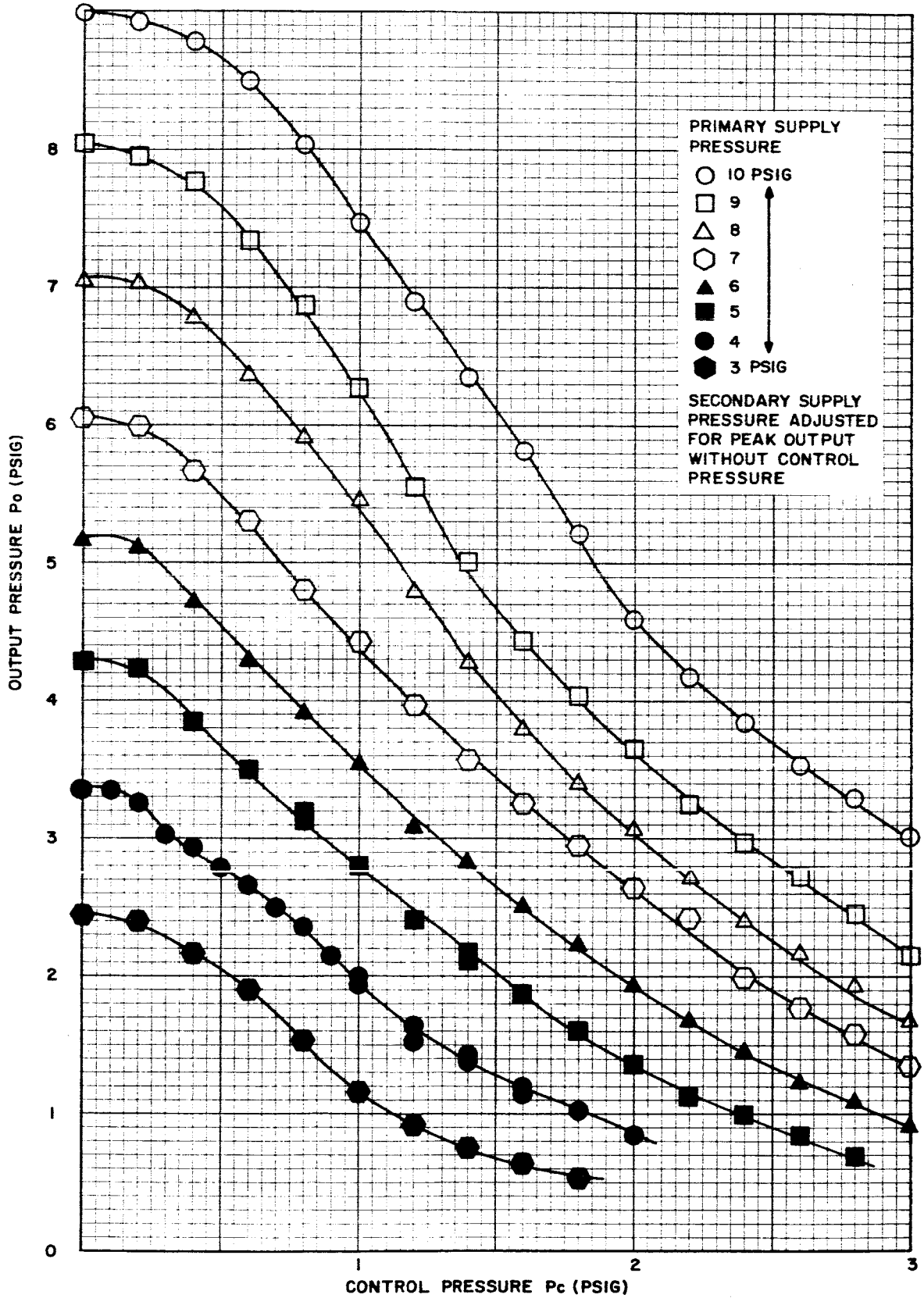

FIGURE 2-3A. IMPACT MODULATOR, EFFECT OF CONTROL PRESSURE

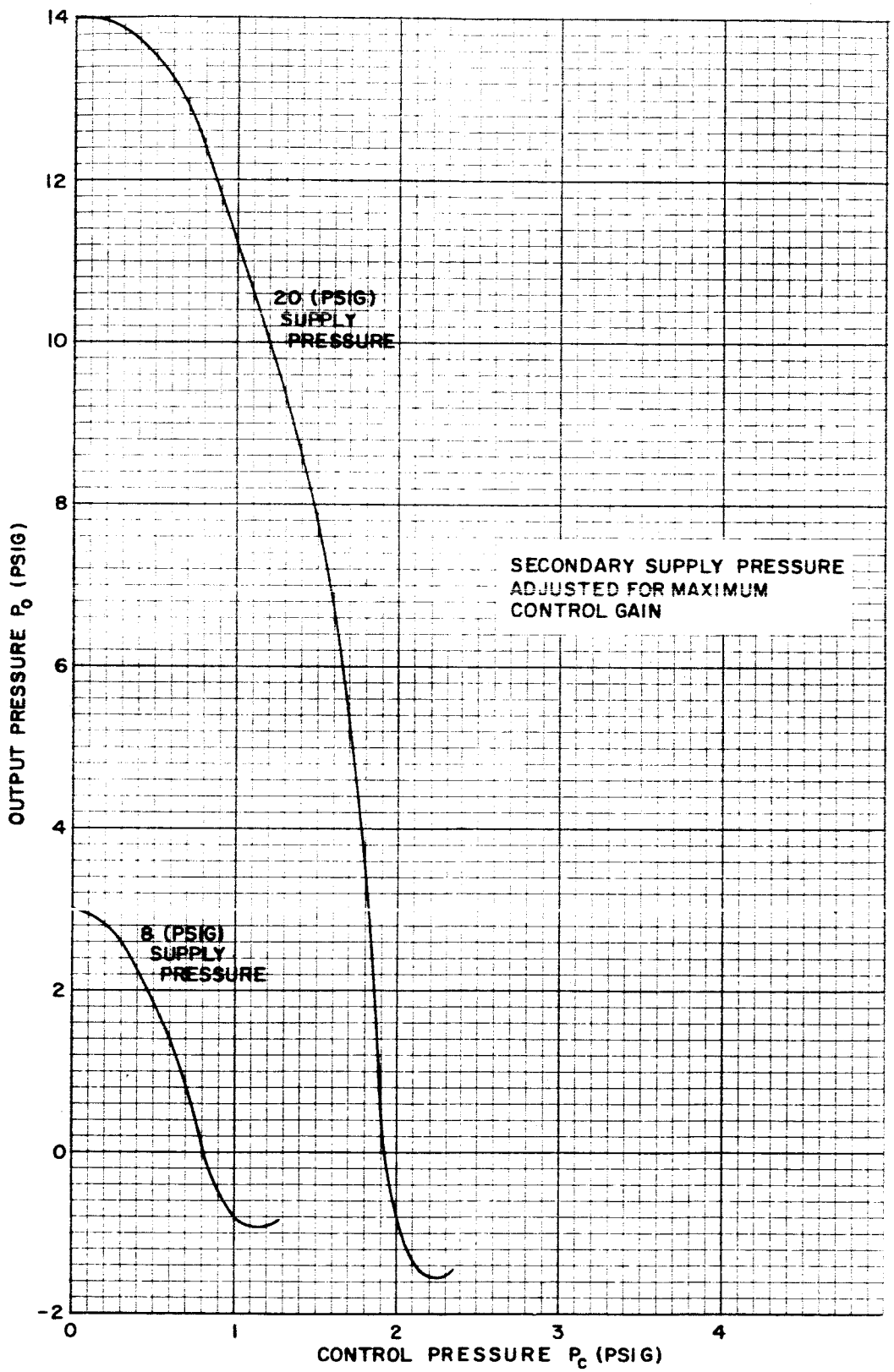

FIGURE 2-3B. IMPACT MODULATOR, EFFECT OF CONTROL PRESSURE

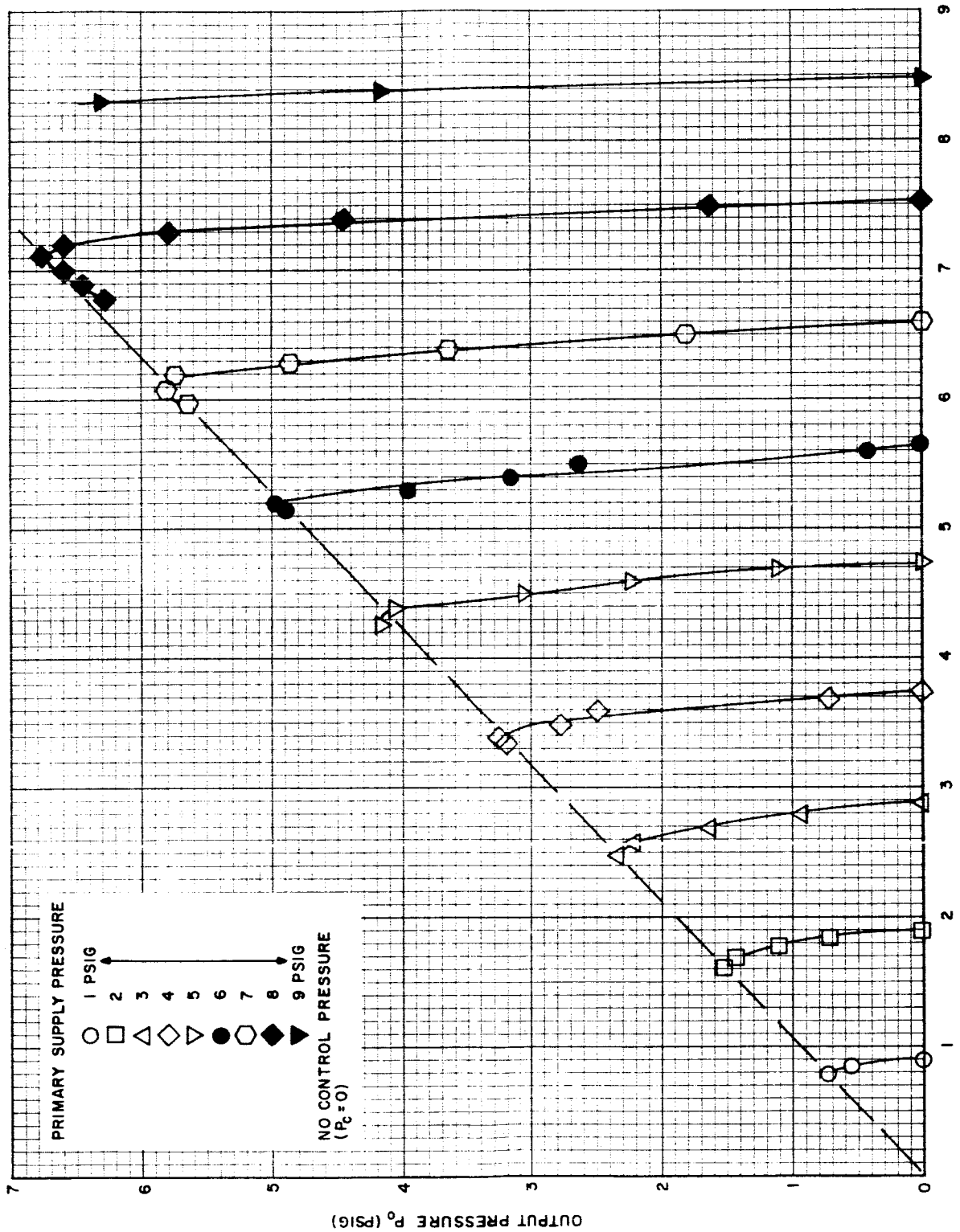

FIGURE 2-4. IMPACT MODULATOR EFFECT OF SECONDARY SUPPLY PRESSURE VARIATIONS.

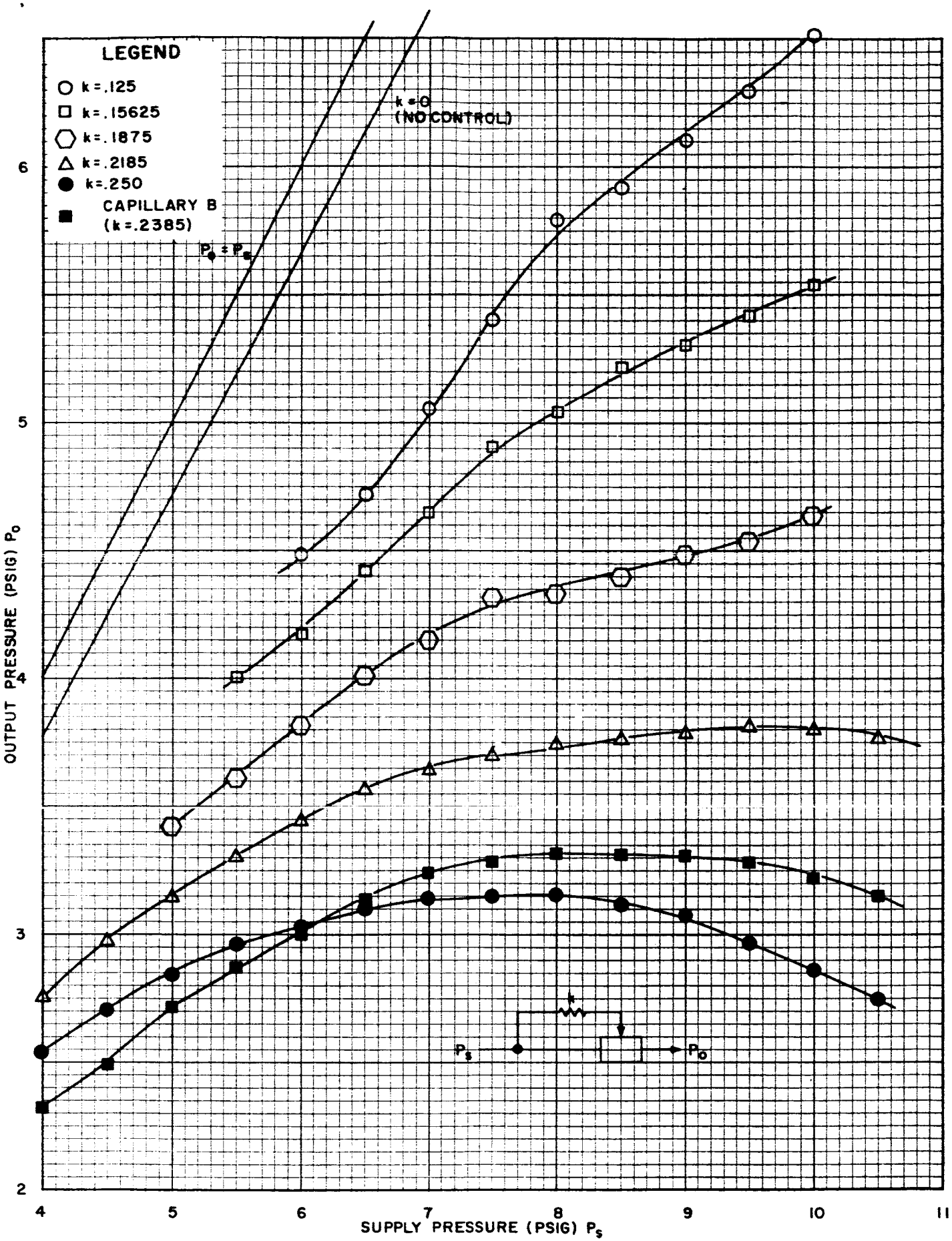

FIGURE 2-5. SELF REGULATED IMPACT MODULATOR

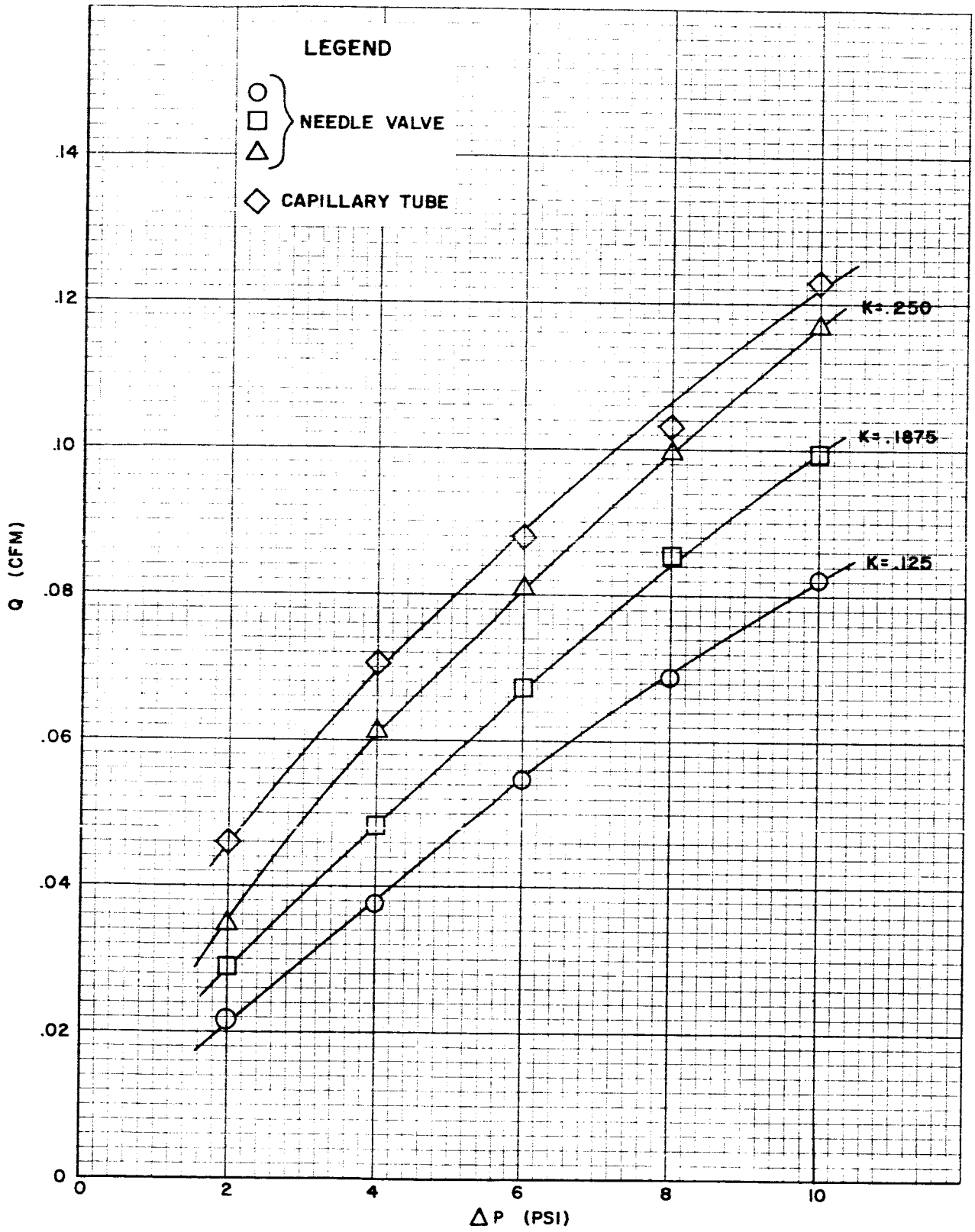

FIGURE 2-6. RESISTANCE CALIBRATION, NEEDLE VALVE AND CAPILLARY TUBE.

taken as the nominal value, then the unit has regulated its output pressure to within ±2% while the supply pressure has varied ±20%.

Although the concept of self regulation for supply pressure variations has been demonstrated in both theory and experiment, it must be noted that at this point the demonstrations have little value. The unit used in the experiment had a blocked output. Although this was consistent with the theory, which made no stipulations about output flow, it would be of little value as a pressure regulator in a system where other components have to be driven by the regulator's output. However, it will be shown that the conclusion drawn in the pressure-based theory above — e.g., equation 2-3 — is still valid when the derivation is based upon flow considerations. This is a by-product of the study of self regulation when both supply pressure and load variations are considered, and that is the next topic of discussion.

2.3 Self Regulation - Variable Supply Pressure and Load

This concept is a simple and logical extension of the one considered above. In this case the regulated pressure, the output of the regulator, is modified by some factor K_2 and fed back to the regulating unit as another control signal. In this case the rate of flow through the load, or the drain of power felt by the regulator, must be considered. The problem is therefore analyzed in terms of flows rather than pressures; each unit within the system is treated as an equivalent orifice. The flow through the load is taken from the orifice equation.

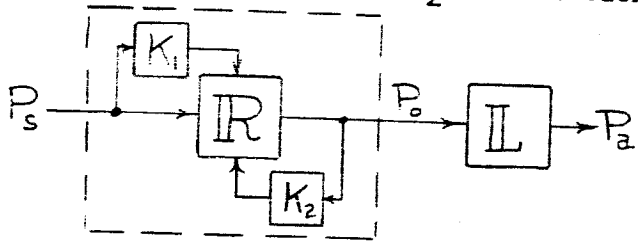

Figure 2-7

$$Q_L = k_L A_L \sqrt{\frac{2}{\rho}(P_o - P_a)}$$

$$= K_L \sqrt{(P_o - P_a)} \qquad (2\text{-}5)$$

Similarly, the regulator without control is described as

$$Q_R = k_R A_R \sqrt{\frac{2}{\rho}(P_s - P_o)}$$

$$= K_R \sqrt{(P_s - P_o)} \qquad (2\text{-}6)$$

With control,

$$Q_R = K_R \sqrt{(P_s - P_o)} + \frac{\partial Q_R}{\partial Q_L}\left[K_s \sqrt{(P_s - P_a)} + K_o \sqrt{(P_o - P_a)} \right] \qquad (2\text{-}7)$$

In this case K_s and K_o are equivalent crifice constants for the control

signals from the supply and output sides of the regulator, respectively. They account for the combined effects of the functions K_1 and K_2, and the control jet.

$$K_s\sqrt{P_s-P_a} = K_1\sqrt{P_s-P_1} = K_c\sqrt{P_1-P_a} \tag{2-8}$$

$$K_o\sqrt{P_o-P_a} = K_2\sqrt{P_o-P_2} = K_c\sqrt{P_2-P_a} \tag{2-9}$$

The pressures P_1 and P_2 are the pressures existing between the functions K_1 and K_2 and the control jet. These equations represent the control flows from the two sides of the regulating unit.

The flow through the regulating unit must equal the sum of the flows on the output side.

$$Q_R = Q_{c_o} + Q_L \tag{2-10}$$

$$K_R\sqrt{P_s-P_o} + \frac{\partial Q_R}{\partial Q_c}K_s\sqrt{P_s-P_a} = \left\{K_L + K_o\left(1-\frac{\partial Q_R}{\partial Q_c}\right)\right\}\sqrt{P_o-P_a} \tag{2-11}$$

The effect of supply pressure variations upon output pressure is found by taking the partial derivative:-

$$\frac{\partial P_o}{\partial P_s} = \frac{\dfrac{K_R}{2\sqrt{P_s-P_o}} + \dfrac{\partial Q_R}{\partial Q_c}\dfrac{K_s}{2\sqrt{P_s-P_a}}}{\dfrac{K_R}{2\sqrt{P_s-P_o}} + \left\{K_L + K_o\left(1-\dfrac{\partial Q_R}{\partial Q_c}\right)\right\}\dfrac{1}{2\sqrt{P_o-P_a}}} \tag{2-12}$$

To make the output pressure independent of supply pressure variations, the numerator of this equation must vanish.

$$\frac{K_R}{2\sqrt{P_s-P_o}} + \frac{\partial Q_R}{\partial Q_c}\frac{K_s}{2\sqrt{P_s-P_a}} = \frac{\partial Q_R}{\partial P_s} + \frac{\partial Q_R}{\partial Q_c}\frac{K_s}{2\sqrt{P_s-P_a}} = 0$$

or

$$\frac{K_s}{2\sqrt{P_s-P_a}} = -\frac{\partial Q_R/\partial P_s}{\partial Q_R/\partial Q_c}. \tag{2-13}$$

In equation (2-8), the constant K_s was shown to be a function of both the function K_1 and the control jet orifice constant K_c. Hence, defining K_s allows further definition of the function K_1. From (2-13) it is seen that the function K_1 is proportional to the regulator output sensitivity to supply pressure, and inversely proportional to the regulator output sensitivity to control flow. This is the same relationship found in (2-3) where pressures alone were considered, so the conclusion drawn there is still valid when the theory is based upon flow rates.

The effect of load variations upon the output pressure can be determined through the partial derivation

$$\frac{\partial P_o}{\partial K_L} = \frac{2\,(P_s - P_o)\,\sqrt{P_o - P_a}}{K_R\sqrt{P_o - P_a} + \left\{K_L + K_o\left(1 - \frac{\partial Q_r}{\partial Q_c}\right)\right\}\sqrt{P_s - P_o}} \quad . \tag{2-14}$$

Since the numerator cannot vanish unless either the regulator or the load do, it is not possible to make output pressure independent of the load. However, the interactions may be minimized by forcing the equation to a minimum value. There is only one parameter that can be varied: K_o, the equivalent orifice constant of the feedback loop. All others are dependent upon the characteristics of the unit used for regulation, and the load it must drive. Since the performance parameter $\partial Q_r / \partial Q_c$ has a negative sign, all terms in the denominator are positive. Hence, the function K_o must be made as large as possible, suggesting that it is not a resistance at all, but an amplifier with considerable gain. Since amplification involves additional components, the regulator is no longer a single unit, and the concept of self regulation must be proclaimed inadequate to regulate output pressures in the presence of variable loads.

2.4 Pressure Regulation System

A pressure regulation system consists of a group of components operating together with the primary purpose of regulating the system output pressure. In its generalized form, the system consists of a controlling apparatus (V), a sensor (S), and intermediate elements (K) as may be required by the components being used. The basic theory of a regulation system is similar to that considered above; the detail theory and analysis is dependent upon the particular components being applied.

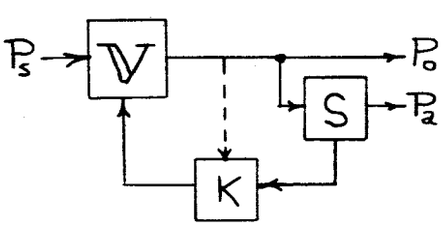

Figure 2-8

2.4.1 Pressure Sensor

There are two approaches to the matter of pressure sensing. The first makes use of a device connected in parallel with the load, and providing an output signal proportional to the pressure ratio across the load. The second makes use of ambient sensitive elements in the feedback loop, operating upon output pressure to provide a control signal. In this manner the functions of the sensor and feedback elements might be combined.

Three types of pressure ratio sensors were considered in this study:

1. Convergent - Divergent Nozzle
2. Orifice - Venturi Combination
3. Pressure Jet Oscillator.

None was found suitable for pressure ratio sensing within the confines of the pressure ratios and accuracies specified earlier in this report.

2.4.1.1 Convergent - Divergent Nozzle

It was proposed to sense the pressure-ratio directly in the form of a pressure difference between the static pressure at the exit of a convergent-divergent Laval nozzle and the ambient pressure. The nozzle's area ratio is chosen to be correct for the desired pressure ratio.

To study the theoretical feasibility of this concept, assume a perfect gas and isentropic flow. Then several basic equations can be written.

$$P = \rho g R T \qquad \text{(perfect gas law)} \tag{2-15}$$

$$m = A \rho u = \text{Const.} \quad \text{(Conservation of mass)} \tag{2-16}$$

$$u = M \sqrt{\gamma g R T} \tag{2-17}$$

$$\frac{P}{P_o} = \left(1 + \frac{\gamma-1}{2} M^2\right)^{-\frac{\gamma}{\gamma-1}} \tag{2-18}$$

$$\frac{T}{T_o} = \left(1 + \frac{\gamma-1}{2} M^2\right)^{-1} \tag{2-19}$$

Consider the convergent-divergent nozzle, and take any two points, $(\ )_1$ and $(\ )_2$, within it. Then

$$\frac{A_1}{A_2} = \frac{\rho_2 u_2}{\rho_1 u_1} = \frac{P_2 T_1}{P_1 T_2} \cdot \frac{M_2}{M_1} \sqrt{\frac{T_2}{T_1}} = \frac{P_2}{P_1} \frac{M_2}{M_1} \sqrt{\frac{T_2}{T_1}} \tag{2-20}$$

at $(\ )_2$,

$$\frac{P_2}{P_o} = \left(1 + \frac{\gamma-1}{2} M_2^2\right)^{-\frac{\gamma}{\gamma-1}} \tag{2-21}$$

and at $(\ )_1$,

$$\frac{P_1}{P_o} = \left(1 + \frac{\gamma-1}{2} M_1^2\right)^{-\frac{\gamma}{\gamma-1}} \qquad (2\text{-}22)$$

Then

$$\frac{P_2}{P_1} = \left(\frac{1 + \frac{\gamma-1}{2} M_2^2}{1 + \frac{\gamma-1}{2} M_1^2}\right)^{-\frac{\gamma}{\gamma-1}} \qquad (2\text{-}23)$$

but

$$\left(1 + \frac{\gamma-1}{2} M_2^2\right)^{-1} = \frac{T_2}{T_o} \qquad (2\text{-}24)$$

and

$$\left(1 + \frac{\gamma-1}{2} M_1^2\right)^{-1} = \frac{T_1}{T_o} \qquad (2\text{-}25)$$

Then

$$\frac{P_2}{P_1} = \left(\frac{T_2}{T_1}\right)^{\frac{\gamma}{\gamma-1}} \qquad (2\text{-}26)$$

Going back to the area ratio equation with this last expression,

$$\frac{A_1}{A_2} = \left(\frac{T_2}{T_1}\right)^{\frac{\gamma}{\gamma-1}} \frac{M_2}{M_1} \left(\frac{T_1}{T_2}\right)^{1/2} = \frac{M_2}{M_1} \left(\frac{T_2}{T_1}\right)^{\frac{\gamma+1}{2(\gamma-1)}} \qquad (2\text{-}27)$$

At the throat, $(\ )_T$, the Mach number is 1.0. Then

$$\frac{A_T}{A} = M \left(\frac{T_T}{T}\right)^{\frac{\gamma+1}{2(\gamma-1)}} = M \left[\frac{2}{\gamma+1}\left(1 + \frac{\gamma-1}{2} M^2\right)\right]^{-\frac{\gamma+1}{2(\gamma-1)}} \qquad (2\text{-}28)$$

$$\frac{P_T}{P} = \left[\frac{2}{\gamma+1}\left(1 + \frac{\gamma-1}{2} M^2\right)\right]^{\frac{\gamma}{\gamma-1}} \qquad (2\text{-}29)$$

If the pressure in the denominator of the ratio is taken as the supply pressure p_s, then the corresponding Mach number is zero at the source, as the supply is assumed to be very large as compared to the flow rates.

Then,

$$\frac{P_T}{P_s} = \left(\frac{2}{\gamma+1}\right)^{\frac{\gamma}{\gamma-1}} \qquad (2\text{-}30)$$

for air, $\gamma = 1.4$, and $\frac{P_T}{P_s} = 0.527$, the critical pressure ratio.

If the pressure in the denominator of the pressure ratio is taken as exhaust pressure, at the nozzle exit, and that pressure is assumed to be ambient, then

$$\frac{P_T}{P_a} = \left[\frac{2}{\gamma+1}\left(1+\frac{\gamma-1}{2}M_e^2\right)\right]^{\frac{\gamma}{\gamma-1}} \tag{2-31}$$

Solving for exhaust Mach number,

$$M_e^2 = \frac{2}{\gamma-1}\left[\frac{\gamma+1}{2}\left(\frac{P_T}{P_a}\right)^{\frac{\gamma-1}{\gamma}} - 1\right] \tag{2-32}$$

This can be written in terms of the total pressure drop across the nozzle by writing

$$\frac{P_T}{P_a} = \frac{P_T}{P_s}\cdot\frac{P_s}{P_a} \tag{2-33}$$

and remembering that

$$\left(\frac{P_T}{P_s}\right)^{\frac{\gamma-1}{\gamma}} = \frac{2}{\gamma+1} \tag{2-34}$$

Then

$$M_e^2 = \frac{2}{\gamma-1}\left[\left(\frac{P_s}{P_a}\right)^{\frac{\gamma-1}{\gamma}} - 1\right] \tag{2-35}$$

Now that all the nozzle equations that might be needed have been developed, go back and take a look at the initial proposition. It said the nozzle would be designed to operate at a given pressure ratio $(P_s/P_e)_*$, such that $P_e=P_a$. That is, the air is completely expanded at the nozzle exit. The nozzle's design parameters are then described by equations (2-28) and (2-35). To define the areas more specifically, that is, to describe the throat and exit areas as areas rather than ratios, requires an additional requirement, presumably a maximum allowable flow rate.

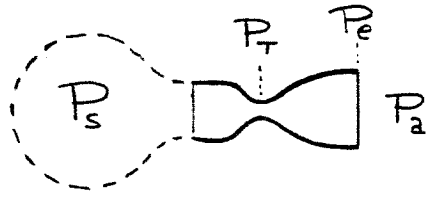

Figure 2-9

Equations (2-28) and (2-35) can be combined to yield the design area ratio

$$\left(\frac{A_T}{A_e}\right)_* = \sqrt{\frac{2}{\gamma-1}}\left[\left(\frac{P_s}{P_a}\right)_*^{\frac{\gamma-1}{\gamma}} - 1\right]^{1/2}\left\{\frac{2}{\gamma+1}\left[1+\left(\frac{P_s}{P_a}\right)_*^{\frac{\gamma-1}{\gamma}} - 1\right]\right\}^{-\frac{\gamma+1}{2(\gamma-1)}}$$

$$= \sqrt{\frac{2}{\gamma-1}}\left(\frac{2}{\gamma+1}\right)^{-\frac{\gamma+1}{2(\gamma-1)}}\left[\left(\frac{P_s}{P_a}\right)_*^{\frac{\gamma-1}{\gamma}} - 1\right]^{1/2}\left(\frac{P_s}{P_a}\right)_*^{-\frac{\gamma+1}{2(\gamma-1)}} \tag{2-36}$$

The additional requirement — maximum mass flow — can be derived from the Conservation of Mass equation (2-16).

$$\dot{m} = \rho A u \tag{2-16}$$

where ρ is mass density (slugs/cu.ft.). Inserting equations (2-15) and (2-17),

$$\dot{m} = \frac{P}{gRT} AM\sqrt{\gamma g R T}$$

$$= \sqrt{\frac{\gamma}{gRT}} AMP \tag{2-37}$$

At the throat, $M_T = 1.0$, $P = P_T = \left(\frac{\gamma+1}{2}\right)^{-\frac{\gamma}{\gamma-1}} P_s$ from (2-30). The supply pressure can be described in terms of the ambient through the design pressure ratio, $P_o = \left(\frac{P_o}{P_a}\right)_* P_a$. Then,

$$\dot{m} = \sqrt{\frac{\gamma}{gRT}} A_{T*} \left(\frac{\gamma+1}{2}\right)^{\frac{-\gamma}{\gamma-1}} \left(\frac{P_s}{P_a}\right)_* P_a \tag{2-38}$$

Given a maximum allowable mass flow $\bar{m}$, the throat area becomes

$$A_{T*} = \sqrt{\frac{gRT}{\gamma}} \left(\frac{\gamma+1}{2}\right)^{\frac{\gamma}{\gamma-1}} \frac{\bar{m}}{\left(\frac{P_s}{P_a}\right)_* P_a} \tag{2-39}$$

Given the nozzle designed for a given pressure ratio, the pressures through it are related as

$$\frac{P_s}{P_e} = \frac{P_s}{P_T} \cdot \frac{P_T}{P_e} \tag{2-40}$$

But $\frac{P_s}{P_e} = \left(\frac{P_o}{P_a}\right)_*$ the design pressure ratio, and P_s/P_t was given by equation (2-30) as the critical pressure ratio. Hence, the above becomes

$$\left(\frac{P_s}{P_a}\right)_* = \left(\frac{\gamma+1}{2}\right)^{\frac{\gamma}{\gamma-1}} \frac{P_T}{P_e} \tag{2-41}$$

The rate of change of exhaust pressure with supply pressure is

$$\frac{\partial P_e}{\partial P_s} = \frac{\partial P_e}{\partial P_T} \cdot \frac{\partial P_T}{\partial P_s} \tag{2-42}$$

The first term on the right is taken from (2-41),

$$\frac{\partial P_e}{\partial P_T} = \frac{\left(\frac{\gamma+1}{2}\right)^{\frac{\gamma}{\gamma-1}}}{\left(\frac{P_s}{P_a}\right)_*} \tag{2-43}$$

The second term on the right is taken from equation (2-30),

$$\frac{\partial P_T}{\partial P_s} = 1 \tag{2-44}$$

Then,

$$\frac{\partial P_e}{\partial P_s} = \left(\frac{\gamma+1}{2}\right)^{\frac{\gamma}{\gamma-1}} \cdot \frac{1}{\left(P_s/P_a\right)_*} \tag{2-45}$$

For air, $\gamma = 1.4$, and

$$\frac{\partial P_e}{\partial P_s} = \frac{1.892}{\left(P_s/P_a\right)_*} \tag{2-46}$$

or

$$\frac{\partial P_e}{P_e} = 1.892 \frac{\partial P_s}{P_s} \tag{2-47}$$

Since $\frac{P_s}{P_e} = \left(\frac{P_s}{P_a}\right)_*$. This says that if the supply pressure P_s is to be regulated to within two per cent $\left(\frac{\partial P_s}{P_s} = .02\right)$, then the exhaust pressure must be sensed to within 3.8 per cent. Since the nominal exhaust pressure is ambient, or atmospheric pressure, the maximum variation in exhaust pressure will be about 0.56 psi at sea level (P_a = 14.7 psia). That is, the maximum output of the sensor is 0.56 psi.

From a practical point of view, it behooves us to investigate what size the convergent-divergent nozzle sensor will be for the pressure ratios in question. Regulation is required for supply pressures running two to three times ambient. Notice that the lowest pressure ratio that can be sensed with the convergent-divergent nozzle sensor is the reciprocal of the critical ratio, or 1.892.

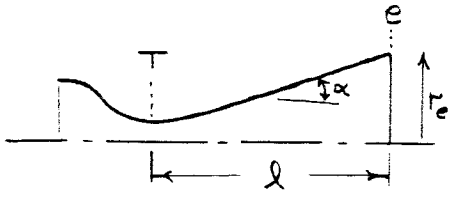

Figure 2-10

The ratios of throat to exit area are given by equation (2-36). The throat area is given by equation (2-39). Given a nozzle expansion half angle α, the length of the divergent portion of the nozzle is given as

$$\ell = \frac{r_e - r_T}{\text{Tan}\,\alpha} = \frac{d_e - d_T}{2\,\text{Tan}\,\alpha}$$

or

$$\frac{\ell}{d_T} = \frac{d_e}{d_T}\,\frac{1 - \frac{d_T}{d_e}}{2\,\text{Tan}\,\alpha} = \frac{1 - \sqrt{\left(\frac{A_T}{A_e}\right)_*}}{\sqrt{\left(\frac{A_T}{A_e}\right)_*}\;2\,\text{Tan}\,\alpha} \qquad (2\text{-}48)$$

To get some numerical values of a practical nozzle, assume three flow rates — 0.25, 0.50 and 0.75 lbs/minute — and the two pressure ratios, 2 and 3.

Wt. Flow, lbs/min.	.25		.50		.75	
lbs/sec.	.00416		.00833		.0125	
Flow Rate, CFM	.0545		.109		.1635	
Mass Flow, slug/sec.	1.292×10^{-4}		2.59×10^{-4}		3.88×10^{-4}	
$(P_s/P_a)_*$	2	3	2	3	2	3
$A_T\times10^4$, sq. ft.	.461	.308	.925	.616	1.383	.923
$d_T\times10^2$, ft.	.767	.626	1.085	.886	1.33	1.083
d_T in.	.092	.0751	.1301	.1061	.1596	.13
$\left[\left(\frac{P_s}{P_a}\right)_*^{.286} - 1\right]$	.2196	.3685				
$\left[\left(\frac{P_s}{P_a}\right)_*^{.286} - 1\right]^{1/2}$	.468	.606				
$(P_s/P_a)_*^{-.857}$	.553	.39				
$(A_T/A_e)_*$	.998	.914				
$(d_T/d_e)_*$	.999	.956				
ℓ/d_T $(\alpha = 6°)$	.0476	.2290				
length, in.	.00438	.0172	.00619	.0243	.0075	.02977

These figures are plotted in figure 2-11. Note that the numbers are very small — that is, the throat diameters and nozzle lengths are very small, but the latter is noticeably so. With nozzles of such sizes it is hardly practical to insert a static pressure tap at the nozzle exit since the divergent section of the nozzle is barely longer than the tap itself. For the pressure ratio of 2.0, the ratio is only slightly higher than the critical ratio (1.892), so the throat is barely choked and the flow at the exit is barely supersonic. From the point of view of using the convergent-divergent nozzle as a pressure ratio sensor, it must be concluded that the pressure ratios of interest are too low to make this sensor a practical device.

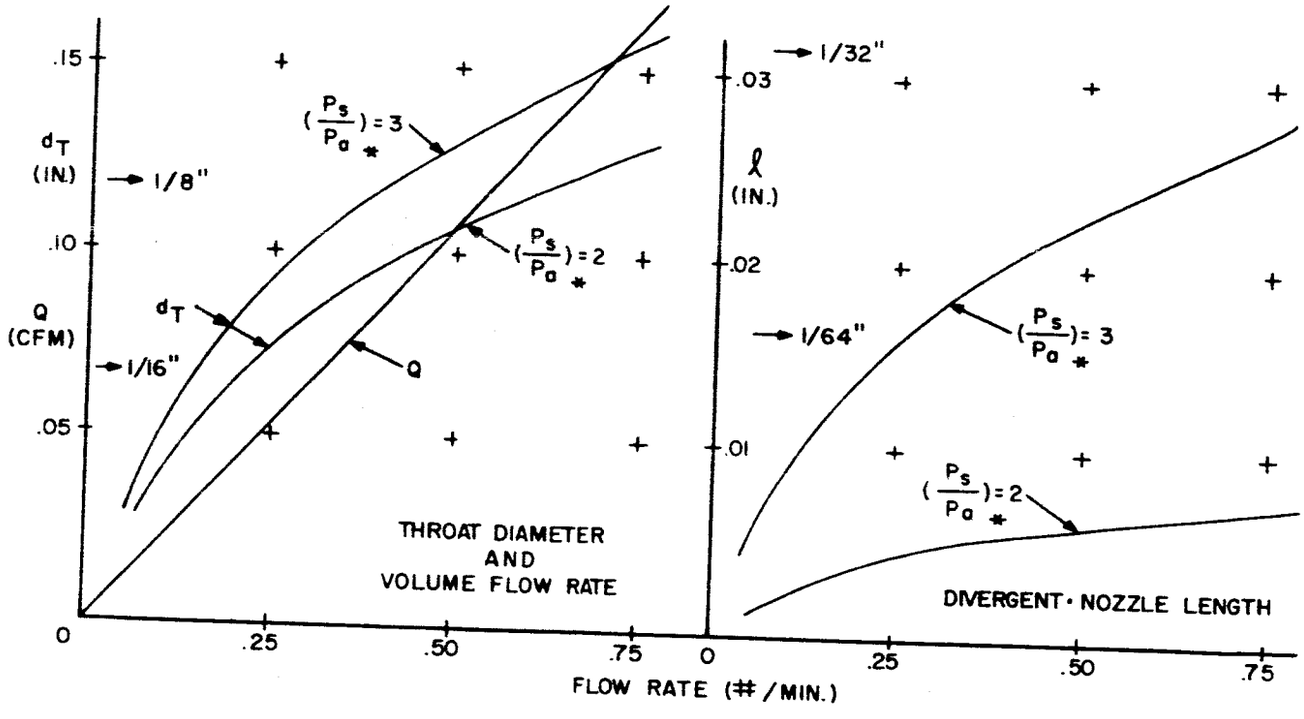

Convergent-Divergent Nozzle
Figure 2-11

2.4.1.2. Venturi - Orifice Combination

The venturi tube has been proposed as an alternate sensor for the pressure regulator. There were probably two reasons behind this suggestion: 1) the convergent-divergent nozzle failed to present an adequate solution to the sensor problem because the pressure ratios of interest were too low. The venturi tube, being a device for low pressure ratios - or low pressure differences - may have been envisioned as an adequate solution to the convergent-divergent nozzle's shortcoming. 2) A pressure ratio regulator had been developed by or for the Lycoming Division of Avco for use as a control device on a gas turbine engine. It was reported that this was a pure fluid device, and therefore excited no small amount of interest.

Unfortunately, both reasons failed to live up to their promise. The Lycoming device, while it did use a venturi tube as a sensor, was not a pure fluid device. It made use of diaphram operated poppet valves and spring loaded pistons, and must, therefore, be discarded from further consideration in this study.

That the venturi tube operates at low pressure ratios or low pressure differences is true, but if the venturi alone is used at pressure ratios of 2 or 3, the device will be choked, since even the lower ratio is greater than the critical pressure ratio. The pressure at the throat is then

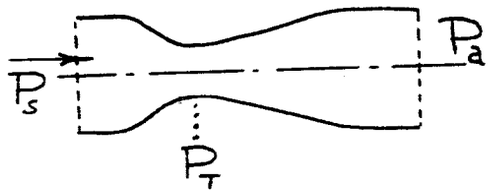

Figure 2-12

$$P_T = \frac{P_s}{\left(\frac{P_s}{P}\right)_{crit.}} \qquad (2\text{-}49)$$

and the pressure difference usually sensed by the venturi tube is

$$P_s - P_T = P_s \frac{\left(\frac{P_s}{P}\right)_{crit.} - 1}{\left(\frac{P_s}{P}\right)_{crit.}} \qquad (2\text{-}50)$$

and has no bearing upon the pressure ratio of interest (P_s/P_a). It is necessary to decrease the pressure drop across the tube to something less than the critical value. This can be done by placing the venturi tube in series with a flow control orifice. Consider both the orifice

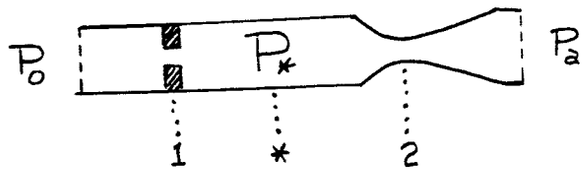

Figure 2-13

and the venturi to have the effect of a simple orifice, and to restrict the flow according to the orifice law.

$$Q_i = K_i A \sqrt{\frac{2(P_o - P)}{\rho}} \tag{2-51}$$

The coefficient for the orifice $(\ )_1$ has a value of about 0.6 for diameter ratios (D_1/D) less than 0.30, while the coefficient for the venturi has a value of about 0.96 for a tube of small diameter.

The flow through the orifice and venturi are, respectively,

$$Q_1 = K_1 A_1 \sqrt{\frac{2(P_o - P_*)}{\rho}} \tag{2-52}$$

$$Q_2 = K_2 A_2 \sqrt{\frac{2(P_* - P_a)}{\rho}} \tag{2-53}$$

Equating these two equations, since the flow through both restrictions must be the same,

$$\left(\frac{K_1 A_1}{K_2 A_2}\right)^2 (P_o - P_*) = (P_* - P_a)$$

$$P_* \left[1 + \left(\frac{K_1 A_1}{K_2 A_2}\right)^2\right] = P_a + \left(\frac{K_1 A_1}{K_2 A_2}\right)^2 P_o$$

$$\frac{P_*}{P_a} = \frac{\left(\frac{K_1 A_1}{K_2 A_2}\right)^2 \frac{P_o}{P_a} + 1}{\left(\frac{K_1 A_1}{K_2 A_2}\right)^2 + 1} \tag{2-54}$$

Assuming the first orifice is the critical one for flow regulation, the flow rate is

$$Q = K_1 A_1 \left\{\frac{2}{\rho}\left[P_o - \frac{\mathcal{K} P_o - P_a}{1 + \mathcal{K}}\right]\right\}^{1/2} \tag{2-55}$$

where

$$\mathcal{K} = \left(\frac{K_1 A_1}{K_2 A_2}\right)^2$$

To determine the characteristics of the flow through the venturi tube it is necessary to go to Bernoulli's equation,

$$\frac{V_2^2 - V_*^2}{2g} + \frac{P_2 - P_*}{w} = 0 \qquad (2\text{-}56)$$

and solve for the throat pressure, P_2.

$$P_2 = P_* - \frac{\rho}{2}(V_2^2 - V_*^2) \qquad (2\text{-}57)$$

The area of the pipe upstream of the venturi is A_*. The velocity of flow in this pipe is $V_* = Q/A_*$, and the velocity in the throat is $V_2 = Q/A_2$. Then

$$P_2 = \frac{KP_0 + P_a}{1+K} - \frac{Q^2\rho}{2}\left[\frac{A_*^2 - A_2^2}{A_*^2 A_2^2}\right] \qquad (2\text{-}58)$$

Inserting the square of equation (2-55), we find

$$\frac{P_2}{P_a} = \frac{K\frac{P_0}{P_a} + 1}{1+K} - (K_1 A_1)^2\left(\frac{A_*^2 - A_2^2}{A_*^2 A_2^2}\right)\left[\frac{P_0}{P_a} - \frac{K\frac{P_0}{P_a} - 1}{1+K}\right]$$

$$= \frac{1 + K_1^2 A_1^2 \mathbb{R}}{1+K} + \left[\frac{K - K_1^2 A_1^2 \mathbb{R}}{1+K}\right]\frac{P_0}{P_a} \qquad (2\text{-}59)$$

where

$$\mathbb{R} = \frac{A_*^2 - A_2^2}{A_*^2 A_2^2}$$

The pressure P_2 is the output pressure of the venturi tube. To find the effect of variations in supply pressure P_0 upon the sensed pressure P_2, take the derivative of equation (2-59) with respect to P_0.

$$\frac{\partial P_2}{\partial P_0} = \frac{K - K_1^2 A_1^2 \mathbb{R}}{1+K} = \frac{\left(\frac{K_1 A_1}{K_2 A_2}\right)^2 - K_1^2 A_1^2 \frac{A_*^2 - A_2^2}{A_*^2 A_2^2}}{1 + \left(\frac{K_1 A_1}{K_2 A_2}\right)^2}$$

$$= K_1^2 \bar{A}_1^2\left[\frac{(1 - K_2^2) + K_2^2 \bar{A}_2^2}{K_1^2 \bar{A}_1^2 + K_2^2 \bar{A}_2^2}\right] \qquad (2\text{-}60)$$

The terms $\bar{A}_i$ represent the ratios of A_i to the tube area A_*.

Assuming the orifice coefficient to be $K_1 = 0.6$, and the equivalent orifice coefficient of the venturi to be $K_2 = 0.96$, and assigning the venturi ratio $\bar{A}_2 = 0.25$ (i.e., $\bar{d}_2 = 0.5$), equation (2-60) becomes

$$\frac{\partial P_2}{\partial P_o} = \frac{.0482\,\bar{A}_1^2}{.36\bar{A}_1^2 + .0576} \qquad (2\text{-}61)$$

Numerical solution of this equation yields the following:

$\bar{A}_2 = 0.25$, $K_1 = 0.6$, $K_2 = 0.96$

$\bar{A}_1$	.6	.5	.4	.3	.2	.1	0
$\partial P_2/\partial P_o$	.0925	.0816	.0669	.0481	.0268	.00788	0

It had been assumed that the orifice ( )$_1$ is the limiting factor in the flow rate. Hence, the maximum orifice area ratio $\bar{A}_1$ which is valid here is that ratio which allows $\bar{A}_1 K_1 = \bar{A}_2 K_2$. Then

$$\bar{A}_{1\ \max} = \frac{\bar{A}_2 K_2}{K_1} = .25\,\frac{.96}{.6} = .40$$

If the venturi area ratio $\bar{A}_2 = 0.0625$ (i.e., $\bar{d}_2 = 0.25$), the above becomes

$$\frac{\partial P_2}{\partial P_o} = \frac{.02875\,\bar{A}_1^2}{.36\,\bar{A}_1^2 + .0036} \qquad (2\text{-}62)$$

and the numerical solution is

$\bar{A}_2 = 0.0625$, $K_1 = 0.6$, $K_2 = 0.96$

$\bar{A}_1$	.3	.2	.1	.05	0
$\partial P_2/\partial P_o$	.0719	.064	.04	.016	0

The limiting orifice area ratio is

$$\bar{A}_{1\ \max.} = \frac{\bar{A}_2 K_2}{K_1} = .0625\ \frac{.96}{.6} = .10$$

The pressure ratio across the second orifice, the venturi tube, was given in equation (2-54). The pressure ratio across the first orifice can be computed from the relationship

$$\frac{P_o}{P_*} = \frac{P_o/P_a}{P_*/P_a} \tag{2-63}$$

For the first set of conditions ($\bar{A}_2 = 0.25$), equation (2-54) becomes

$$\frac{P_*}{P_a} = \frac{1.0\ \bar{A}_1^{\,2} + .0576}{.36\ \bar{A}_1^{\,2} + .0576} \tag{2-64}$$

The pressure ratios across the two orifices are computed as:

$\bar{A}_2 = 0.25$, $K_1 = 0.6$, $K_2 = 0.96$, $P_o/P_a = 3.0$

$\bar{A}_1$	.5	.4	.3	.2	.1	0
P_*/P_a	2.22	2.002	1.72	1.40	1.118	1.0
P_o/P_*	1.35	1.50	1.74	2.14	2.68	3.0

For the second set of conditions ($\bar{A}_2 = 0.0625$), equation (2-54) becomes

$$\frac{P_*}{P_a} = \frac{1.08\ \bar{A}_1^{\,2} + .0036}{.36\ \bar{A}_1^{\,2} + .0036} \tag{2-65}$$

and the pressure ratios across the orifices become:

$\bar{A}_2 = 0.0625$, $K_1 = 0.6$, $K_2 = 0.96$, $P_o/P_a = 3.0$

$\bar{A}_1$	.15	.10	.05	0
P_*/P_a	2.385	1.86	1.40	1.0
P_o/P_*	1.256	1.61	2.14	3.0

These data are plotted in figure 2-14.

The magnitude of the pressure sensed at the throat $(\ )_2$ is given by equation (2-59). When expanded, this equation becomes

$$\frac{P_2}{P_a} = \frac{K_2^2\left[\bar{A}_2^2 + K_1^2\bar{A}_1^2(1-\bar{A}_2^2)\right] + K_1^2\bar{A}_1^2\left[1-K_2^2(1-\bar{A}_2^2)\right]\frac{P_o}{P_a}}{K_1^2\bar{A}_1^2 + K_2^2\bar{A}_2^2} \tag{2-66}$$

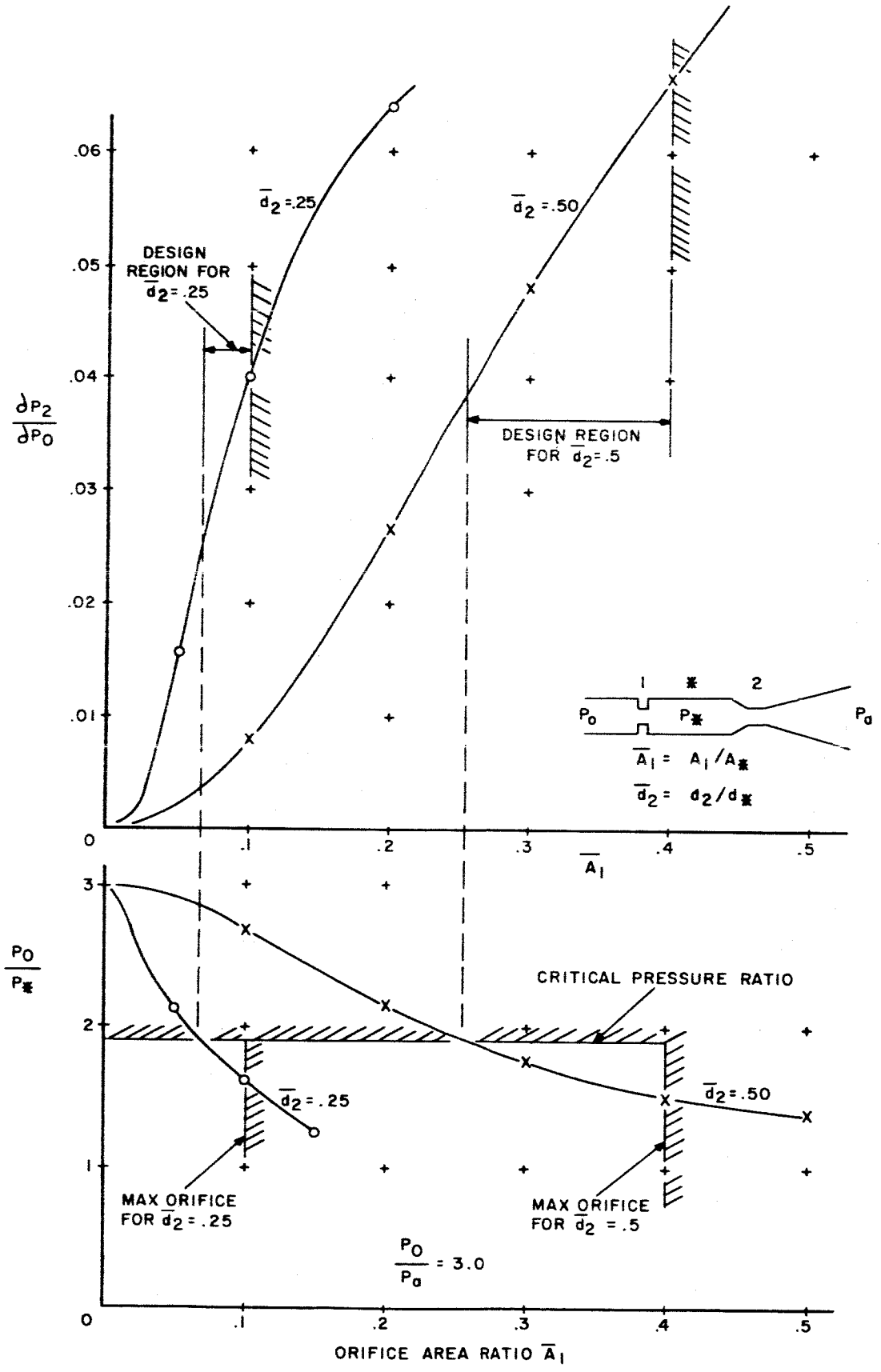

FIGURE 2-14. ORIFICE-VENTURI COMBINATION

For the first set of assumed conditions ($\bar{A}_2 = 0.25$) and a pressure ratio of 3.0 from supply to ambient, the numerical values of the equation become:

$$\frac{P_2}{P_a} = \frac{.0576 + .4573\,\bar{A}_1^2}{.0576 + .36\,\bar{A}_1^2} \qquad (2\text{-}67)$$

$\bar{A}_2 = 0.25$, $K_1 = 0.6$, $K_2 = 0.96$, $P_o/P_a = 3.0$

$\bar{A}_1$	.5	.4	.3	.2	.1	0
P_2/P_a	1.163	1.132	1.098	1.052	1.019	1.0

For the second set of assumed conditions ($\bar{A}_2 = 0.0625$) and a supply pressure ratio of 3.0, the numerical values become:

$$\frac{P_2}{P_a} = \frac{.0036 + .417\,\bar{A}_1^2}{.0036 + .36\,\bar{A}_1^2} \qquad (2\text{-}68)$$

$\bar{A}_2 = 0.0625$, $K_1 = 0.6$, $K_2 = 0.96$, $P_o/P_a = 3.0$

$\bar{A}_1$	.15	.10	.05	0
P_2/P_a	1.11	1.08	1.03	1.0

These data are found plotted in figure 2-15.

The pressures sensed at the venturi throat are seen to vary from 1.05 to 1.13 times ambient, depending upon the design parameters. For a nominal sea level atmospheric ambient ($P_a = 14.7$ psi), the sensed pressures will vary from 0.7 to 1.9 psig. These are adequate pressures, but it must be noted that the throat pressure alone gives no information about the supply pressure ratio. It only indicates the supply pressure. The supply pressure ratio is given when the throat pressure ratio is used; that is, the ratio of pressure from the throat to ambient. This implies the use of ambient sensitive components in the feedback element.

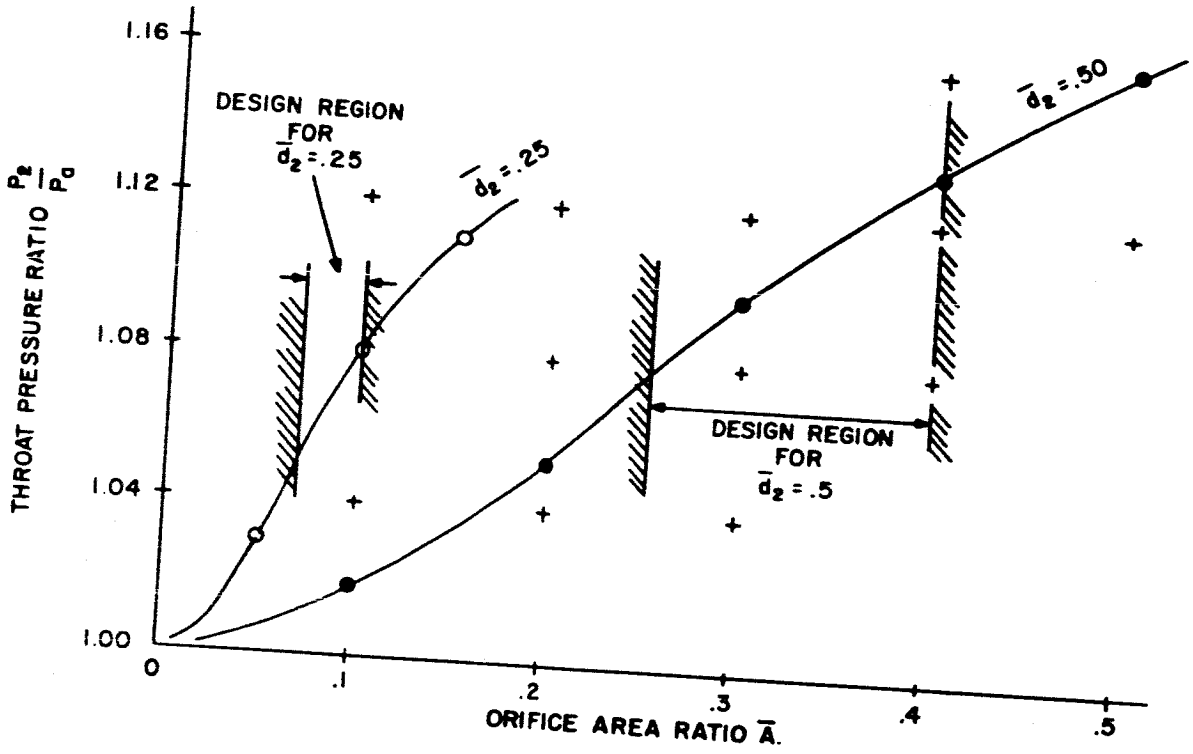

Venturi Throat Pressure Ratios
Venturi-Orifice Combination
Figure 2-15

In its standard mode of utilization, the venturi tube gives a pressure difference between the input -- P_*, in this case -- and throat pressures. This is given by a difference between equations (2-54) and (2-66).

$$\frac{P_* - P_2}{P_a} = \frac{K_1^2 \bar{A}_1^2 K_2^2}{K_1^2 \bar{A}_1^2 + K_2^2 \bar{A}_2^2} (1 - \bar{A}_2^2)\left(\frac{P_0}{P_a} - 1\right) \qquad (2\text{-}69)$$

In terms of pressures rather than ratios,

$$P_* - P_2 = \frac{K_1^2 \bar{A}_1^2 K_2^2}{K_1^2 \bar{A}_1^2 + K_2^2 \bar{A}_2^2} (1 - \bar{A}_2^2)(P_0 - P_a) \qquad (2\text{-}70)$$

Again, the pressure difference given by the venturi tube gives no information about the supply pressure ratio, but rather the supply guage pressure.

One other point should be made about the use of the venturi; it concerns the practical aspects of applying this unit as a pressure sensor. As with the convergent-divergent nozzle, it is the practical aspects of the application that cause the unit to be discarded. In this case it concerns the rate of change of sensed throat pressure with supply pressure as shown in the graph. Values of the derivative vary from 0.025 to 0.067. For a supply pressure variation of two per cent, the sensed pressure will have a maximum variation of 0.05 to 0.134 per cent, or only 0.035 to 0.255 psi. If the sensor parameter can be selected such that it operates closer to the upper figure, it can be practical. However, even in this case, the need for the sensor must be seriously questioned since the feedback elements must still be capable of interpreting the signal as representing a ratio rather than a pressure. If they are able to do that, they should be able to do the same thing when supplied with the regulated supply pressure directly. Hence, the venturi - orifice combination, while being a workable solution to the sensing problem, does not offer all that might be desired.

2.4.1.3 Pressure Jet Oscillator

The pressure jet oscillator is a device consisting of two convergent nozzles, each opening through a plate or wall whose area is large compared to the throat area, oriented such that their nozzles face one another on a common axis. One nozzle is supplied with air at the supply pressure, while the other is connected to a closed volume, known as the chamber. The pressure jet oscillator has a characteristic of providing an oscillation in chamber pressure, accompanied by a well defined and distinctive change in sound when it switches. The frequency of oscillation is a function of the supply pressure, chamber volume and separation between the two nozzles. The frequency is stable and consistent. Figure 2-16 shows typical variations in chamber pressure as the separation is varied. For all separations greater than 0.026 inches, there are oscillations, some with rather large variations in chamber pressures.

While making preliminary tests on this unit, it was found that the chamber pressure seemed to be proportional to the supply pressure when the unit was not oscillating. It was therefore suggested that the pressure jet oscillator, used in a nonoscillating mode, might be an adequate sensor for the pressure regulator.

A series of tests were run on an oscillator with small gap (0.007 inches) and relatively low supply pressures such as would be used for the pressure regulator. A small pressure chamber was used to test the unit in ambient pressures greater than local atmospheric pressure. The results of these

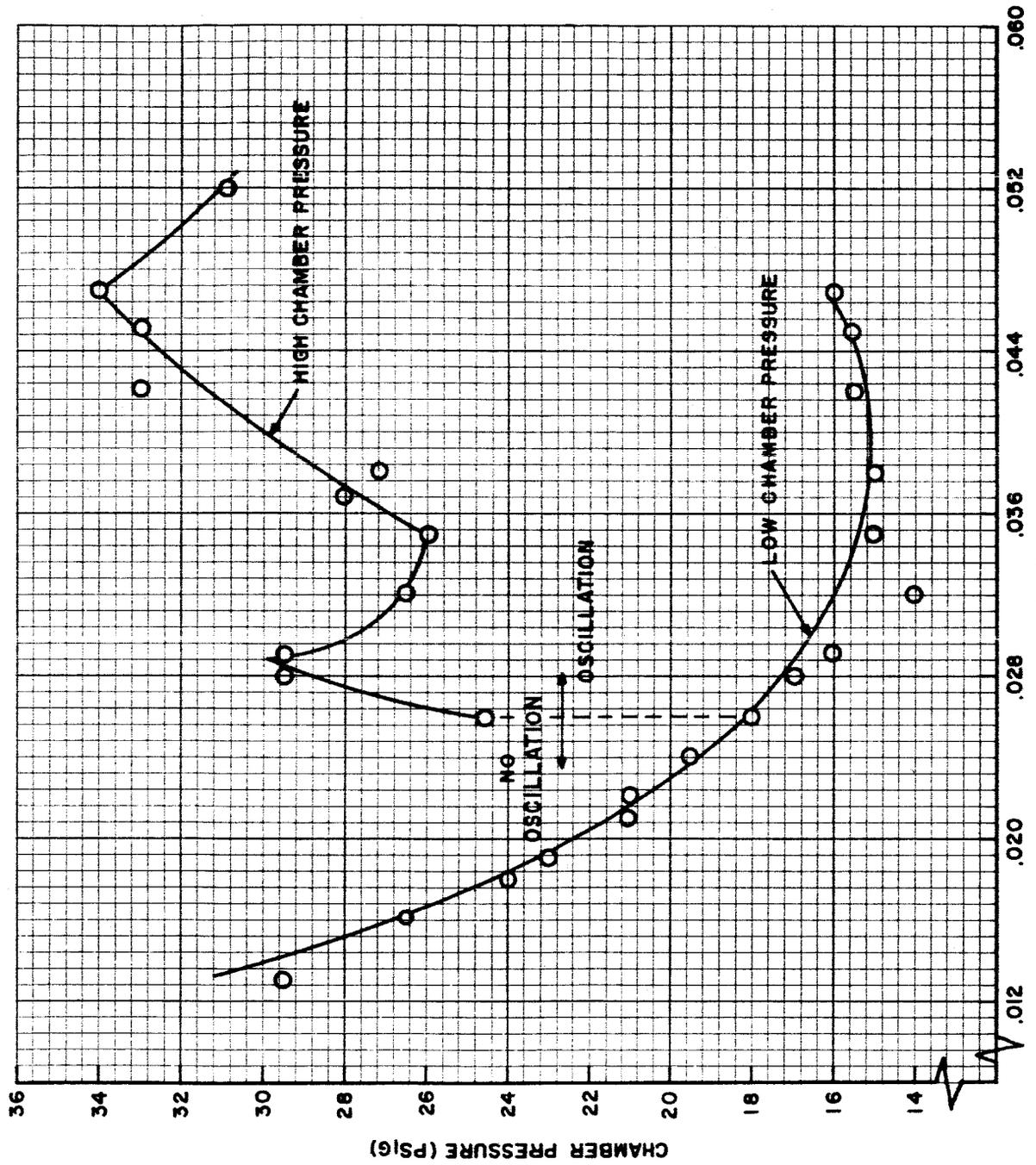

FIGURE 2-16. PRESSURE JET OSCILLATOR Mk O, HIGH AND LOW CHAMBER PRESSURE DURING OSCILLATION, 60 PSIG SUPPLY PRESSURE

tests are shown in figure 2-17. Due to instrumentation limitations, it was necessary to vent the chamber to limit the measured pressures. The vent was adjusted to give a 6 psig chamber pressure at a supply pressure ratio $P_a/P_s = 0.5$ when the ambient was atmospheric pressure. This vent shifts the curves to the left, but does not otherwise affect the operation of the unit. Note that chamber pressure turns out to be a function of ambient pressure as well as supply pressure ratio. Attempts to remove this ambient pressure dependency failed. The separation gap was increased to 0.125 inches, but caused very little change in the shape or character of the curves.

The experimental data just described has a strong similarity to data recently published in the literature. In NASA CR-101, "Fluid Amplifier State of the Art", Volume I, October 1964, there is brief mention of a pressure regulator credited to the Harry Diamond Laboratories (page 6-7). Except to say that the device uses a vortex, the report contains no description, but does have a figure supposedly showing the performance of the unit. The figure has neither numbers nor identification for its scales, but when compared to figure 2-17, it is apparent that the vertical scale represents an output signal while the horizontal scale is $(P_s - P_a)/P_s$, or possibly the ratio P_s/P_a. The same shape of curve and the same scatter of data is present as is found for the pressure jet oscillator. The data for higher ambient pressures do not extend as far up the scales as those for lower ambient pressures, a direct result of instrumentation limitations also found in the present experiments. Hence, the HDL device and the pressure jet oscillator share the same curious operational characteristics. It was only through an attempt to generate the same data theoretically that the true nature of both units was revealed.

Since variations in separation between the two nozzles made little difference in the operation of the unit, it was hypothisized that the same would be true if the gap were decreased to zero. The pressure jet oscillator then becomes a simple pipe supplying air at the supply pressure to the chamber, and chamber pressure then equals the supply pressure. The ratio of ambient to supply can be written as

$$\frac{P_a}{P_s} = \frac{P_{at} + \Delta P}{P_{s(G)} + P_{at} + \Delta P} \qquad (2\text{-}71)$$

where P_{at} is the local atmospheric pressure, the nominal ambient, and Δp is the difference between the ambient and atmospheric pressures. The term $P_{s(G)}$ represents gage supply pressure. Chamber pressure relative to the ambient is equal to this gage supply pressure. Using these definitions, curves of chamber pressure as a function of supply pressure ratio were drawn for various ambient pressures. These are shown in figure 2-18. It is seen that the shape and character of the curves are similar to those generated by experimental means.

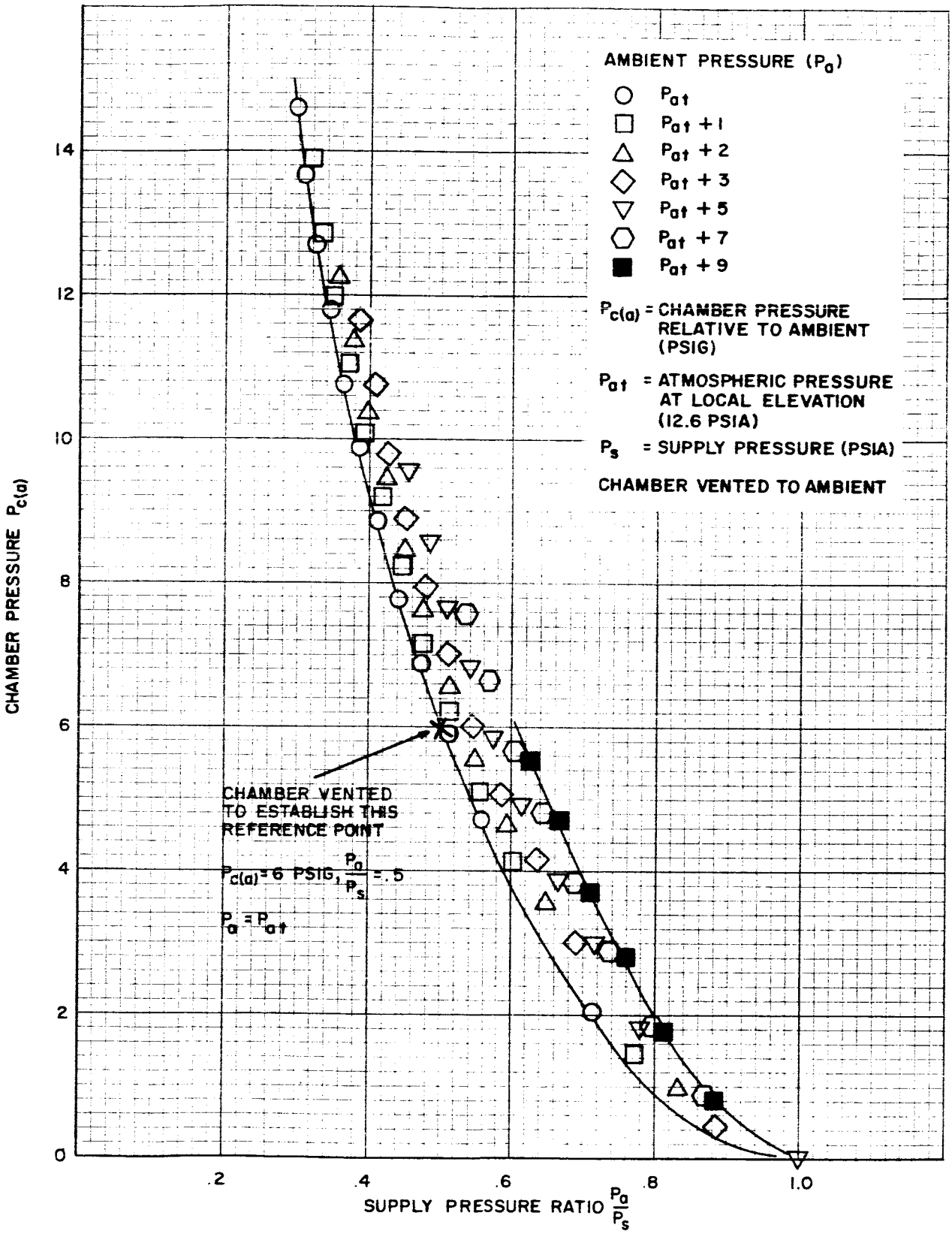

FIGURE 2-17. CHAMBER PRESSURE, PRESSURE JET OSCILLATOR Mk.I, .007" GAP

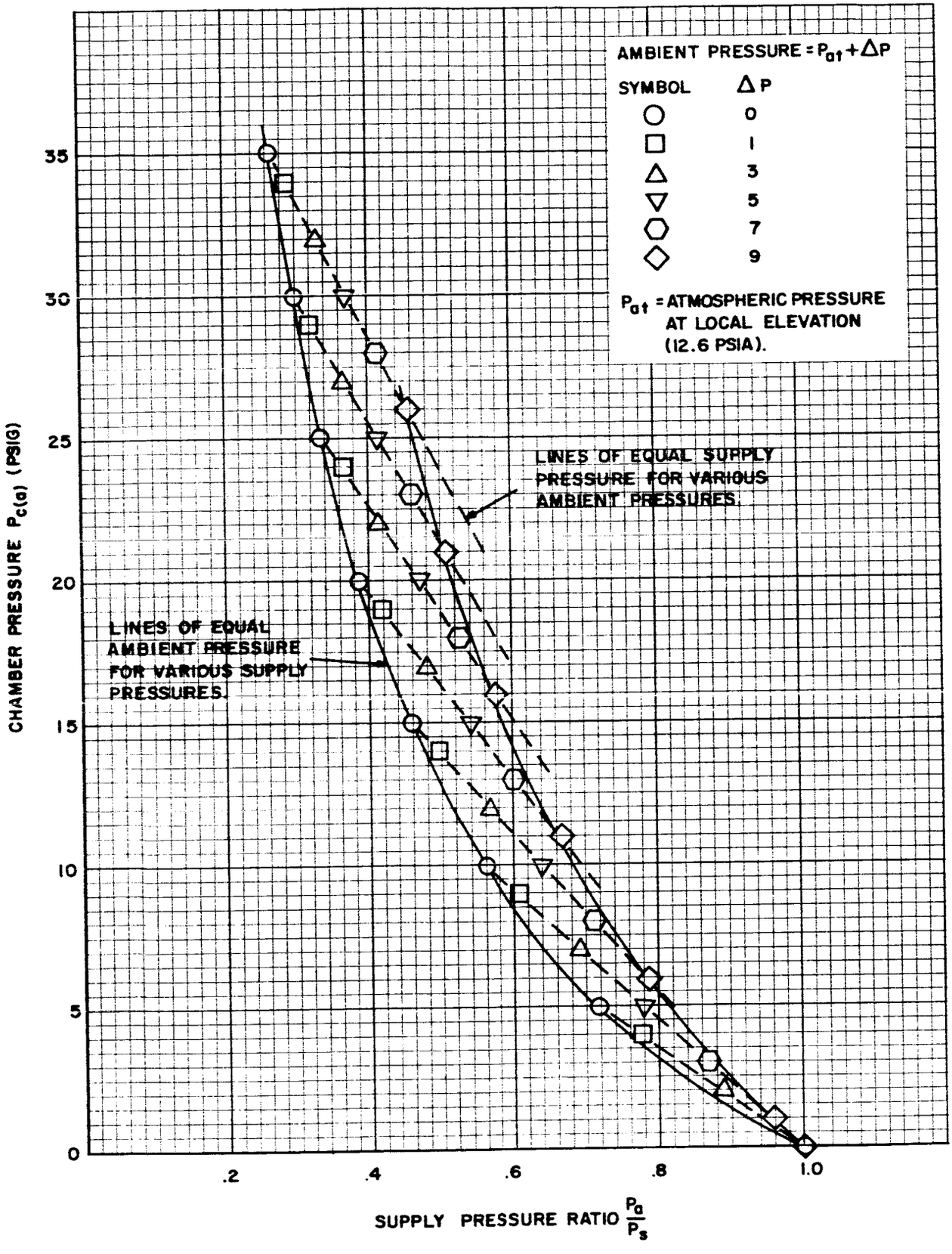

FIGURE 2-18. THEORETICAL CHAMBER PRESSURE

If a chamber pressure ratio is used for the ordinate, the ratio can be defined as

$$\frac{P_c}{P_a} = \frac{P_{s\,(G)} + P_{at} + \Delta P}{P_{at} + \Delta P} = \left(\frac{P_a}{P_s}\right)^{-1} \qquad (2\text{-}72)$$

The last equality is a result of equation (2-71). This shows that the curve of chamber pressure ratio should be independent of ambient pressure changes. When the experimental data shown in figure 2-17 are placed into a chamber pressure ratio form and plotted, they give a curve as shown in figure 2-19. As suggested above, all data falls on the same curve, showing no effect of ambient pressure variations. The theory, equation (2-72), is also plotted in the figure, but does not agree with the experimental data due to the chamber vent used for the latter. This can be corrected by remembering that

$$P_c = P_a + (P_c - P_a) \qquad (2\text{-}73)$$

and that a vent to ambient operates on the basis of the pressure difference in the parentheses. Only some fraction of that increment will be present, so the new chamber pressure is

$$P_{c_*} = P_a + K\,(P_c - P_a)$$

or

$$\left(\frac{P_c}{P_a}\right)_* = 1 + K\left(\frac{P_c}{P_a} - 1\right) \qquad (2\text{-}74)$$

In terms of supply pressure, since chamber and supply pressures are, theoretically, the same,

$$\left(\frac{P_c}{P_a}\right)_* = 1 + K\left(\frac{P_s}{P_a} - 1\right)$$

$$= 1 + K\left[\left(\frac{P_a}{P_s}\right)^{-1} - 1\right] \qquad (2\text{-}75)$$

For the vent setting used to obtain the experimental data, the value of the constant is K= 0.466. Equation (2-75) is also plotted in figure 2-19 and is found to agree perfectly with the experimental data. Thus we have shown that the pressure jet oscillator, when used in a nonoscillating mode, senses nothing more than supply pressure, which could have been done with a simple T-fitting in the supply line. Therefore, the pressure jet oscillator cannot be considered to be a potential pressure ratio sensor.

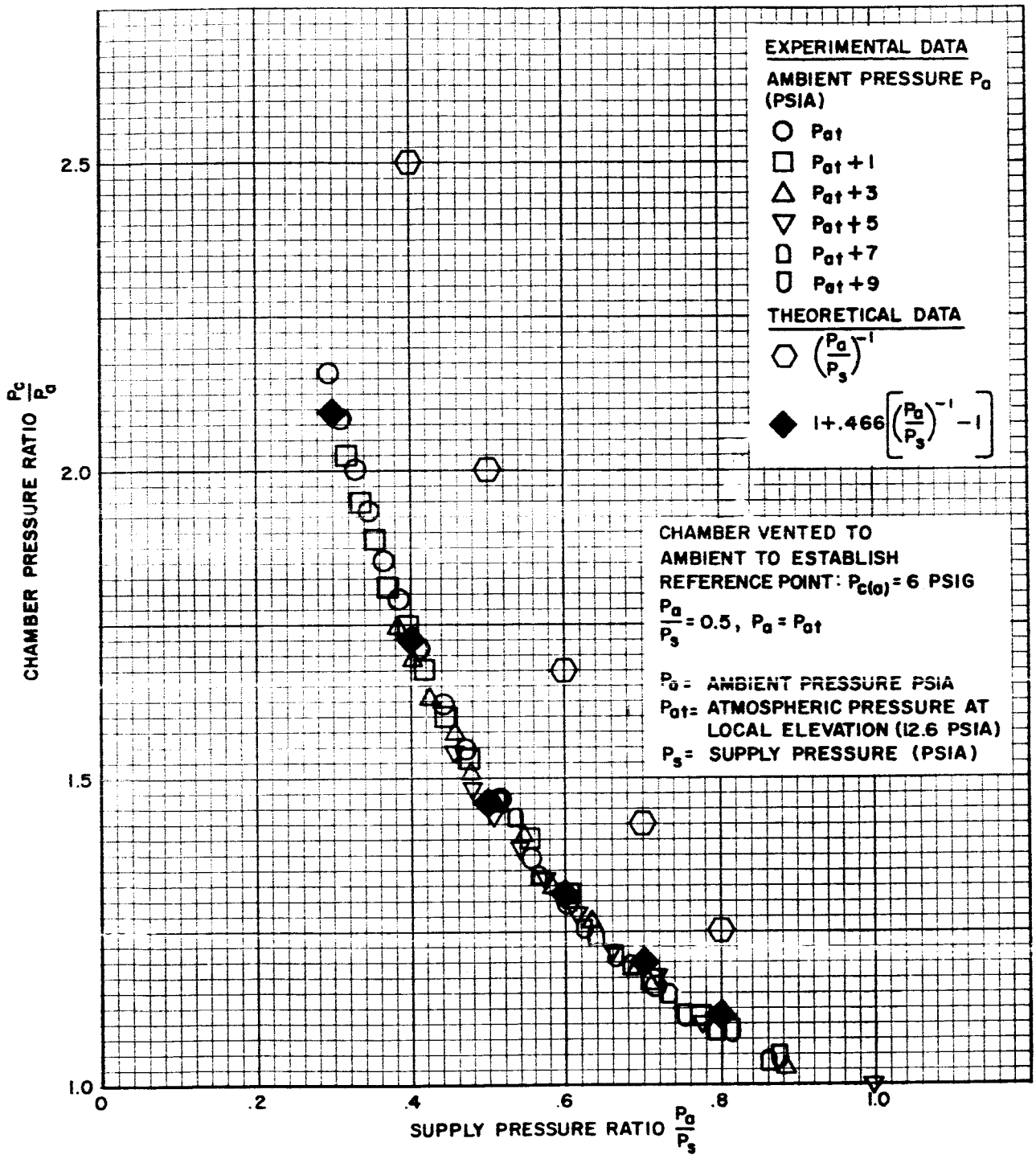

FIGURE 2-19. PRESSURE JET OSCILLATOR, CHAMBER PRESSURE RATIO MK. I, .007"GAP

2.4.2 Control Valve

The control valve poses the most difficult problem in a pure fluid pressure regulation system. By their very nature, pure fluid valves do not provide high output pressures and flows simultaneously. This may be an acceptable state of affairs for control or amplification applications, where flow requirements are small, but the pressure regulator must be capable of supplying all flows demanded, from zero to the maximum specified, at the same constant output pressure.

2.4.2.1 Vortex Valve

The vortex valve was originally proposed to be used in the pressure regulator. The fact that this valve can handle large flows, has reasonable pressure recoveries, and can control output pressures over a three to one range, led it to be considered the ideal component. However, vortex valves have a singular disadvantage which effectively rules out their use as a single, isolated component acting as a control valve. That is, they require control pressures in excess of their supply pressures. If the supply pressure is the unregulated source pressure for the system, as is the case in the pressure regulator, where does the higher control pressure originate? The vortex valve must be rejected as a simple control valve.

The true value of the vortex valve becomes apparent when it is used in combination with other units, or used in an unconventional or unique manner. When used in a servo valve application, it has been used in combination with another device; the vortex valve, operating at pressures well under the system pressure, acted as a controlling device for the other, primary valve. (Reference: NASA CR-54463, "Final Report. Design, Fabrication, and Test of a Fluid Interaction Servovalve", prepared by Bendix Corporation for NASA, 17 May 1965.)

The vortex valve with a portion of the supply pressure fed into the control port can be used as a pressure step-down device, while another, smaller valve, whose output is vented to ambient, can be used as the pressure control device. This has the disadvantage of dumping excess fluid to ambient, but that is the nature of pure fluid systems: pure fluid systems do not make efficient use of their working fluid.

2.4.2.2 Momentum Valve

The momentum valve (figure 2-20) was investigated as a possible device for either the self contained pressure regulator, or as the primary control valve in a pressure control loop. The momentum vlave consists of two convergent nozzles facing one another on a common axis. A control jet is located normal to the axis of the

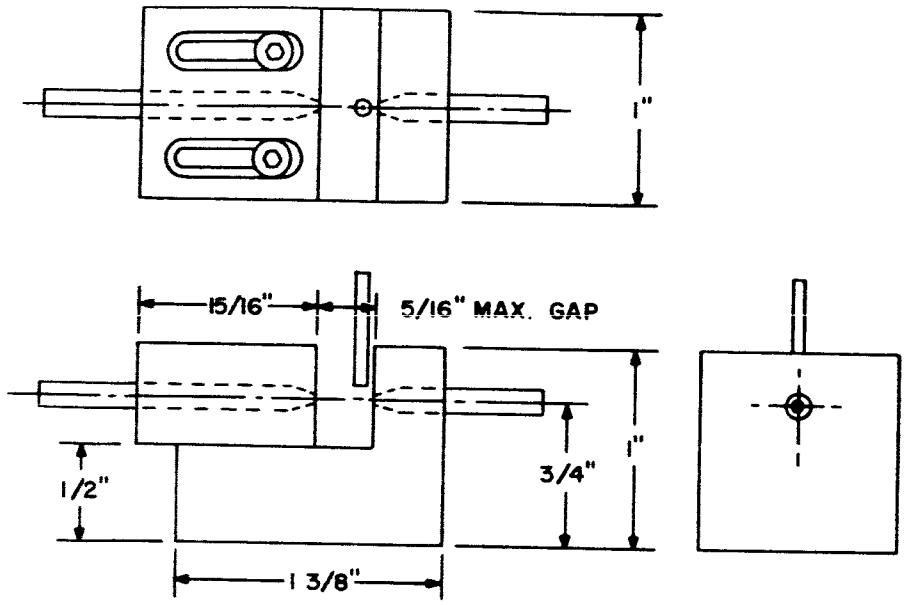

Momentum Valve
Figure 2-20

nozzles. In the sketches, the input side is on the right, while the output side is on the left. The control jets used in the tests were over eight inches long, an arbitrary length, and 0.033 and 0.063 inches in inside diameter. They were located against or nearly against the wall on the supply side of the gap, with the outlet at the edge of the supply nozzle. Tests were also run with the input jet withdrawn a distance of 0.050 inches. All tests were run with a momentum valve gap of 0.250 inches.

Figures 2-21 and 2-22 summarize the experimental data for the larger and smaller diameter control jets, respectively. Each figure has curves of 5, 10, 15 and 20 psig supply pressures and two control jet positions. Also shown is a 20 psig supply pressure curve where the control pressure was taken from the output of the unit. The limiting control pressure for this configuration is, of course, at that point where the control and supply pressures are equal.

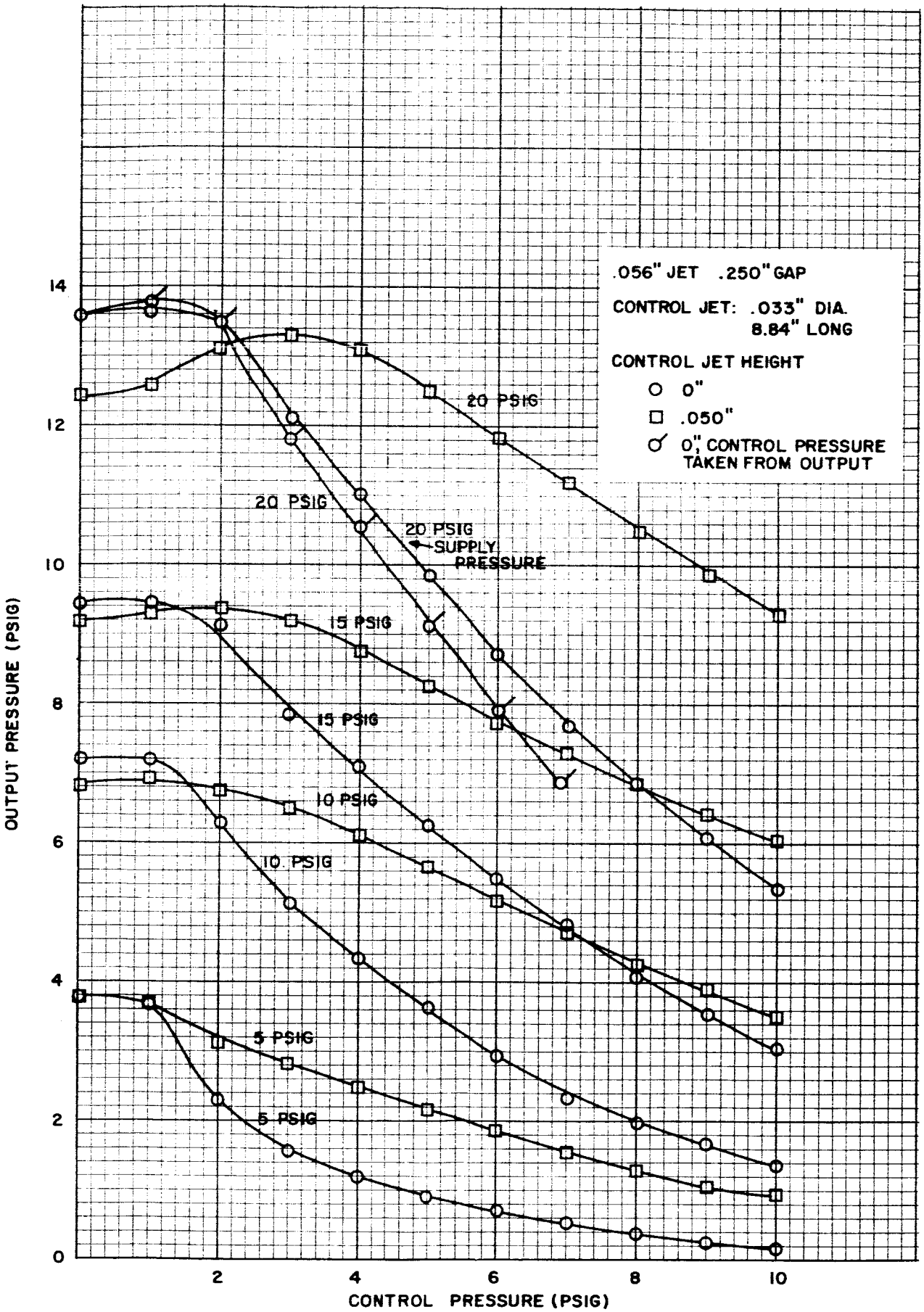

FIGURE 2-21. MOMENTUM VALVE PERFORMANCE

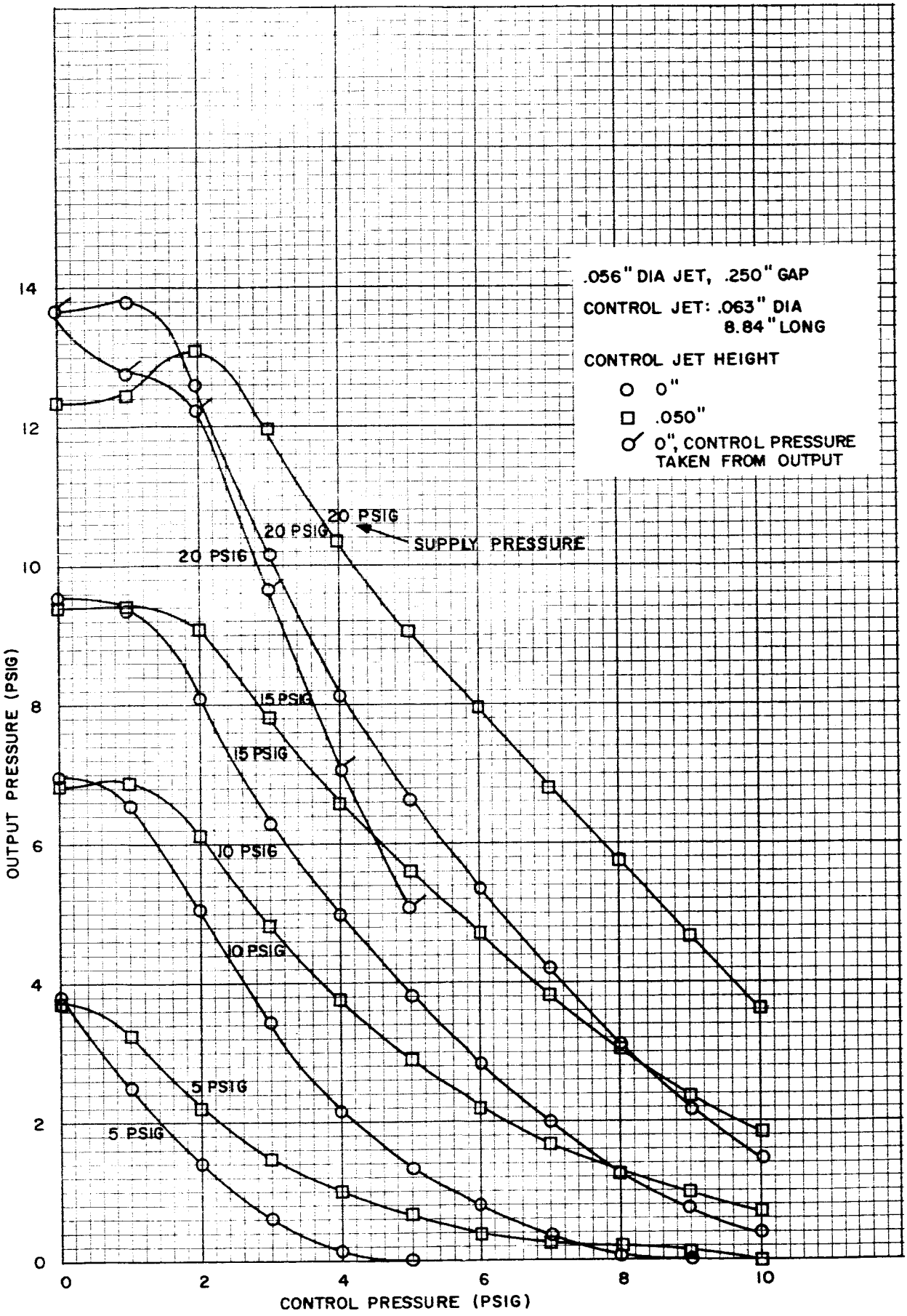

FIGURE 2-22. MOMENTUM VALVE PERFORMANCE

Except for the 5 psig supply pressure data, the curves can be linearized for a portion of their lengths. In the first figure, the slopes of output to control pressures are found to vary between -1.0 and -1.75, depending upon the curve used. The slopes of output to supply pressures vary from 0.33 to 1.0, again depending upon the location at which the slope is taken.

Due to instrumentation limitations, data could not be taken at higher supply pressures, but the usefulness of such data is questionable when such a small unit is used. For application as a primary flow or pressure control valve, it is envisioned that a much larger unit be used, the nozzle diameters being sized for the flow rates required downstream. However, the unit does have rather poor pressure recoveries, which may limit its usefulness in this application.

2.4.3 Feedback Elements

As was mentioned in the heading to this section, the choice of feedback or intermediate elements is dependent upon the requirements placed upon them by the sensor and the primary control valve. Until those elements are chosen, and the nature of output and input signals are known, the requirements for the feedback elements cannot be defined. However, the nature of the task to be performed is such that most of the available proportional devices, such as the impact modulator, can be used with satisfaction.

2.5 Conclusion

In the studies discussed above, it has been found that a single unit, operating in a self regulating mode, cannot correct for changes in load. However, it can compensate for supply pressure variations. In order to regulate the pressure in the presence of load variations it is necessary to introduce amplification in the feedback loop. The single unit, self contained regulator then becomes a pressure regulating system. Components of the system were discussed, the possibilities were presented and the problem areas reviewed.

Although a pure fluid pressure ratio regulator has not been fabricated and tested as a part of this study, the concept of pure fluid pressure regulation is considered feasible and practical. The few problem areas that remain to be faced can be surmounted by a continuing effort. Such effort should place primary emphasis upon the performance of components that might serve as sensors, feedback elements, and primary control valves, with special attention being paid to the effect of variations in their operating ambient pressures. Given such basic performance data, supported by continuing conceptual studies using the component data, it would be possible to fabricate and test a practical pressure regulator.

2.6 List of Symbols for Chapter 2

A	area; orifice area
$\bar{A}_i$	ratio of area i to tube area, in orifice-venturi combination
$\mathbb{R}$	ratio of areas, see equation (2-59)
d	diameter
g	gravity
k, K	various constants, orifice constant, control constant
$\mathcal{K}$	ratio of areas and orifice constant, see equation (2-55)
ℓ	length of divergent portion of nozzle
m	mass flow
$\bar{m}$	maximum mass flow
M	Mach number
ΔP	pressure increment
P	pressure
Q	volume flow rate
r	radius
R	universal gas constant
T	absolute temperature
V, u	velocity
w	weight flow rate
α	nozzle half angle
γ	ratio of specific heats
ρ	mass density

Subscripts

a	ambient
at	atmosphere
C	control; chamber
C_o	control from output side
e	exit
L	load
o	output; initial condition
R	regulator
S	supply
T	throat
1	forward control gain; arbitrary point; orifice in the orifice-venturi combination
2	feedback control gain; arbitrary point; venturi in the orifice-venturi combination
*	design condition; intermediate point in the orifice-venturi combination